# Respiratory Viral Coinfection Ameliorates Disease Severity in Mice

A Dissertation

Presented in Partial Fulfillment of the Requirements for the

Degree of Doctor of Philosophy

with a

Major in Microbiology, Molecular Biology & Biochemistry

in the

College of Graduate Studies

University of Idaho

by

Andres J. Gonzalez

Major Professor: Tanya A. Miura, Ph.D.

Committee Members: Elizabeth Fortunato, Ph.D.; Diana Mitchell, Ph.D.;

Santanu Bose, Ph.D.

Department Administrator: James Nagler, Ph.D

May 2019

## Authorization to Submit Dissertation

This dissertation of Andres J. Gonzalez, submitted for the degree of Doctor of Philosophy with a major in Microbiology, Molecular Biology & Biochemistry and titled "Respiratory Viral Coinfection Ameliorates Disease Severity in Mice," has been reviewed in final form. Permission, as indicated by the signatures and dates below, is now granted to submit final copies to the College of Graduate Studies for approval.

Major Professor: _____ Date:_____

Tanya A. Miura, Ph.D.

Committee Members: _____ Date:_____

Elizabeth Fortunato, Ph.D.

_____ Date:_____

Diana Mitchell, Ph.D.

_____ Date:_____

Santanu Bose, Ph.D.

Department Administrator: _____ Date:_____

James Nagler, Ph.D.

# Abstract

Improvements to viral diagnostic techniques led to increased detection of multiple respiratory viral pathogens from single samples. These co-detections of multiple viruses are known as viral coinfections. Viral coinfections are reported to lessen, increase, or not affect disease severity compared to individual virus infections. The literature is unclear as to what infection parameters or immune responses drive the disease severity aberrations. Clinical data cannot determine the timing of virus infections concerning each virus or the initial severity of each infection. We developed a mouse model of respiratory viral coinfection that allows us to control infection parameters. We can control for the timing, order, severity, and pairing of each virus. Using this model, we have determined that a less pathogenic virus can attenuate the disease severity of a more pathogenic virus. We used a minor group rhinovirus (RV) to attenuate the disease severity of influenza A virus (IAV), pneumonia virus of mice (PVM), and mouse hepatitis virus (MHV) when viruses were inoculated two days apart. We then determined that coinfection-mediated disease attenuation was not unique to RV, but MHV could also attenuate IAV and PVM disease severity. Further research found coinfection-mediated disease attenuation was dependent upon timing between virus infections and the severity of infections. Coinfection induced an early interferon response in mice, but the level of induction was dependent upon the specific viral pairing. Early type I interferon signaling was blocked in coinfected mice by intranasal administration of an antibody specific to the type I interferon receptor. We determined type I interferon was not a required mechanism for coinfection-mediated disease attenuation during RV and PVM coinfection. We then depleted neutrophils by intraperitoneal injection of an antibody specific to Ly6G high neutrophils. Depletion of neutrophils early during coinfection did not affect coinfection-mediated disease attenuation during coinfection with RV and PR8. Further experiments targeting other components of the innate immune system will be required to elucidate the critical mechanisms of respiratory viral coinfection-mediated disease attenuation.

# Acknowledgments

I want to give the highest appreciation to my major professor, Dr. Tanya Miura. I know sometimes teaching me must have felt like teaching a rock to breathe. But you persevered and helped me to the end. You truly are one of the most intelligent people I know and a very capable scientist. You provided me with many opportunities to grow professionally and academically. I appreciate everything you taught me, and I will work hard to improve myself based on your mentorship.

I would also like to express my appreciation for Ann Norton, former director of the IBEST Imaging Core. You were always around to provide help for all of my microscopy and flow cytometry questions. Without your assistance, I would have struggled much more in that cold, upstairs room.

My experiences teaching the general microbiology laboratory class opened my eyes to the enjoyment of being a teacher. My experience was enriched by having Tim Steffens as a teaching mentor and boss. He is essential to the course and helps the teaching assistants feel comfortable with the class material. Without Tim's help, I would not be half as prepared to move into teaching as an occupation.

Lastly, I would like to thank my committee members: Drs. Lee Fortunato, Diana Mitchell, and Santanu Bose. I always enjoyed Lee's spontaneous appearances in my laboratory and her commentary on life; she provided a nice spice to the day. I want to thank Diana for teaching me some of the tricks of flow cytometry. I also appreciated Diana allowing me to guest lecture in her immunology course. It was a scary experience but quite enjoyable once I started lecturing. I didn't get to interact with Santanu as much as my other committee members because of location differences. However, I appreciate how much he made me think during our committee meetings. His questioning helped me grow as a student and prepare for the future.

# Dedication

There are too many people I would like to thank for helping me maintain my sanity. It was a long five years, and I wasn't always a pleasant person, so I would like to express my gratitude to anyone who had to interact with me during this time. There are many friends I would like to reach out to who helped me along the way. You may not have realized it, but just staying around helped keep my life together.

I need to thank my mom most of all. She is stuck dealing with during the good and the bad. She has listened to everything I have had to say during this journey, or at least I think she was listening, and still supported me along the way. I wouldn't be anywhere without her. For all of your guidance, support, sympathy, lectures, reprimands, chastising, teachings, help, and love I will fulfill my promise and ensure your retirement yurt has indoor plumbing and not an outhouse. I hope you remain as proud of me in the future as you are now.

I want to single a few friends out who were essential to my survival during graduate school. First, I want to thank my best friend, Nick Flynn. I needed all the crazy experiences we had to remind me I cannot be an undergraduate forever and that someday I need to grow up. You truly helped relieve a lot of stress over the years, and I look forward to sharing climbing trips and drinks for a very long time. Next, I want to thank Savannah Patterson. You were my first friend in graduate school at the University of Idaho. We shared many enjoyable times that I will cherish and laugh about for the rest of my life. Lastly, I want to thank John Clary. You always supported me, even when you should have been chastising me for my choices. You made work a fantastic experience, and I'm truly grateful that we are friends. I look forward to keeping all three of you in my life forever.

I should probably thank all the past and present members of my laboratory. You all had to deal with me the most, and I know that wasn't easy. I would especially like to thank Frankie for always being a ray of sunshine for us, even when we just wanted to be rain clouds. Big Andy (the only time I'll ever use that!), we are too similar, but that is what made our friendship so fun. Thank you for being one of the most genuine people I have ever met. I cannot wait to go to your wedding. Thank you, Sierra, for being "lab mom" and sponsoring baked goods Monday. I would also like to thank Elijah, Manny, and Kevin for putting up with me and providing the most interesting conversations.

Finally, I would like to thank the climbing community that helped me find my place in this world. I also want to thank my friends from volleyball for always being available to play pick-up games and help me relieve stress by hitting something hard, especially Niels and Michaila. I want to thank my dog, Grace, too. You're a good dog.

I would also like to dedicate this work to all the mice that gave their lives for this project.

# Table of Contents

# List of Figures

# List of Tables

# CHAPTER 1

# Introduction

## 1.1 Prevalence of respiratory viral coinfection

Current research has uncovered that multiple concurrent viral infections may heavily influence respiratory disease. The phenomenon of multiple interacting infections is known as a coinfection, and these types of infections have been reported to be both viral-bacterial (1-3) or viral-viral (4-6) in nature. During the 2009 influenza pandemic, one study reported that 55% of autopsied samples revealed secondary bacterial pneumonia complications in conjunction with the influenza-related disease (7). Clinical studies report that 11-26% of virus infections in the respiratory tract are viral-viral coinfections and not single virus infections (8-11). However, the prevalence of coinfection has also been reported at much higher levels too: 34% (2), 45% (12), or 62% (13). One study reported that 71% of positive respiratory syncytial virus infections involved another virus (14). Rhinovirus is often the most common co-detected pathogen with respiratory syncytial virus (12, 14, 15), but another study reported that rhinovirus and respiratory syncytial virus coinfection was under detected (16). The incidence of coronavirus infections being co-detected with at least one other respiratory pathogen is reported between 50-70% of total coronavirus infections (17-19). Once again rhinovirus, respiratory syncytial virus, and influenza virus were reported as common co-pathogens in these studies. When assessing pandemic influenza A virus (IAV) coinfection, the most common pathogens co-detected are rhinovirus followed by respiratory syncytial virus (20). These studies demonstrate that respiratory viral coinfections are prevalent and certain viruses have a high co-detection rate compared to other virus pairings. This could mean that certain virus pairings are more compatible with sharing a host while other viruses are excluded by viral interference. One alternative is these studies may be biased by which viruses are chosen for screening during each study, allowing a potential underreporting for many virus pairings. These studies also varied in their patient demographics (age, immunocompromised, location, etc.), sampling periods (year-round vs seasonal), and sample population sizes. Differences in these parameters could affect the

prevalence of coinfection detection, and more research is necessary for determining what parameters allow viral coinfections to persist in a population.

### 1.2 Study demographics

An important aspect of studying coinfection is the population demographics. One contribution to the wide range of reported coinfections could be the varied populations sampled. Studies vary between sampling hospitalized patients (13, 21) and monitoring infections within the community (14, 22). This sampling discrepancy separates the identification of potentially severe viral coinfections from those that may not cause any signs of disease. It would be difficult to piece together a strong picture of coinfection virus pairings if these studies did not sample in the same locations and screen for the same viruses. The age of the sample population is also an important parameter as one study found viral coinfection is associated with increased hospitalization in patients younger than 23 months old compared to patients older than 23 months (23). One study focused on the prevalence of human bocavirus (HBoV) infections and found 57.2% of HBoV infections involve at least one other virus with the majority of infections being in children 1-2 years old (24). Another study reported that an increased prevalence of coinfection in children younger than five years old (20). In a study focusing on children < 5 years old in South Africa, coinfection rates of respiratory syncytial virus (RSV) infection were 51.1% (25). Enteroviruses and rhinoviruses were the most commonly co-detected viruses with human metapneumovirus (HMPV) when the sample population included all age groups and community/hospital-based specimens (26). However, when the population demographic was narrowed down to younger, hospitalized patients, the most common co-detected virus with HMPV was RSV (27) or HBoV (28). These studies imply that patient demographics may bias which coinfections are detected and the prevalence of each coinfection. It will be difficult to understand the true scope of respiratory viral coinfection until a universal sampling method is utilized.

### 1.3 Improvements in respiratory pathogen detection

Respiratory viral coinfection has become more recognized as a common occurrence because of relatively recent improvements in viral detection methods. Classically, viral pathogens were screened using various *in vitro* cell culture and immunofluorescence methods. These techniques are time-consuming, heavily rely on available reagents for identification and are often limited to identifying single pathogens in a sample. Classical techniques have since been improved upon by the use of quantitative polymerase chain reaction (qPCR) and, more recently, multiplex qPCR. Multiplex qPCR allows for testing of multiple pathogens simultaneously in a single specimen. Using multiplex qPCR increases the detection rates of viral pathogens while identifying unique strains within a family missed by conventional methods (29, 30). Larger multiplex qPCR kits are being developed to screen for more pathogens while also increasing test sensitivity for accurate pathogen identification (31, 32). One drawback of these highly sensitive techniques is the identification of viral genetic material from a previous infection (33-36). Identification of persistent viral genetic material can confound the identification of current viral infections and interfere with determining how coinfection affects disease severity. It is difficult to determine between a current, previous, and latent infections, which could change the question of how respiratory viral coinfection affects disease severity to how a previous infection with one virus can predispose the immune response to respond differently during a new infection. It may be more prudent to combine virus identification methods and culture samples alongside multiplex qPCR assays. This combination approach would help investigators tease out current infections and identify how current viral coinfections may affect disease compared to single virus infections.

### 1.4 Coinfections alter disease severity compared to single virus infections

Viral coinfection is a concern because it has been documented to alter disease severity compared to individual viral infections (8, 13, 22, 25, 37-42). It is unclear how coinfection affects disease severity and what parameters drive these changes. Changes in

disease severity could be due to sample population demographics or dependent upon the specific viruses involved in coinfection. Below are examples from the literature that demonstrate the relationship between respiratory viral coinfection and disease severity.

**Disease exacerbation**

Arguably the most worrisome effect of respiratory viral coinfection is when coinfection exacerbates disease compared to individual virus infections. Many studies implicate coinfection with RSV increasing disease severity compared to its partnered coinfection virus alone. Children coinfected with both human rhinovirus (HRV) and RSV are more likely to belong to a high-risk group (37) and chances to develop severe lower respiratory tract disease increase compared to single HRV infection (38). Another group determined that HRV and RSV coinfection significantly increased bronchiolitis severity and admission to the pediatric intensive care unit (PICU) compared to single virus infections (39). Similar to HRV and RSV coinfection, RSV and HMPV coinfection increases the likelihood of admittance to the PICU compared to either HMPV or RSV single infection (40). Obstructive airway disease is increased in infants coinfected with adenovirus (AdV) and either RSV or HRV compared to single AdV infections (38). Exacerbated disease during coinfection goes beyond the involvement of RSV and can include a plethora of infections. Coinfections involving parainfluenza virus 3 (PIV-3), IAV, AdV, HMPV, and HBoV are all associated with an increase in hospitalization compared to their single virus counterparts (25). These studies reveal that one virus may play a dominant role in determining the medical outcome for a patient during coinfection.

**Disease attenuation**

Respiratory viral coinfection can also reduce disease severity compared to single virus infections. One epidemiological study in Spain determined that infections with multiple viruses resulted in decreased hospital admission and oxygen treatment (13). Other studies claim HRV and RSV coinfection reduces hospitalization duration compared to single virus infections (25, 41). Although not correlated with disease severity, coinfection with either AdV or parainfluenza virus 1 (PIV-1) reduces the viral load of both AdV and PIV-1 compared to their single virus infections (8). Martin *et al*. also determined that coinfection reduced the hospitalization admittance/duration and oxygen treatment compared to patients

with single infections. Lastly, coinfection with HRV and IAV reduces hospitalization and oxygen use compared to single IAV infections (22, 42). Interestingly, Esper *et al.* found HRV and IAV coinfection did not affect IAV titers, similar to Martin *et al*., but Pascalis *et al.* reported that this coinfection decreased IAV shedding compared to single IAV infections. These studies report conflicting data on whether coinfection increases or decreases disease severity.

**No change in disease**

Coinfection has been well-documented to alter disease severity compared to single virus infections, but other studies report that coinfection also does not affect disease severity. No significant differences in hospitalization or oxygen treatment were detected in patients under 14 years old with single infections compared to coinfections (23, 43). A group in Taiwan found respiratory viral coinfection did not significantly change any clinical symptoms associated with acute lower respiratory tract infections compared to single virus infections (44). Interestingly, although other studies implicate RSV coinfection in increasing disease severity and IAV coinfection reducing disease severity, the titer of neither virus is affected by coinfection compared to single infection (45). RSV and IAV viral loads are at equivalent levels during single and coinfection, regardless of age or being immunocompromised. To help corroborate this, another group found no significant differences in patients with single virus infections versus coinfections when hospitalization and treatment were assessed (46). This was interesting because this study identified 20 out of 54 coinfections involved RSV and HRV. Another study found that RSV and IAV coinfection did not increase the risk for lower respiratory tract infections compared to single virus infections (47). Yoshida *et al*. expanded this further and reported that IAV coinfection, in general, did not increase the likelihood of a lower respiratory tract infection. Finally, one report assessed coinfection during the H1N1 influenza outbreak of 2009 and found no differences in clinical cases between H1N1 2009 coinfection or seasonal IAV coinfection compared to their respective single virus infections (48).

Altogether these data paint a contradicting picture of coinfection and its effects on disease severity. RSV has been reported to increase, decrease, and cause no change to disease severity compared to single virus infections. These contradictions may be dependent

upon the age of the patient, location of the study, or on what viruses were assessed. This could also be due to qPCR results picking up RNA remnants of previous infections and not representing a true coinfection. More information, including larger population studies with increased sampling frequency to monitor disease progression, is needed to understand how coinfection affects disease severity.

### 1.5 Viruses utilized in these studies

We are interested in coinfections involving HRV, RSV, IAV, and coronaviruses (CoV) because these viruses are commonly found in single and multiple respiratory tract infections. It is common for HRV to coinfect with either RSV (14, 47) or IAV (20, 21). The studies referenced above reported mixed effects on disease severity for HRV and RSV coinfections. However, HRV and IAV coinfections seem to decrease IAV-induced disease severity compared to single virus infections. One explanation is that HRV is reported to interfere with IAV infection and subsequent spread of IAV pandemics (49, 50). This implies that an initial infection with HRV can stimulate an immune response, creating a more inhospitable environment for a secondary viral infection. This could also be highly dependent on the specific immune arms recruited and if those responses are effective or not at clearing the second pathogen. Coinfection with CoV is interesting because of the prevalence of co-detecting a second viral pathogen during a CoV infection. CoV coinfection rates are reported between 59-70% of CoV-positive infections (19, 51). Our investigation will use a minor group rhinovirus, mouse-adapted IAV, pneumonia virus of mice (PVM), and murine hepatitis virus strain 1 (MHV). Mice are not susceptible to major group HRV because of receptor incompatibility, but minor group rhinovirus 1B (RV) can infect and elicit an immune response in mice (52). IAV is also not a natural mouse pathogen, but influenza virus A/PR/8/34 (H1N1) (PR8) has been mouse-adapted and causes dose-dependent disease severity in mice (53). PVM is a mouse pathogen closely related to RSV and is commonly used to investigate severe RSV-related mechanisms using mice as a model (54). Finally, we will use the respiratory-tropic strain of MHV (strain 1) as a model coronavirus (55). We will use these viruses to establish a mouse model of respiratory viral

coinfection to investigate how coinfection can manipulate the immune response to alter disease severity.

### 1.6 Viral recognition

One potential mechanism for coinfection-mediated disease attenuation is faster recognition of a secondary virus infection. The first step to eliciting an immune response against a pathogen is recognition by pattern recognition receptors (PRR). PRRs are groups of receptors that recognize specific pathogen-associated molecular patterns. When these receptors bind their pathogen-associated molecular patterns (PAMP), the innate immune system is alerted to the presence of a pathogen via cytokine and chemokine production. RV, MHV, PVM, and PR8 are all recognized by PRRs on epithelial cells and innate immune cells such as macrophages and dendritic cells. Some PRRs are shared between these viruses, while others are unique to each virus. Stimulation of these PRRs with multiple PAMPs from each virus may help supplement and coordinate the immune response during coinfection.

Shared activation of PRRs could help the immune system overcome inhibitory mechanisms associated with viruses. Plasmacytoid dendritic cells (pDCs) use endosomal toll-like receptor (TLR) 7 to recognize viral pathogens. Once TLR7 is activated, pDCs will begin producing type I interferon (IFN). TLR7 recognizes IAV, PVM, and mouse hepatitis virus strain A59 in pDCs (56-60). Similarly, RV and mouse hepatitis virus type 3 (MHV3) activate TLR2 on the surface of macrophages (61, 62). Activation of innate immune cells could help increase presentation to adaptive immune cells resulting in increased control of viral infection.

Epithelial PRRs also recognize these viruses. The dominant PRR during IAV infection of primary and transformed alveolar epithelial cells is retinoic acid-inducible gene I (RIG-I) (63). RIG-I knockout in mice delays clearance of PR8 and increases mortality associated with infection (64). RV infection in mice induces RIG-I expression (65), but induction of type I and III IFNs is debatable (65, 66). There is evidence of PVM nonstructural proteins causing ubiquitination of RIG-I, leading to its degradation (67). PVM may activate RIG-I signaling mechanisms during infection, but the virus has developed an

effective means for controlling this response. Other epithelial PRRs activated by RV and IAV infection are TLR3 (63, 66, 68) and melanoma differentiation-associated gene 5 (MDA5) (66, 68-70). These receptors contribute to type I and III IFN production during RV and IAV infection. Lastly, MHV and RSV infection, which is closely related to PVM, induces expression of TLR4 and the loss of TLR4 signaling fails to control RSV (71) and increases MHV mortality (72) in mice. However, no differences are observed in PVM-induced disease between wild type and TLR4 knockout mice during PVM infection (73). Inducing expression of shared PRRs could increase the likelihood of recognizing a second virus during coinfection.

Not only do these viruses have shared PRR activation, but activation of some PRRs is unique to each virus. HRV infection in human epithelial cells stimulates the production of interleukin-6 by activation of TLR2, 7, and 8 pathways (69). Infection with MHV3 stimulates TLR2 signaling in macrophages, but MHV3 TLR2 activation also occurs in endothelial cells (74). Finally, various strains of mouse hepatitis virus induce cytokine production from macrophages by stimulating MDA5 activation (75). This stimulation of PRRs unique to each virus infection can help supplement immune responses to unrelated viruses.

Immune responses are initiated by PRR recognition of viral pathogens. Our viruses activate TLR2, 3, 4, 7, RIG-I, and MDA5 signaling during infection in various cell types. This shared signaling could benefit coinfection by increasing the numbers of PRRs expressed in the cells while also initiating shared pathways for cytokine production. This increases the chances of detecting and controlling a second virus. Activation of cytokine production by unique PRRs helps supplement immune responses because it can bypass the inhibitory effects on PRR signaling observed during PR8 and PVM infections. Production of IFNs and cytokines are initiated by many PRRs, and increasing the number of potential signaling pathways could help control a secondary virus infection during coinfection.

### 1.7 Murine model for human viruses

We are using RV, PR8, PVM, and MHV in our model of coinfection because they represent common viruses found in coinfection of humans. Not only do they represent common coinfecting viruses, but these four unrelated viruses elicit varying degrees of respiratory pathogenesis in mice.

Since mice have no known rhinoviruses, investigators use RV (strain 1B) to study rhinovirus infections (52, 76, 77). RV is a minor group rhinovirus that uses the low-density lipoprotein receptor (LDLR) to enter respiratory epithelial cells (52, 78). Major group rhinoviruses are restricted to using human intercellular adhesion molecule 1 as a receptor, whereas minor group rhinoviruses use the LDLR in both mice and humans. RV infection in mice generates a rapid production of type I and III interferon, chemokines, inflammatory cytokines, and mucin. Shortly after infection of airway epithelium, neutrophils migrate into the airways followed by lymphocytes. RV RNA and viral load decline within 24 hours of inoculation (52). Although RV does not establish a lasting infection in mice, it provides the best model for studying rhinovirus infection in a mouse model.

Influenza viruses are not natural pathogens of mice. To study influenza-induced disease, PR8 has been adapted to mice by serial passaging. PR8 creates dose-dependent disease severity in mice where higher doses induce more severe pathology. The primary sites of infection for IAV are respiratory epithelia, including bronchiolar and alveolar epithelia (79, 80). After a lethal dose of PR8 induces rapid production of chemokines and inflammatory cytokines correlating with an early peak in viral load (53, 81). Initially, neutrophils and macrophages are the first responding cell types in the lungs after infection. Then T lymphocytes migrate to the lungs with PR8-specific CD8 T cells increasing as viral titers decrease (82). Infected lungs are marked by severe pulmonary inflammation, lesions on the lungs, and edema (80). Late stage PR8 infection is associated with diffuse alveolar damage and acute respiratory distress.

MHV is used as a model of severe acute respiratory syndrome-associated coronavirus (SARS-CoV) in A/J mice and a milder form of SARS-CoV in BALB/c mice (55, 72, 83). MHV replicates in primary alveolar epithelial cells (84) and a transformed murine lung epithelial cell line *in vitro* (85). High numbers of MHV virions were detected

within macrophages by electron microscopy (55). MHV infection is associated with extensive macrophage recruitment, severe pulmonary inflammation, and late-stage hyaline membrane formation and fibrin deposition. Cytokines remain elevated during infection, correlating with mortality (55). However, MHV infection in BALB/c mice induces pulmonary inflammation and recruitment of inflammatory cells into the airways before eventual clearance of the virus and survival (55, 72). Using BALB/c mice and lower doses of MHV can be beneficial for studying severe coronavirus infections.

PVM is a natural mouse pathogen used to study severe RSV infections in BALB/c mice (86). PVM initially replicates in alveolar epithelial cells before progressing to bronchiolar epithelial cells at later time points (87). PVM infection induces pulmonary inflammation and edema with infiltration of macrophages before neutrophils at higher inoculation doses (88). Early cytokine production is induced using high dose PVM, but lower doses of PVM delays cytokine production. Increased cytokine production correlated with higher histopathology scores and inflammatory cell infiltration. PVM replicates to high levels in mice, but peak titer is reached early before plateauing for several days.

### 1.8 Current research on respiratory viral coinfection

Respiratory viral-viral coinfections are poorly understood, and the literature does not reflect many studies focusing on this topic. Many studies focus on how viral-bacterial coinfections affect disease severity (89-91). However, some studies discuss the implications of viral-viral coinfections within different model organisms. One of the earliest studies of respiratory viral coinfection found that initial infection with a mouse hepatitis virus (not strain 1) delayed seroconversion to a subsequent PVM infection along with a reduction of PVM specific antibody levels (92). This group also used an initial mouse hepatitis virus infection to reduce Sendai virus-induced mortality dramatically. Another group studied viral coinfection between IAV and RSV in mice. IAV inoculation 24 hours before, simultaneously with, or 24 hours after RSV reduces histopathology associated with either IAV or RSV single infections (93). Attenuation of pulmonary inflammation is associated with an increase in early NK and CD4 T cell recruitment and reduced cytotoxic T cells

compared to controls. Reduction in cytotoxic T cells could be limiting damage to alveoli while increased CD4 T cells could be regulating inflammation in these mice.

Coinfection with RSV and IAV has also been studied using a ferret model. Pre-infection with IAV three days before RSV prevents RSV infection, whereas pre-infection with IAV seven days before RSV only reduces the level of RSV infection (94). Interestingly, pre-infection with RSV at any time point before IAV does not alter the establishment of PR8 infection but reduces IAV-induced disease. These effects are associated with IAV infection inducing a stronger proinflammatory response, which could limit RSV infection. Coinfection of weanling pigs with porcine reproductive and respiratory syndrome virus ten days before porcine respiratory coronavirus increases fever and pneumonia compared to single virus infections (95). Exacerbation of disease severity is linked to an attenuated interferon-α response and NK cell activity. Coinfection is also associated with a shift to T-helper 1 responses and a decrease in T-helper 2 responses.

Further research is necessary to understand how respiratory viral coinfection can alter immune responses to be protective versus detrimental to the host. Respiratory viral-viral coinfections are reported to affect disease severity compared to individual virus infections in humans. *In vivo* models of viral coinfection find that certain virus pairings prevent a secondary virus infection while other virus pairings only reduce disease severity of a second virus infection. Changes to inflammatory responses and lymphocyte responses are thought to be the mechanism of action underlying the effects of coinfection. However, other cell types may play a critical role, orchestrating the switch to a less detrimental role for adaptive immune responses. It is necessary to investigate the roles of the early innate immune responses and how these responses influence the progression of disease during coinfection. These studies also used pathogenic viruses as model viruses for coinfection. We are interested in studying if a mildly virulent virus, one that causes little to no disease, could protect the host from a highly virulent virus.

# CHAPTER 2

# Materials and Methods

## 2.1 Virus stocks and cell lines

Madin-Darby canine kidney cells (MDCK) (ATCC CCL-34), murine fibroblast line 17Cl.1 (provided by Dr. Kathryn Holmes, University of Colorado Denver School of Medicine), murine fibroblast line L929 (provided by Dr. Wendy Brown, Washington State University), and HeLa cells (ATCC CCL-2) were grown in Dulbecco's modified Eagle medium (DMEM) supplemented with 10% fetal bovine serum (FBS; Atlanta Biologicals), and 1X antibiotic-antimycotic (ThermoFisher). Murine lung epithelial cells (LA-4) (ATCC CL-196) were grown in Ham's F12 (Kaign's modified) medium (F12K; Caisson) supplemented with 10% to 15% FBS and antibiotics. Murine alveolar macrophages (MH-S) (provided by Dr. Santanu Bose, Washington State University) were grown in RPMI 1640 (RPMI) medium supplemented with 10% FBS and antibiotics. Baby hamster kidney cell line (BHK) (provided by Dr. Kathryn Holmes, University of Colorado Denver School of Medicine) were grown in minimal essential media (MEM) supplemented with 10% FBS and 1X antibiotics. Influenza A virus PR8 (A/Puerto Rico/8/1934 [H1N1]), obtained from BEI Resources (NR-3169), was grown and titrated by 50% tissue culture infectious dose ($TCID_{50}$) assay in MDCK cells. Mouse hepatitis virus MHV-1 (ATCC VR-261) was grown and titrated by plaque assay in 17Cl.1 cells. Rhinovirus RV1B (ATCC VR-1645) was grown and titrated by $TCID_{50}$ assay in HeLa cells. RV1B stocks were concentrated by centrifugation through 30% sucrose, and the virus pellet was resuspended in phosphate-buffered saline containing 2% FBS (PBS/2% FBS). Pneumonia virus of mice (PVM) strain 15 (ATCC VR-25) was grown and titrated by $TCID_{50}$ assay in BHK cells. Vesicular stomatitis virus expressing green fluorescent protein (VSV-GFP) (provided by Dr. Victor DeFilippis, Oregon Health and Science University) was grown and titrated by $TCID_{50}$ assay in BHK cells.

**2.2 Mouse infections**

All experimental protocols were approved by the University of Idaho Institutional Animal Care and Use Committee, following the *Guide for the Care and Use of Laboratory Animals* (206). As described below, mice were monitored daily and were euthanized by an overdose of sodium pentobarbital if they reached humane endpoints.

Six-to-eight-week-old female BALB/c mice were purchased from Harlan Laboratories/Envigo. Mice were housed in individually vented cages with controlled light/dark cycles and regulated temperature maintained by University of Idaho Lab Animal Research Facilities and received food and water *ad libitum*. The mice were allowed to acclimatize to the facility for five to 12 days before experiments were performed under animal biosafety level 2 (ABSL2) conditions. Mice were anesthetized with inhaled isoflurane and inoculated intranasally with 50 µl of the virus. The following inoculation scheme was used:

| Coinfection | Day -2 | Day 0 | Day 2 |
|---|---|---|---|
| RV/Mock | RV | Mock | |
| Mock/PR8 | Mock | PR8 (Low, Med, Hi) | |
| RV/PR8 | RV | PR8 (Low, Med, Hi) | |
| RV/PVM | RV | PVM | |
| RV/MHV | RV | MHV (Severe) | |
| MHV/Mock | MHV | Mock | |
| MHV/PR8 | MHV (mild, moderate, severe) | PR8 | |
| MHV/PVM | MHV | PVM | |
| RV+PR8 | | RV and PR8 (Low, Med) | |
| PR8/RV | | PR8 | RV |
| RV+PVM | | RV and PVM | |
| PVM/RV | | PVM | RV |

**Table 2.1. Respiratory viral coinfection scheme.**

Control mice received mock inoculations of the same buffer or medium used for the respective virus: RV (PBS/2% FBS), PR8 (DMEM/1% bovine serum albumin [BSA]), PVM

(DMEM/2% FBS), or MHV (DMEM/10% FBS). See results and figure legends for viral doses and the number of mice used in each experiment.

Mice were weighed and observed for clinical signs of disease daily and were humanely euthanized if they lost more than 25% of their starting weight or exhibited severe clinical signs of disease. Mice were given a daily severity score of 0 to 3 in each of four categories: ruffled fur, lethargy, labored breathing, and hunched posture. The daily scores were totaled for each mouse and averaged across the group of mice.

### 2.3 *In vitro* coinfection

LA-4 cells were inoculated with RV (multiplicity of infection [MOI] of 1 or 2) either 2, 6, or 12 hours before or simultaneously with PR8 (MOI of 1 or 2). After 1 hour of incubation with the inoculum, cells were washed twice with serum-free medium and then incubated in Ham's F12K medium with 2% FBS and antibiotics at 37°C. The supernatant medium was collected from the cells at 6, 12, 18, 24, 48, 72, and 96 h after PR8 inoculation, and PR8 was titrated by $TCID_{50}$ assay using MDCK cells.

LA-4 cells were inoculated with PR8 (MOI of 1 or 2) either 6 or 12 hours before or simultaneously with RV (MOI of 1 or 2). After 1 hour of incubation with the inoculum, cells were washed twice with serum-free medium and then incubated in Ham's F12K medium with 2% FBS and antibiotics at 37°C. The supernatant medium was collected from the cells at 6, 12, 18, 24, 48, 72, and 96 h after RV inoculation and RV was titrated by $TCID_{50}$ assay using HeLa cells.

MH-S cells were either inoculated with RV (MOI of 1) 12 hours before PR8 (MOI of 1) or, the reverse, PR8 (MOI of 1) 12 hours before RV (MOI of 1). After 1 hour of incubation with inoculum, cells were washed once with serum-free medium and then incubated in RPMI medium with 2% FBS and antibiotics at 37°C. The supernatant medium was collected from cells 24 hours after secondary virus inoculation. $TCID_{50}$ assay was used to titrate RV (HeLa cells) and PR8 (MDCK cells).

### 2.4 PR8 quantification

Right lobes of the lungs were flash-frozen and stored at -80°C. Frozen tissues were weighed and homogenized in DMEM with 2% BSA and 1% antibiotics, and PR8 was quantified by $TCID_{50}$ assay on MDCK cells (96).

We tested if the presence of RV or MHV would interfere with the titration of PR8 in coinfected samples. We performed a 1:2 dilution of PR8 with either media, RV, or MHV. Then quantified PR8 by $TCID_{50}$ assay on MDCK cells. We found no significant differences between PR8 combinations with media (Mock/PR8), RV (RV/PR8), or MHV (MHV/PR8) (Table 2.2). We also inoculated MDCK cells with RV and MHV and we did not observe any cytopathic effects in MDCK cells with either virus.

| | Mock/PR8 | RV/PR8 | MHV/PR8 |
|---|---|---|---|
| PR8 Titer | 2.10E+06 | 3.48E+07 | 1.96E+07 |

**Table 2.2. Titration of PR8 when mixed with media, RV, or MHV.**

### 2.5 Histology

The tracheas of euthanized mice were cannulated, and the lungs were inflated with 10% formalin before submerging the lungs in 10% formalin. After fixation, lungs were embedded in paraffin, cut in 5-µm sections, and stained with modified Harris hematoxylin and eosin (VWR Scientific).

### 2.6 Flow cytometry

Left lobes of lungs were incubated in RPMI containing 1 mg/mL type IV collagenase (MP Biomedicals) and 0.5 mg/mL DNase (Spectrum) for one hour. Lobes were manually homogenized during incubation before passing through a 70 µm strainer. Red blood cells were lysed before blocking Fc receptors using TruStain fcX αCD16/CD32 (BioLegend). Cells were stained for 20 minutes in 96-well plate in 100 µL volumes of flow cytometry staining buffer (PBS/1% BSA/0.1% sodium azide) containing the following antibodies: αCD11b-Alexa Fluor 488 (cat #53-0112-82), αLy6G-APC (cat #17-9668-82), αCD3-PerCP-Cy5.5 (cat #45-0031-82), αCD8-APC (cat #17-0083-81) all from eBiosciences; αCD64-PE (cat #139304) and αCD4-Alexa Fluor 488 (cat #100423) from BioLegend; and αSiglecF-

PerCP-Cy5.5 (cat #565526) from BD Biosciences. Stained cells were incubated in BD Stabilizing Fixative (BD Biosciences) for 30 minutes before replacing with flow cytometry staining buffer. Cells were analyzed using BD FACS Aria (BD Biosciences). Gates were made with FlowJo software (Treestar, Costa Mesa, CA).

| Cell type | Antibodies |
|---|---|
| Neutrophil | CD11b+ Ly6G+ |
| Activated neutrophil | CD11b+ Ly6G+ CD64+ |
| Interstitial macrophage | CD11b+ Ly6G- CD64+ |
| Alveolar macrophage | CD11b- CD64+ SiglecF+ |
| CD8 T cell | CD3+ CD8+ |
| CD4 T cell | CD3+ CD4+ |

**Table 2.3. Immune cell surface markers.**

### 2.7 Type I interferon bioassay

Samples for bioassay were cell-free lavage fluid (days 4 and 7) and lung homogenates (day 2). Cell-free lung homogenates and lavage fluid were added to a 96-well plate and UV-inactivated using a 2000 J/$m^2$ dose (LabX Stratagene Stratalinker 1800). Sodium pyruvate was added to each well to quench free radicals. Samples were diluted by serial 2-fold dilutions down the plate, followed by addition of $3.0x10^4$ L929 cells to each well, and the plate was incubated for 24 hours at 37°C and then cell media was replaced with VSV-GFP inoculum at MOI of 10. Cells and inoculum were incubated for 24 hours at 37°C. Wells were then washed with PBS and fluorescence was analyzed using BMG Labtech FLUOstar OPTIMA. Data were normalized to positive virus control (no type I interferon present) and displayed as 2-fold dilution versus fluorescence.

### 2.8 Quantitative RT-PCR

Lung tissue was stored in RNALater, and RNA was extracted using TRIzol (Invitrogen) or RNeasy Plus (Qiagen) according to the manufacturer's recommendations. One microgram of RNA was reverse transcribed using SuperScript IV VILO with ezDNase digestion

(Invitrogen). Quantitative PCR was performed using PowerUp SYBR green and the StepOne Plus instrument (Applied Biosystems) using previously published IFN-β (97), glyceraldehyde-3-phosphate dehydrogenase (GAPDH) (98), and interferon-induced GTP-binding protein Mx1 (Mx1) (99) primer sets. Fold change compared to the values for mock-inoculated mice was calculated using the $2^{-\Delta\Delta Ct}$ method (100).

**2.9 TNF-α protein quantification**

TNF-α enzyme-linked immunosorbent assay (eBioscience) was performed on BAL fluid samples (collected in the same fashion as for IFN Bioassay (2.7)).

**2.10 Neutrophil depletion**

Neutrophil depletion was accomplished by administering the antibody specific to mouse Ly6G clone 1A8 (Bio X Cell) or rat IgG2a isotype control antibody (52). Mice initially received 0.5 mg of 1A8 or isotype control antibody intraperitoneally (i.p.) one day before RV inoculation. On day -2, 0.2 mg of 1A8 or isotype control antibody was delivered intranasally with RV. Neutrophil depletion was then maintained by administering 0.2 mg 1A8 or isotype control antibody on days -1, 1, and 3 i.p. in respect to PR8 inoculations.

**2.11 Bronchoalveolar lavage cell counts**

To ensure neutrophil depletion did occur, we counted cells from BAL samples. Lungs were inflated with 1 mL PBS and then lavage fluid was collected and counted recovered cells. Samples were centrifuged to pellet cells for resuspension in red blood cell lysis solution. Cells were then spun onto a glass slide and stained using PROTOCOL HEMA 3 Stain Set (PROTOCOL). Cells were then categorized into cell types based on staining and converted to percentage of each cell type based on total cells counted.

**2.12 Block of type I interferon receptor**

Type I interferon signaling was blocked by administering the antibody specific to type I interferon α/β receptor clone MAR1-5A3 (IFNAR, Bio X cell) or mouse IgG1k isotype control antibody (171). Mice were intranasally administered 0.05 mg MAR1-5A3 or isotype control antibody with RV on day -2 and again with PVM on day 0.

### 2.13 $RT^2$ profiler PCR array

RNA was isolated from mouse lung tissue stored in RNAlater using QIAamp Viral RNA Mini Kit from QIAGEN (cat #52904). General RNA screen was performed using the $RT^2$Profiler PCR Array System from SA Biosciences (cat #1022A). Data are expressed as RV/PR8 coinfection gene expression fold-increase compared to Mock/PR8 single infection.

### 2.14 RNAseq

RNAseq samples were prepared and analyzed as described in Van Leuven *et al.*, currently in preparation for publishing.

### 2.15 Statistics

Statistical analyses were performed using GraphPad Prism 7 software. Survival curves were compared using log-rank Mantel-Cox curve comparison. Weight loss and clinical score data were compared using multiple Student's *t*-tests. PR8 titers from mouse lungs, cell culture experiments, recruited immune cells, and RT-qPCR results were compared using Student's *t*-tests without correction for multiple comparisons.

# CHAPTER 3

# Effects of Coinfection on Influenza A Virus and Rhinovirus Replication *In Vitro*

## 3.1 Overview

Our bodies are constantly assaulted by viruses that routinely manipulate their environments to ensure replicative success. This creates opportunities for related or unique viruses to interact while attempting to establish an infection. These viral interactions contribute to the phenomenon known as viral interference. Viral interference occurs when a cell infected by one virus becomes less susceptible to infection (or re-infection) by another virus. This response is not limited to individual cells but can be conveyed to entire organs as well. Stimulation of interferon-regulated pathways (101), antigenic presentation (102), or down-regulation of viral receptors on a cell's surface (103) are all mechanisms of interference.

Evidence of viral interference among respiratory viruses has been widely established through epidemiological studies tracking seasonal virus circulation. Recent interest has been focused on epidemic H1N1 influenza infections and delays in circulation. Many studies report findings of HRV circulation coinciding with the delay in epidemic influenza circulation. These studies have been conducted in countries across the world: China (104), Norway (49), France (105), and Sweden (106). The global scope of this interference is important because it indicates this is not an isolated event that is unrepeatable, but a small-scale viral arms race that has many recorded incidences across several years. Another group reported that HRV was not limited to interfering with influenza circulation but hindered the circulation of other seasonal respiratory viruses (50). It is also possible for a previous virus infection to generate a strong enough immune response within a population to prevent re-infection of the population for subsequent years. One outbreak of adenovirus in China generated a strong antibody response among the infected population, causing a two-year delay before adenovirus circulation returned to normal (104).

These studies provide evidence for viral interference occurring at the population-level, but there is also evidence for interference at the tissue-specific level using *in vitro* methods. Human lung epithelial cells and canine kidney cells were simultaneously coinfected with H5-mCherry IAV and either H1-GFP or H5-GFP IAV. Coinfection with H1-GFP and H5-mCherry resulted in lower GFP expression in both cell lines compared to coinfection with H5-GFP and H5-mCherry (107). Not all viral interactions are detrimental to the virus. Simultaneous coinfection of African green monkey kidney cells with IAV and human parainfluenza virus type 2 resulted in increased IAV titers compared to single virus controls (108). Coinfection increased influenza titers because parainfluenza virus stimulates cell-cell fusion, allowing IAV to spread easily to neighboring cells. Evidence of viral interference has also been established in more controlled studies using *in vivo* models. Using a ferret model, primary IAV infection prevents a secondary infection by an influenza B virus (IBV) when viruses are inoculated 1, 3, 5, or 7 days apart (109). Similarly, primary infection with IAV in ferrets prevents a secondary infection by RSV when viruses were inoculated 3 or 7 days apart (94). IAV may be interfering with secondary viral infections by inducing a strong proinflammatory response, including the production type I IFN. These *in vitro* and *in vivo* data, demonstrate that IAV can interfere with the replication of related and unrelated viruses.

Another viral mechanism of interference is superinfection exclusion (SIE). SIE is similar to viral interference, but SIE refers to an initial virus infection interfering with the establishment of a second identical or similar virus infection. SIE of hepatitis C virus *in vitro* using human cell lines has been well-documented. Studies suggest that interference occurs after viral entry into the cell and is active at the viral replication step (110, 111). The influenza neuraminidase (NA) glycoprotein is a known mediator of SIE. Influenza hemagglutinin (HA) binds sialic acids on cellular membranes to gain entry into a cell, and NA limits superinfection by cleaving these sialic acids, thus preventing influenza HA from binding its receptor (112). Cleavage of sialic acids by NA inhibits entry of a secondary influenza virus and pseudotyped retroviruses expressing HA. Treatment of IAV with NA-inhibitors restored the ability for the secondary virus to establish infection and propagate. Sindbis virus infection in mosquito cells reduces replication of both homologous viruses and closely-related arenaviruses when the viruses are cultured together i*n vitro* (113). The

nonstructural alphavirus protease from the initial infection may be cleaving viral proteins required for minus-strand RNA synthesis during the secondary virus infection. Citrus tristeza virus also demonstrates that SIE during infection of citrus trees is through mechanisms dependent upon the virus' p33 protein, a virus membrane component involved in stimulating the release of reactive oxygen species during infection (114, 115). SIE across a broad host range suggests that this is not a mechanism utilized solely by pathogens of vertebrates, but a mechanism that has developed and refined over a long period.

Taken together, these studies demonstrate that viral interference is not as simple as one virus establishing an infection before another virus, but rather a complex network of interactions that lead to adverse or even beneficial effects depending on which viruses are coinfected together. Because HRV infection is proposed to interfere with pandemic IAV circulation, we are interested if this viral interference is dependent upon the host immune system or SIE mediated through viral infection. To test this, we used a cell line, LA-4, susceptible to both RV (116) and IAV (117) as a model for *in vitro* coinfection. Both viruses were inoculated simultaneously with, and 2-, 6-, and 12-hours apart from each other and viral titers measured at various time points post-infection. Any changes in viral titers during coinfection compared to single virus infections would inform some role of viral interference, e.g., competition or decreased susceptibility to a secondary infection. If no changes are measured, then the immune system is required to inhibit secondary viral infections. This distinction is imperative to understanding the model of respiratory viral coinfection because it will provide insight into what mechanisms control attenuation or exacerbation of disease severity during coinfection.

## 3.2 Results

### 3.2.1 Pre-infection with RV did not affect PR8 replication *in vitro*

We wanted to determine if RV can interfere with IAV growth kinetics during coinfection. Potential routes of interference are competition for susceptible cells, variable surface expression of virus receptors, or exclusion of infection by inducing innate immune mechanisms. To test if RV interferes with PR8 replication *in vitro*, we inoculated the murine

lung epithelial cell-line, LA-4, with either Mock (media) or RV (MOI=1) simultaneously with, 2, 6, or 12 hours before inoculation with PR8 (MOI=1). Infected LA-4 cells were incubated for 48 to 96 hours, and media overlaying the monolayer were collected at 6, 12, 18, 24, 48, 72, and 96 hours post-inoculation (hpi). PR8 was titrated by $TCID_{50}$ assay on MDCK cells.

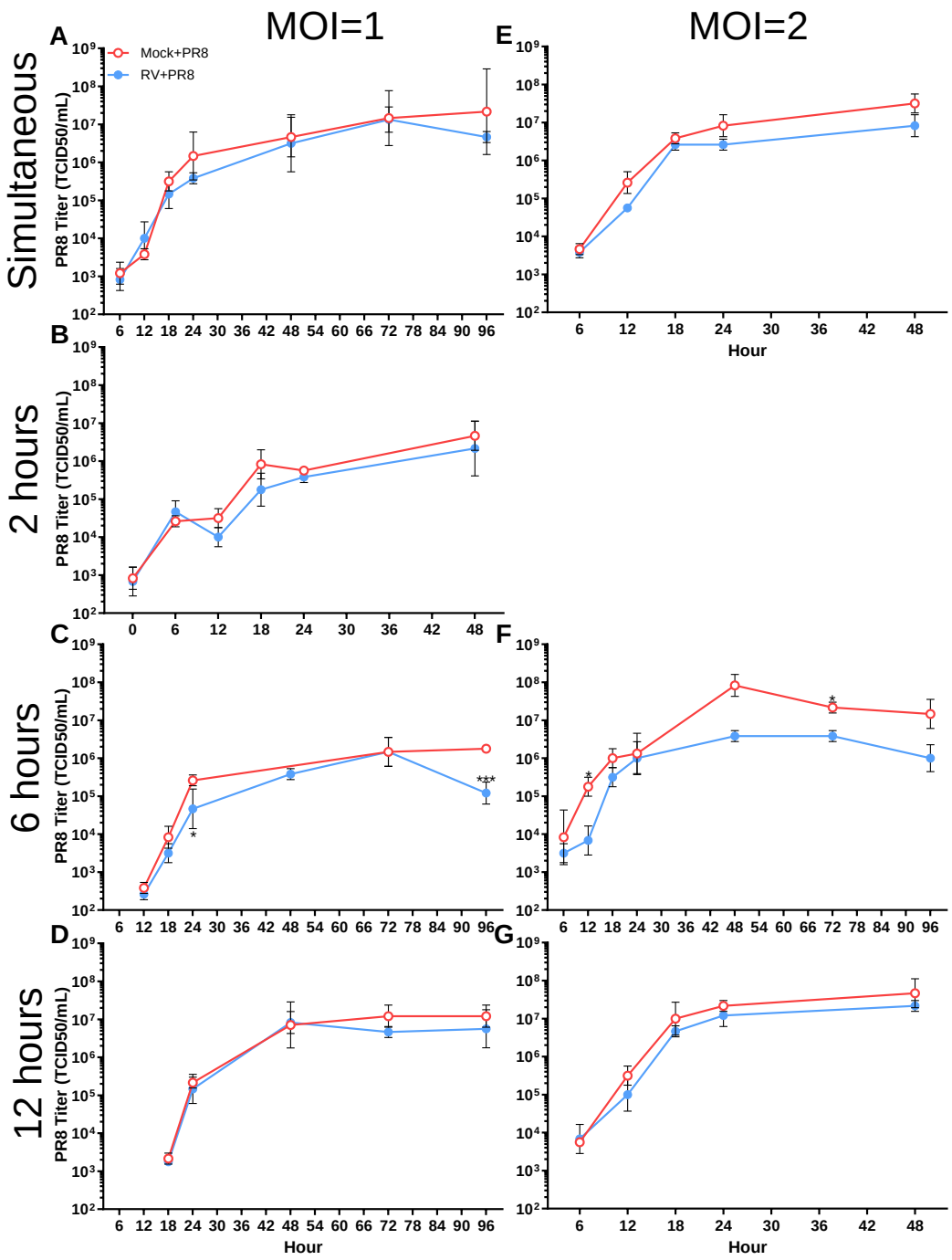


**Figure 3.1. PR8 replication was not affected by coinfection with RV.** LA-4 cells were either inoculated with Mock (media) or RV 2, 6, or 12 hours before or simultaneously with PR8. Cells were incubated for 48-96 hours, and media were collected at 6, 12, 18, 24, 48, 72, and 96 hours post-inoculation, and PR8 was quantified by $TCID_{50}$ assay on MDCK cells. PR8 titer from single infected cells (Mock+PR8) is open, red circles and PR8 titer from coinfected cells (RV+PR8) is closed, blue circles. A) Simultaneous coinfection; MOI=1. B) RV inoculated 2 hours before PR8; MOI=1. C) RV inoculated 6 hours before PR8; MOI=1. D) RV inoculated 12 hours before PR8; MOI=1. E) Simultaneous coinfection; MOI=2. F) RV inoculated 6 hours before PR8; MOI=2. G) RV inoculated 12 hours before PR8; MOI=2. Significance versus Mock/PR8 was determined by unpaired Student's *t*-test of triplicate samples. P-values are shown by * ≤ 0.05 or *** ≤ 0.001.

PR8 replication was unaffected by coinfection in a mouse lung epithelial cell-line with RV at multiple timings. Initially, we tested how simultaneous coinfection affected PR8 titers. The same trend in PR8 replication was seen during PR8 alone (Mock+PR8) and coinfected (RV+PR8) samples (Fig. 3.1A). PR8 titers in both single- and coinfection increased throughout 72 hours. However, no significant differences were found at any time point between single- and coinfection. Viral interference may be influenced by individual virus replication kinetics and a sufficient amount of time to establish an initial infection may be required to see full effects. We decided to test a larger range of time intervals between viral inoculations to try and capture any subtleties involved. However, no major effects of viral interference were found when RV was inoculated either 2 (Fig. 3.1B), 6 (Fig. 3.1C), or 12 hours (Fig. 3.1D) before PR8 (RV/PR8) compared to PR8 alone (Mock/PR8). The only significant difference found between single (Mock/PR8) and coinfection (RV/PR8) PR8 titers was when RV was inoculated 6 hours before PR8 at 96 hours. This implies that PR8 replication is unaffected by the presence of another virus regardless of the timing of infections.

One potential problem with previous coinfection schemes is the inoculation dose could be too low to ensure sufficient interactions between RV and PR8. We decided to double the inoculation dose of both viruses in hopes of increasing viral interactions and improving the chances of both viruses coinfecting individual cells. LA-4 cells were either Mock- (media) or RV-inoculated (MOI=2) simultaneously with, 6, or 12 hours before PR8-inoculation (MOI=2). Infected cells were incubated for 48-96 hours, and media overlaying the monolayers were collected at 6, 12, 18, 24, 48, 72, and 96 hours after virus inoculation. PR8 was titrated using the $TCID_{50}$ assay on MDCK cells.

Increasing the dose of each virus during coinfection had timing-specific effects on PR8 replication. As seen earlier, with lower doses, PR8 titers during simultaneous coinfection (RV+PR8) were not significantly different than PR8 alone (Mock/PR8) titers (Fig. 3.1E). A similar trend was seen when RV was inoculated 12 hours before PR8 (Fig. 3.1G). No significant differences in PR8 titers were seen during coinfection (RV/PR8) compared to a single infection (Mock/PR8). However, when RV was inoculated 6 hours before PR8, PR8 titers during coinfection (RV/PR8) were significantly lower at 12 and 72

hpi compared to PR8 alone (Mock/PR8) (Fig. 3.1F). Coinciding with these significant differences, PR8 titers in RV/PR8 samples were also lower at 48 and 96 hpi, but these differences did not reach a significant level. These differences may be specific to a small window of inoculation timings for these viruses and inoculating outside this window negates potential for viral interference. This small window could be due to how RV replication is affecting cellular processes because RV would be producing immediate early genes shortly after entering a cell. Replication of RV and LA-4-specific cellular responses would need to be measured to assess how this would affect PR8 inoculation at different times.

### 3.2.2 Rhinovirus replication was altered during *in vitro* coinfection at low inoculation doses

Since coinfection with RV had little to no effect on PR8 replication, we were interested if PR8 affected RV replication. The LA-4 cell-line was inoculated with either Mock (media) or PR8 (MOI=1) simultaneously with, 6, or 12 hours before inoculation with RV (MOI=1). Infected LA-4 cells were incubated for 48 to 96 hours, and media overlaying the monolayer were collected at 6, 12, 18, 24, 48, 72, and 96 hpi. RV was then titrated by $TCID_{50}$ assay on HeLa cells.

When we analyzed RV titers, there was a more obvious effect of coinfection on virus replication. Simultaneous coinfection with RV and PR8 (RV+PR8) reduced RV titers compared to RV alone (Mock+RV) infected samples (Fig. 3.2A). But when PR8 was inoculated 6 hours before RV, RV titers during coinfection (PR8/RV) were significantly higher at 24 hpi compared to RV alone infection (Mock/RV) (Fig. 3.2B). However, when PR8 was inoculated 12 hours before RV, coinfected samples (PR8/RV) had reduced RV titers at both 48 and 72 hpi compared to RV alone (Mock/RV) infected samples (Fig. 3.2C). These data infer that RV is more susceptible to viral interference than PR8 during coinfection. However, RV gained a replicative advantage when PR8 was inoculated 6 hours before RV. This advantage correlated with the eclipse phase of the PR8 replication cycle, which could help set the stage for RV.

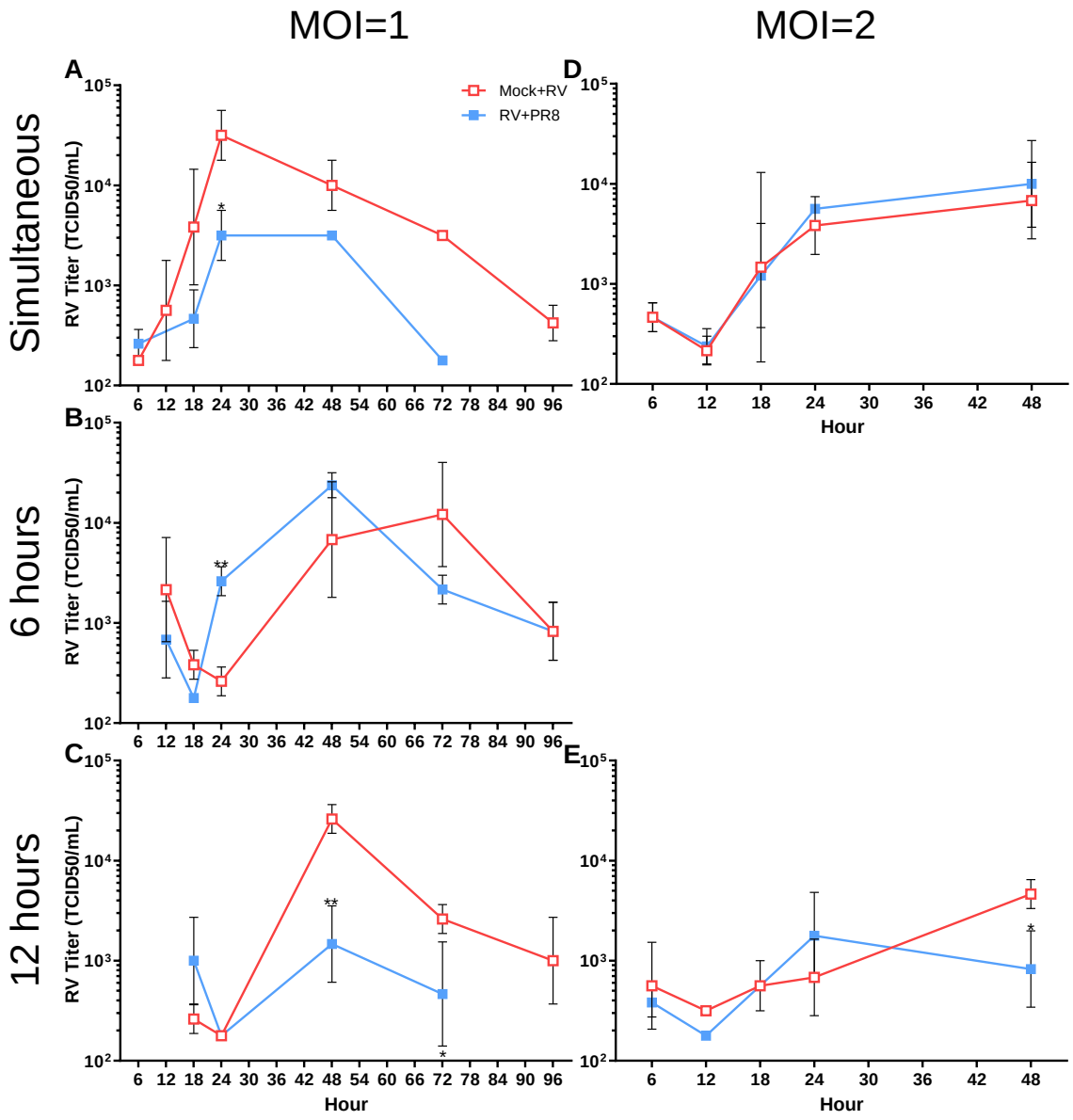


**Figure 3.2. RV replication was affected by coinfection with PR8 at lower inoculation doses.** LA-4 cells were either inoculated with Mock (media) or PR8 6 or 12 hours before or simultaneously with RV. Cells were incubated for 48-96 hours, and media were collected at 6, 12, 18, 24, 48, 72, and 96 hours post-inoculation and RV was quantified by $TCID_{50}$ assay. RV titer from single infected cells (Mock+RV, Mock/RV) is open, red squares, and RV titer from coinfected cells (RV+PR8) is closed, blue squares. A) Simultaneous coinfection; MOI=1. B) PR8 inoculated 6 hours before RV; MOI=1. C) PR8 inoculated 12 hours before RV; MOI=1. D) Simultaneous coinfection; MOI=2. E) PR8 inoculated 12 hours before RV; MOI=2. Significance versus Mock/RV was determined by unpaired Student's *t*-test of triplicate samples. P-values are shown by * ≤ 0.05 or ** ≤ 0.01.

We also tested how increasing the inoculation dose of each virus affected RV titers during coinfection. LA-4 cells were either Mock- (media) or PR8-inoculated (MOI=2)

simultaneously with or 12 hours before RV-inoculation (MOI=2). Infected cells were incubated for 48 hours, and media overlaying the monolayers were collected at 6, 12, 18, 24, and 48 hours after virus inoculation. RV was titrated using the $TCID_{50}$ assay on HeLa cells.

Interestingly, we did not see any differences in RV titers between coinfection (PR8/RV) and RV alone (Mock/RV) infected samples when the inoculation dose was increased. Whether PR8 and RV were coinfected simultaneously (Fig. 3.2D) or 12 hours apart (Fig. 3.2E), RV titers in single infected samples matched RV titers in coinfected samples. The only significant difference recorded was at 48 hpi when PR8 was inoculated 12 hours before RV (Fig. 3.2E). This may need further investigation into later time points to see if this reduction in RV titers during coinfection is maintained. These data suggest that coinfection can alter RV replication, but it is dependent upon the amount of virus inoculated and timings between inoculations.

### 3.2.3 Testing coinfection viral interference in a mouse alveolar macrophage cell line

We initially observed mixed results for coinfection-mediated viral interference in a murine lung cell-line, but now we wanted to try similar experiments in another pulmonary-related cell line. Alveolar macrophages are a frontline defense against anything attempting to gain access to the lower respiratory tract. These macrophages would be another cell type encountered by each virus during infection; we wanted to test if the replication of either virus would be affected by coinfection of these cells.

In the following study, we chose to use the murine alveolar macrophage cell-line MH-S because it is susceptible to RV (118) and PR8 (119). MH-S cells were inoculated with either Mock (media) or RV (MOI=1) 12 hours before inoculation with PR8 (MOI=1). The reverse, PR8 12 hours before RV, was also tested. Infected cells were incubated for 24 hours before media were collected, and both RV and PR8 were titrated by $TCID_{50}$ assay on HeLa and MDCK cells, respectively.

Coinciding with results obtained from coinfecting a lung cell-line, RV growth was affected by coinfection more than PR8. Both PR8 alone (Mock/PR8) and coinfected (RV/PR8) samples had PR8 titers around $10^5$ $TCID_{50}$/mL at 24 hpi (Fig. 3.3A), which

demonstrated that PR8 growth was not disturbed by coinfection in MH-S cells. When MH-S cells were inoculated with RV alone (Mock/RV), RV titers were slightly above $10^2$ $TCID_{50}$/mL at 24 hpi whereas RV titers from coinfected (PR8/RV) samples were undetectable (Fig. 3.3B). These data provide further evidence for RV growth being more sensitive to the effects of coinfection in alveolar macrophages than PR8 growth.

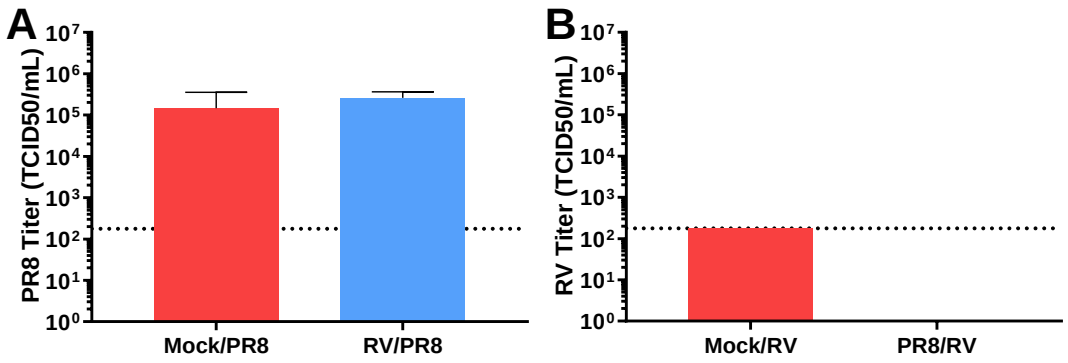


**Figure 3.3. Coinfection in murine alveolar macrophages interfered with RV replication.** MH-S cells were either inoculated with Mock (media), RV (MOI=1), or PR8 (MOI=1) 12 hours before either PR8 (MOI=1) or RV (MOI=1) inoculation. Cells were incubated for 24 hours after the second virus inoculation before collecting media. PR8 and RV were quantified by $TCID_{50}$ assay on MDCK and HeLa cells, respectively. A) PR8 titer from single infected cells (Mock/PR8) is a red bar, and PR8 titer from coinfected cells (RV/PR8) is a blue bar. B) RV titer from single infected cells (Mock/RV) is a red bar, and RV titer from coinfected cells (PR8/RV) is a blue bar. The limit of detection for this assay is represented by the dotted line.

## 3.3 Discussion

Viral interference can be influenced by several subtleties of infection that combine to produce the effects seen. Some infection components are the viruses involved, inoculation dose of each virus, the timing of each virus, etc. Which viruses are involved relates to what immune responses are induced by infection and establishment of a strong versus weak antiviral state. Inoculation doses affect whether all susceptible cells are infected by each virus or if there are pockets of infection that limit potential interactions between coinfecting viruses. Inoculation timings are imperative because it establishes if one virus has an advantageous head start on replication over another virus.

The goal of this study was to establish if viral interference witnessed *in vivo* was attributed to virus-virus interactions or if it were dependent upon large scale immune responses. To test this, we inoculated a murine lung epithelial cell-line with RV and PR8 while varying timings and doses of inoculations. We also inoculated a murine alveolar macrophage cell line with RV and PR8 (only using one timing and dose scheme) to determine if any of the effects that were seen were cell line specific. In summation, PR8 replication was more or less unaffected by the presence of another virus, whereas RV replication kinetics were altered during coinfection.

PR8 growth curves during coinfection were consistently similar to growth curves from PR8 alone samples regardless of inoculation timing or dose. Interestingly, the only significant differences in PR8 titers recorded were when RV was inoculated six hours before PR8 at both an MOI of 1 and 2 (Fig. 3.1C and F). This PR8 titer decline in coinfected samples may be due to an initial infection by RV induced an antiviral response causing a reduction in the number of susceptible cells for PR8. But this option seems unlikely because we did not observe any evidence of this in earlier time points, and an antiviral state would have been initiated by 24 hpi (85). Similar results were obtained from another lab using RSV and IAV. IAV titer was unaffected by simultaneous coinfection with RSV, but as timing between inoculations increased, IAV titers began to drop (120). This study suggests that the mechanism behind IAV and RSV interference is the high growth rate of IAV combined with IAV-induced IFN production and interference with protein synthesis between viruses. Contradictory to this, we did not find significant differences when RV was inoculated 12 hours before PR8. This implies that inoculation timing is a critical parameter for determining viral interference, and this can be further convoluted by which viruses are coinfected together. One explanation for why timing is a major factor is the responses to infection generated in the LA-4 cell line. RV infection in LA-4 cells modifies gene expression by 12 hours post-infection and this is maintained through 24 hours (85). Many of these affected genes are related to antiviral, MHC class presentation, and immune responses such as Mx1, 2’-5’-oligoadenylate synthase-related genes, type I IFN, and C-X-C motif chemokine 10. It would then be expected, given enough time, that RV would induce a strong enough antiviral response in LA-4 cells to inhibit PR8 replication. However, this was not the case here, and increasing the timing between inoculations to 12 hours did not affect PR8

replication. IAV has known mechanisms for bypassing antiviral responses such as nonstructural protein 1 (NS1) inhibiting type I IFN responses (121) or NA reducing tetherin functionality (122). The NS1 gene of IAV is capable of binding sequences of dsDNA specific to antiviral genes, preventing binding of transcriptional factors from locating their targets and inducing production of these genes (123). Another key mechanism IAV utilizes is the destruction of the type I interferon receptor (IFNAR). IAV hemagglutinin ubiquitin-tags a subunit of IFNAR, leading to reduced expression of functional IFNAR (124). Reduction of this receptor would then reduce downstream signaling of type I interferon. These mechanisms could help PR8 normally replicate despite the immune responses activated by a prior RV infection.

The effects of coinfection were more apparent when looking at RV replication over time. RV titers were reduced by both simultaneous and PR8 12 hours before RV coinfection (Fig. 3.2). Then when PR8 was inoculated six hours before RV, the coinfected RV growth curve was accelerated compared to RV alone growth curve. The reduction in RV replication fits with gene expression from PR8 infected LA-4 cells. PR8 continually alters gene expression changes in LA-4 cells from 12 hours to 24 hours post-infection with a strong induction of type I interferon, including induction of the type I interferon receptor (85). Induction of the type I receptor would contribute to a stronger type I interferon response by making cells more sensitive to secreted interferon while also further increasing type I interferon through cyclical feedback loops. This mechanism would help explain the reduced RV growth curves during coinfection as time progresses. Another potential mechanism is PR8 may be outcompeting RV for susceptible host cells. PR8 replicated to much higher titers in LA-4 cells than RV. This would allow PR8 to spread to susceptible host cells much faster than RV, potentially excluding RV from coinfecting these cells by increasing TLR3 expression (85) which could thereby limit RV expansion by cytokine and chemokine production (125). It is interesting to note that PR8 inoculation six hours before RV increased RV titers at the early time points of infection (Fig 3.2). One explanation is PR8 may be reducing host cell protein synthesis, allowing RV to more easily establish an infection. But when PR8 is inoculated 12 hours before, PR8 has replicated to high enough degree that it is outcompeting RV for susceptible cells and the host cell responses may have rebounded to interfere with both PR8 and RV infection. Increasing the virus doses lent credence to this

idea because RV replication was no longer strongly affected by coinfection when it was inoculated at a higher dose. Although these mechanisms do not explain how simultaneous RV and PR8 coinfection affects RV replication, it may be that PR8 can replicate at a faster rate and outcompetes RV for susceptible host cells. Further support for this potential is RV replication is limited by innate immune responses in a temperature dependent manner. RV replicates to higher titers at 33°C compared to 37°C, correlating with reduced interferon-*beta* and antiviral responses (126). All experiments were incubated at 37°C, thus putting RV at a disadvantage. Temperature-dependent replication mechanisms in combination with the strong induction of antiviral genes and rapid replication rate by PR8 would explain how coinfection can reduce RV replication when inoculated at a MOI=1.

Virus replication within cells can occur in many different locations of the cell. PR8 replication is unique to RNA viruses because it happens in the nucleus of the cell (127) while RV replicates in the cytoplasm (128). This unique localization could explain why PR8 is less affected by coinfection than RV. PR8 infection induces RIG-I activation and downstream production of type I IFN (129). The RIG-I-dependent pathway is a major contributor to recognition and downstream type I IFN production during RV infection (66). This PR8-mediated induction of RIG-I could prepare cells for a secondary infection, leading to a more rapid recognition and response to RV, thus potentially limiting the extent of RV replication we observe during coinfection. Alternatively, RV induces expression of both RIG-I and TLR3 (65), both of which recognize PR8 (130). However, because PR8 replicates in the nucleus, it can avoid recognition by cytoplasmic recognition receptors such as RIG-I. Our data agreed with this because we did not see many differences in PR8 replication during coinfection. These data further reflect that differences during rhinovirus and influenza coinfection depend on larger scale immune responses, e.g. cellular immune responses and not on virus-virus interactions.

Finally, we were interested if the trends observed during *in vitro* coinfection were cell line specific. We used a murine alveolar macrophage, MH-S, cell line because these would be a common cell type encountered when infections spread to the lower respiratory tract. Again, PR8 was unperturbed by coinfection in macrophages. PR8 titers in coinfected and PR8 alone infected samples reached equivalent levels by 24 hpi (Fig. 3.3A). This result

is a little surprising because other groups report that IAV infection is abortive in similar alveolar macrophage cell types (117, 131, 132). One other group reports that PR8 replication in MH-S cells is minimal (133). MH-S cells have lost some typical features of primary murine alveolar macrophages, which may account for their ability to sustain PR8 infection (119). HRV does not establish a strong infection in human alveolar macrophages, but HRV RNA is detectable up to ten days after inoculation (134). However, HRV and RV are known to attenuate immune responses to subsequent stimuli in human alveolar macrophages (134) and MH-S cells (118). In our experiments, no RV titer was detected for coinfected samples at 24 hpi, whereas a small amount of RV was detected in single infected samples. Failure for RV to replicate in macrophages has been observed in other studies (61, 134, 135). Although RV does not replicate well in macrophages, RV still induces TNF-α and IL-6. This allows RV to still induce an immune response without having to establish an infection. These data in MH-S cells are analogous to the data obtained from LA-4 cells where PR8 replication is unaffected by coinfection while RV replication is reduced during coinfection.

These data demonstrate that the effects of viral interference are dependent upon viruses involved and timing of viral infection. PR8 replication was mostly undisturbed during coinfection with both a lung epithelial cell-line and alveolar macrophages, regardless of the timing of viral inoculations. However, RV replication was altered during coinfection in both lung cell-line and alveolar macrophages. These effects may be dependent upon each viruses' replicative speed in each cell line leading to competition for host cells or how each virus affects gene expression leading to a reduction in susceptible host cells. Future studies will need to be directed at identifying key antiviral genes in each cell line responsible for viral exclusion.

# CHAPTER 4

# Respiratory Viral Coinfection Outcomes are Dependent upon Severity and Timings of Infections

## 4.1 Overview

Respiratory viral coinfections have been observed to reduce or exacerbate disease severity compared to individual virus infections. It is not well understood how these viruses interact to affect disease severity. Although clinical studies can identify the effects of coinfection, they remain a snapshot in time and cannot clearly pinpoint the subtleties of infection that occur behind the scenes. A model system is needed to help identify the parameters of coinfection responsible for ameliorating or exacerbating disease severity.

Many studies have addressed the prevalence of respiratory viral coinfections both in hospitalized patients and community sampled individuals. Instances of patients hospitalized with coinfections range from 18 – 45% of virus-positive samples (2, 8, 11, 12, 38, 136). Interestingly, viral coinfection pairings may not be random and could be influenced by the compatibility of each coinfecting virus. One study reports that coinfections with adenovirus and HRV are more common than expected (11). Nolan *et al*. also report that coinfections with HRV and respiratory syncytial virus (RSV) are less prevalent than expected (11). Although Nolan *et al.* find HRV and RSV coinfection is less frequent than expected, this coinfection is often reported as being quite common in other studies (14, 47, 136). One group observes HRV being the most common virus detected during coinfection, but HRV also reduces the chances of co-detecting several other respiratory viruses (50). Coinfections involving CoV are reported at high frequencies with upwards of 70% of CoV detections involving another virus (8, 18, 19, 137). IAV is not as commonly found in coinfections as HRV or RSV. Martin *et al*. report that IAV is the least likely virus to be involved in a coinfection (8). One study finds IAV is the most commonly co-detected with RSV or HRV (20). However, other studies find HRV interferes with the circulation of IAV (49, 50). More information is needed to understand why some virus pairings are more frequent than others.

There has yet to be a clear consensus for when coinfections are detrimental or beneficial to the host. Coinfections involving RSV typically increase disease severity compared to individual infections (20, 38, 40). These increases in disease severity are linked to increased obstructive airway disease, lower respiratory tract infections, and admittance to prenatal intensive care unit or general wards. However, RSV coinfections are also reported to not affect disease severity compared to single virus infections (14, 47). Coinfections involving RSV have even been observed to lessen disease severity (136). These trends are not unique to RSV and have been reported for HRV as well. HRV increases adenovirus disease severity during coinfection (38) but reduces IAV disease severity during coinfection (42). Once again, this trend is seen during CoV coinfections. CoV coinfections, including coinfections with RSV, are associated with reduced frequency of upper respiratory tract infections compared to CoV single infections (19, 137), whereas pandemic IAV coinfections with CoV have higher clinical severity compared to pandemic IAV infection alone (42). A viral coinfection model is necessary to determine if the effects of coinfection on disease severity are dependent upon virus pairings alone or in combination with other infection parameters that cannot be controlled in clinical studies.

Experimental models of coinfection have been used to explain the effects of coinfection *in vivo*. A ferret model tested coinfection of RSV and a pandemic H1N1 influenza A virus (pH1N1) at different times. Pre-infection with pH1N1 3 and 7 days, but not 11 days, before RSV prevents the establishment of RSV infection in ferrets, whereas pre-infection with RSV does not interfere with subsequent pH1N1 infection (94). pH1N1 infection induces a stronger inflammatory response compared to RSV, lending credence to an initial inflammatory response being the cause for interference with viral replication during coinfection. Another ferret model focused on unrelated influenza virus infections. Once again, pH1N1 prevents infection with a secondary virus, this time an IBV, when pre-infected 1 and 3 days before secondary challenge (109). However, no protection from pH1N1 infection is seen when IBV was inoculated first. pH1N1 was thought to induce an inflammatory cytokine response that interfered with IBV infection, but this was not confirmed. A more common model to study respiratory coinfection is viral-bacterial coinfections, specifically influenza infection predisposing a host to a secondary bacterial infection (138-140). HRV infection predisposes mice to a secondary *Hemophilus influenzae*

infection by attenuating TLR-responses resulting in a decrease in neutrophil responses (118). Intranasal administration of *Lactobacillus* species 21 days before influenza inoculation increases mouse survival compared to mice receiving skim milk (141). These studies introduce important parameters of disease attenuation and exacerbation effects, which are dependent upon the organisms coinfecting the host and timing between coinfections.

A mouse model of respiratory viral coinfection allows for proper control of infection parameters not seen in clinical studies. The ability to vary each parameter individually during infection assists in determining the essential parameters during coinfection. We are interested in testing how specific virus pairings, doses, and order of virus infections alter disease severity compared to individual virus infections. Determining the essential criterion for coinfection effects will explain when a coinfection is detrimental versus beneficial compared to individual virus infections.

Although we observed minimal effects during *in vitro* coinfection, the primary literature reports many examples of HRV preventing IAV infection or even modulating IAV disease. We were interested if coinfection with RV and PR8 would mimic results described in the literature when using a murine model.

## 4.2 Results

### 4.2.1 Rhinovirus attenuates disease severity during coinfection with influenza A virus

Single infection control mice were either inoculated with RV two days before Mock-inoculation (media)(RV/Mock) or Mock-inoculation (media) two days before PR8 (Mock/PR8). Coinfected mice were inoculated with RV two days before inoculation with PR8 (RV/PR8) (Fig. 4.1). Mortality, weight loss, and clinical signs (lethargy, ruffling of fur, hunched posture, and labored breathing) were monitored for 14 days after PR8 inoculation. We designated a 25% weight loss as a humane endpoint for euthanasia.

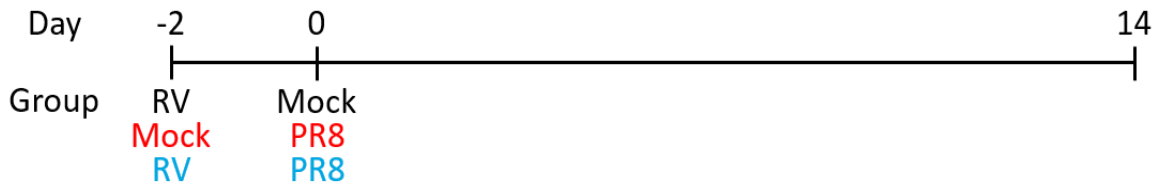


**Figure 4.1. RV and PR8 coinfection inoculation scheme.**

Excitingly, RV attenuated PR8-induced disease severity when coinfected two days apart (Fig. 4.2). Mice inoculated with RV alone (RV/Mock) did not exhibit any signs of disease and remained healthy throughout the study. PR8 alone (Mock/PR8) infection was 40% lethal with 2 of 5 mice succumbing to PR8 infection on day 8 (Fig. 4.2A). Mock/PR8 mice reached 78% of the original weight, the peak of their weight loss, by day 8 before eventually recovering (Fig. 4.2B). Clinical signs were elevated from days 3 to 9 after PR8 infection and limited to minor ruffling (Fig. 4.2C). Day 8 coincided with peak clinical signs, which included minor hunching and shallow or irregular breathing. Coinfected mice (RV/PR8) were protected from PR8-induced mortality with all mice survived until the end of the study (Fig. 4.1A). RV curtailed weight loss associated with PR8, and coinfected mice lost weight at a lower rate compared to PR8-infected mice (Fig. 4.1B). RV/PR8 coinfected mice reached 88% of original weight before recovering, one day before PR8 alone infection. Coinfection significantly reduced weight loss on days 7-14. Coinfection with RV two days before PR8 also reduced clinical signs in mice; RV/PR8 coinfected mice only exhibited minor hunching on days 5 and 6 (Fig. 4.2C).

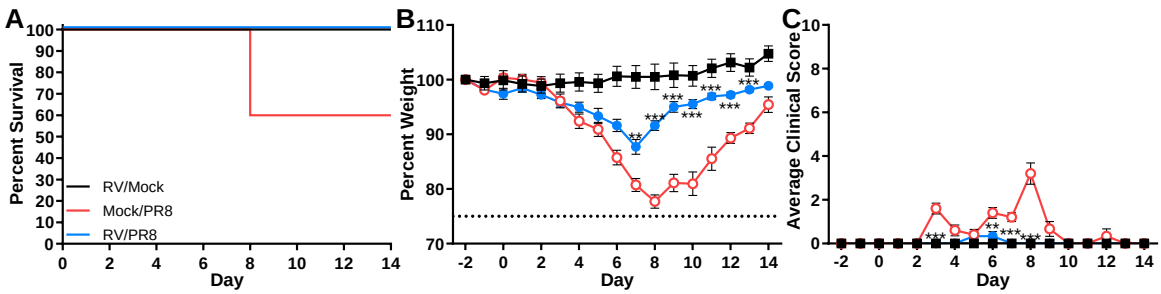


**Figure 4.2. RV attenuates PR8-induced disease when coinfected two days apart.** Groups of 5-6 mice were inoculated with either Mock (media) or RV ($7.6x10^6$ $TCID_{50}$/mouse) on day -2. Two days later on day 0, mice were then inoculated with either Mock (media) or PR8 (77.5 $TCID_{50}$/mouse). Mice were then monitored for mortality, weight loss, and clinical signs (lethargy, ruffled fur, hunched back, labored breathing) for 14 days after PR8 inoculation. (A-C) RV and PR8 coinfection mortality (A), weight loss (B), and clinical scores (C). RV/Mock (black lines, closed squares), Mock/PR8 (red lines, open circles), RV/PR8 (blue lines, closed circles). Survival curves were compared using log-rank Mantel-Cox curve comparison versus Mock/PR8. Weight loss and clinical score data were compared using multiple Student's *t*-tests versus Mock/PR8. P-values are shown as ** ≤ 0.01 or *** ≤ 0.001.

### 4.2.2 Rhinovirus-mediated disease attenuation is not restricted to influenza A virus infection

We were curious if the effects seen during RV and PR8 coinfection were limited to this virus pairing, or if they would apply to coinfections with unrelated viruses. RSV and CoV are also commonly found in clinical coinfections (137). We used PVM and the respiratory-tropic MHV as models for RSV (86) and CoV (55), respectively.

Single infection control mice were either inoculated with RV two days before Mock-inoculation (media)(RV/Mock) or Mock-inoculation (media) two days before PVM (Mock/PVM) or MHV (Mock/MHV). Coinfected mice were inoculated with RV two days before PVM (RV/PVM) or MHV (RV/MHV) (Fig. 4.3). Mice were monitored for mortality, weight loss, and clinical signs for 14 days after PVM or MHV inoculation.


**Figure 4.3. Coinfection scheme for RV and either PVM or MHV.**

Infection with PVM alone (Mock/PVM) was highly lethal and about 80% of mice succumbed to infection by day 8 (Fig. 4.4A). Weight loss in Mock/PVM infected mice began on day 5 and rapidly increased until mice succumbed to disease (Fig 4.4B). Clinical signs appeared on day 4, and quickly increased by day 8, correlating with weight loss (Fig. 4.4C). Clinical signs began as mild ruffling on day 4, and by day 6 mice exhibited moderate lethargy, ruffling, and labored breathing and mild hunching. Mice coinfected with RV two days before PVM (RV/PVM) were all protected from mortality (Fig. 4.4A), weight loss (Fig. 4.4B), and clinical signs (Fig. 4.4C) associated with Mock/PVM infections (Fig. 4.4A). No RV/PVM coinfected mice succumbed to PVM infection. Surprisingly, RV/PVM coinfected mice experienced very minimal weight loss, which was not significantly different than healthy mice inoculated with RV alone. Coinfected mice exhibited minor ruffling on days 8 and 9, but signs were quickly resolved.

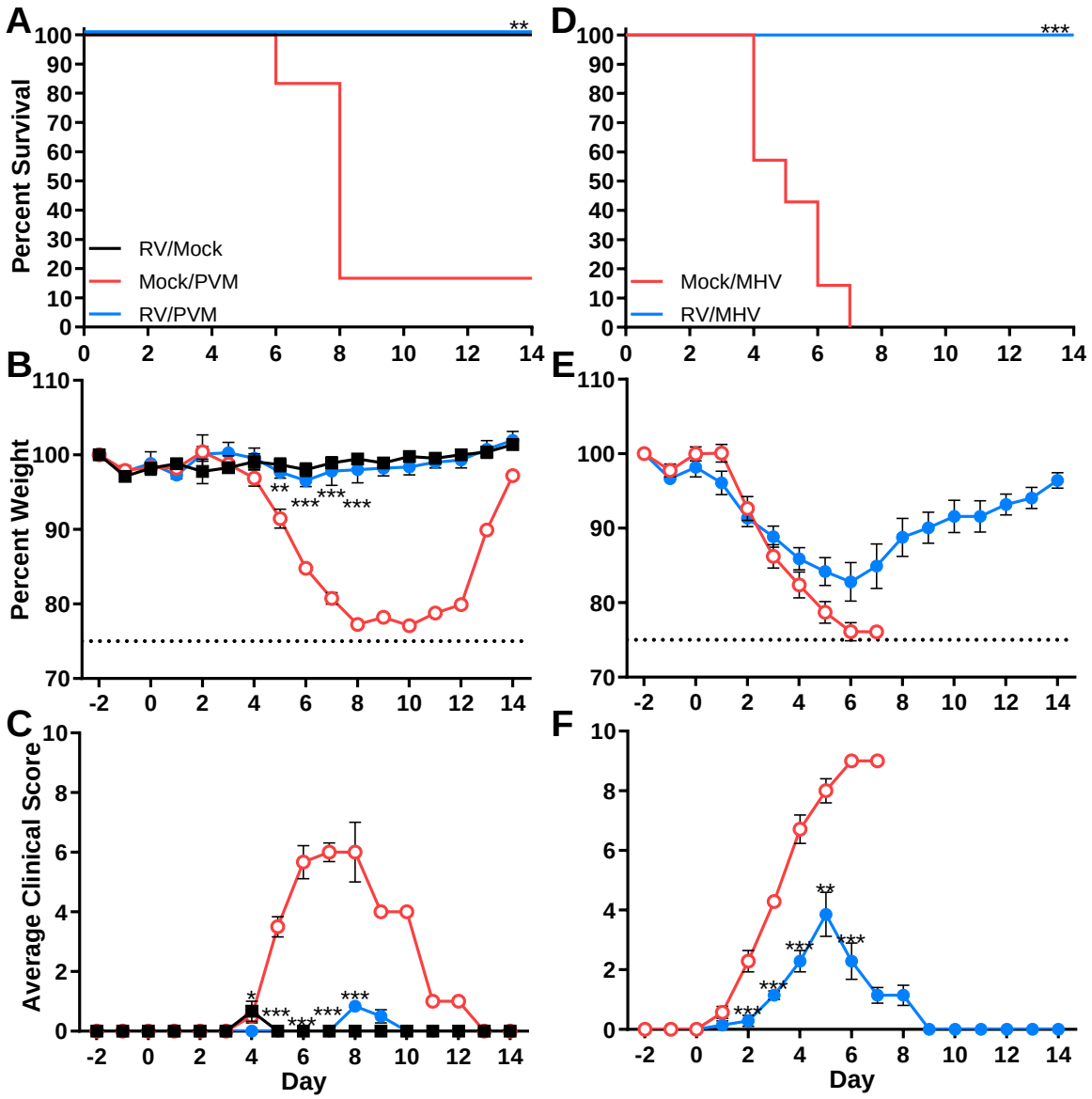


**Figure 4.4. Pre-infection with RV attenuated disease severity of multiple, unrelated viruses.** Mice were either inoculated with Mock (media) or RV ($7.6x10^6$ $TCID_{50}$/mouse) on day -2. On day 0, mice were either inoculated with Mock (media), PVM ($1.0x10^4$ $TCID_{50}$/mouse), or MHV ($2.0x10^5$ PFU/mouse). Mice were monitored for mortality, weight loss, and clinical signs (lethargy, ruffling fur, hunching, labored breathing) for 14 days after PVM or MHV inoculation. (A-C) RV and PVM coinfection mortality (A), weight loss (B), and clinical scores (C). RV/Mock (black lines, closed squares), Mock/PVM (red lines, open circles), RV/PVM (blue lines, closed circles). (D-F) RV and MHV coinfection mortality (A), weight loss (B), and clinical signs (C). Mock/MHV (red lines, open circles), RV/MHV (blue lines, closed circles). Survival curves were compared using log-rank Mantel-Cox curve comparison versus Mock/PVM or Mock/MHV. Weight loss and clinical score data were compared using multiple Student's *t*-tests versus Mock/PVM or Mock/MHV. P-values are shown as * ≤ 0.05, ** ≤ 0.01, or *** ≤ 0.001.

RV/MHV coinfection disease kinetics more closely resembled RV/PR8 rather than RV/PVM coinfections. MHV alone (Mock/MHV) infection was 100% lethal, and mice succumbed to the infection starting day 4 until day 7 (Fig. 4.4D). The onset of weight loss in Mock/MHV infected mice was rapid following MHV inoculation. Mock/MHV mice initially lost weight on day 2 and progressed to day 6 and 7 (Fig. 4.4E). Initial clinical signs observed on day 1 were limited to minor ruffling, but by day 4, signs progressed to mild lethargy and labored breathing with moderate hunching and severe ruffling (Fig. 4.4F). As the study progressed, labored breathing and lethargy increased to moderate severity. Mice coinfected with RV two days before MHV (RV/MHV) were protected from mortality, and all mice survived until day 14 (Fig. 4.4D). However, RV/MHV coinfected mice were not protected from weight loss. Coinfected mice even lost weight on day 1, one day sooner than the Mock/MHV group (Fig. 4.4E). Coinfected mice maintained greater weight loss than Mock/MHV mice until day 2, when the rate of weight loss lessened. RV/MHV coinfected mice continued to lose weight until reaching 83% of the original weight on day 6 before recovering from the infection. Clinical signs in coinfected mice were restricted to ruffling and hunching. Mild ruffling appeared on day 3 and increased to moderate ruffling with mild hunching by day 5 before eventually resolving by day 9 (Fig. 4.4F). Interestingly, RV attenuated both PVM and MHV disease severity, but disease kinetics were unique to each pairing.

### 4.2.3 Disease attenuation during coinfection is not limited to rhinovirus infections

After we discovered that RV attenuated disease severity for multiple, unrelated secondary viral infections, we were then interested if similar outcomes could be achieved when changing the primary infection. We then tested if MHV was capable of protecting mice from PR8 and PVM disease during coinfection. Because our initial studies using MHV were 100% lethal, we chose to reduce the dose by 100-fold, producing a milder MHV infection. To test this, single infection control mice were inoculated with MHV two days before Mock-inoculation (media)(MHV/Mock) or Mock-inoculated two days before PR8 (Mock/PR8) or PVM (Mock/PVM). Coinfected mice were inoculated with RV two days

before PR8 (RV/PR8) or PVM (RV/PVM) (Fig. 4.5). Mortality, weight loss, and clinical signs were monitored daily for 14 days after PR8 or PVM inoculation.


**Figure 4.5. Coinfection scheme for MHV and either PR8 or PVM.**

As opposed to coinfections with RV, coinfections with MHV seemed to be dominated by MHV disease kinetics. No mortality was observed when mice were infected with MHV alone (MHV/Mock) (Fig. 4.6A). However, MHV/Mock-infected mice lost weight on day 0 and continued until reaching 15% weight loss was reached on day 4 before slowly recovering by day 14 (Fig. 4.6B). Clinical signs in MHV-infected mice paralleled increases in weight loss. Clinical signs appeared on day 0 as minor ruffling and hunching and increased by day 5 to include minor breathing changes (Fig. 4.6C). PR8-infected mice (Mock/PR8) exhibited about 80% mortality by day 11 (Fig. 4.6A). Mock/PR8 infected mice lost weight on day 4 and reached peak weight loss of 23% original weight on day 9 before recovery (Fig. 4.6B). PR8-infected mice began displaying clinical signs on day 4 as mild ruffling, which increased to mild lethargy and moderate ruffling, hunching, and labored breathing by day 9 (Fig. 4.6C). Coinfection with MHV two days before PR8 (MHV/PR8) reduced PR8-induced mortality to 0% (Fig. 4.6A), and weight loss of coinfected mice resembled the MHV/Mock group more than the Mock/PR8 group (Fig. 4.6B). Coinfected mice initially lost weight on day 0 and slowly increased until day 9 when peak weight loss was reached at about 17% of original weight. It is important to note that although coinfected mice did not recover on day 4, similar to MHV-infected mice, their peak weight loss was lower than Mock/PR8 mice. MHV/PR8 coinfected mice displayed clinical signs between days 0-6; clinical signs were limited to minor ruffling and hunching with sporadic minor lethargy (Fig. 4.6C).

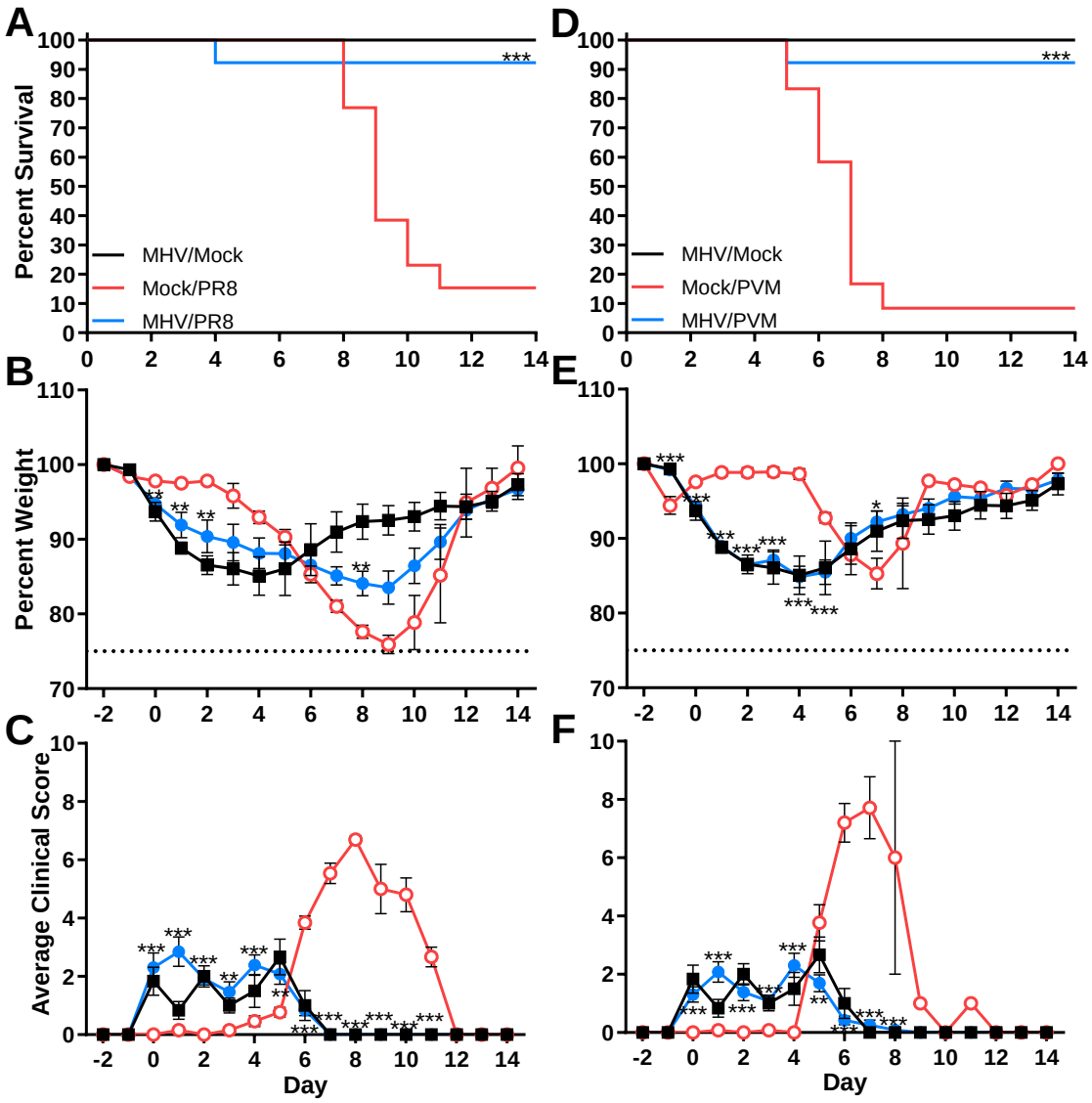


**Figure 4.6. Initial infection by MHV reduced both PR8- and PVM-induced disease.** Mice were either inoculated with Mock (media) or MHV ($2.0x10^3$ PFU/mouse) on day -2. On day 0, mice were either inoculated with Mock (media), PR8 (77.5 $TCID_{50}$/mouse), or PVM ($1.0x10^4$ $TCID_{50}$/mouse). Mice were monitored for mortality, weight loss, and clinical signs (lethargy, ruffling fur, hunching, labored breathing) for 14 days after PR8 or PVM inoculation. (A-C) MHV and PR8 coinfection mortality (A), weight loss (B), and clinical signs (C). MHV/Mock (black lines, closed squares), Mock/PR8 (red lines, open circles), MHV/PR8 (blue lines, closed circles). (D-F) MHV and PVM coinfection mortality (A), weight loss (B), and clinical signs (C). MHV/Mock (black lines, closed squares), Mock/PVM (red lines, open circles), MHV/PVM (blue lines, closed circles). Survival curves were compared using log-rank Mantel-Cox curve comparison versus Mock/PR8 or Mock/PVM. Weight loss and clinical score data were compared using multiple Student's *t*-tests versus Mock/PR8 or Mock/PVM. P-values are shown as * ≤ 0.05, ** ≤ 0.01, or *** ≤ 0.001.

Similar disease attenuation was achieved during MHV/PVM coinfection compared to MHV/PR8 coinfection. PVM-infection (Mock/PVM) was 90% lethal by day 8 (Fig.

4.6D). Mock/PVM mice experienced rapid weight loss from day 5 to 7 (Fig. 4.6E). Clinical signs were observed in Mock/PVM infected mice on day 5 as mild lethargy and moderate ruffling, hunching, and labored breathing (Fig. 4.6F). Signs increased to severe ruffling and moderate-severe lethargy, hunching, and labored breathing. The disease kinetics in MHV/PVM coinfected mice matched that of MHV/Mock infected mice. MHV/PVM coinfected mice were protected from PVM-induced mortality, and 90% of mice survived until the end of the study (Fig. 4.6D). Coinfected mice lost weight from days 0-2 and then plateaued at about 13% weight loss until day 4 before starting to regain weight (Fig. 4.6E). Clinical signs in coinfected mice were mainly limited to minor ruffling and sporadic minor hunching observed through days 0-5 (Fig. 4.6F). These data lend credence to clinical reports that multiple viruses can attenuate disease from unrelated viruses, but the degree of disease attenuation is dependent upon which viruses are involved.

### 4.2.4 Severity of infections influences the effects of coinfection

Clinical studies provide a snapshot of infection but cannot inform on all parameters of infection. One crucial gap in information is clinical data cannot distinguish the severity of individual infections during coinfection. A murine model allows us to vary the dose of each virus inoculated. Thus, we gain the power to control disease severities of the viruses involved. We were interested in testing how varied doses of both primary and secondary infections affected coinfection-mediated disease attenuation.

We first tested if RV could attenuate a moderate or severe PR8 infection when inoculated two days apart. Mice were either inoculated with Mock (media) or RV two days before a low (mild), medium (moderate), or high (severe) dose of PR8 (Fig. 4.7). Mice were monitored daily for mortality, weight loss, and clinical signs for 14 days after PR8 inoculation.

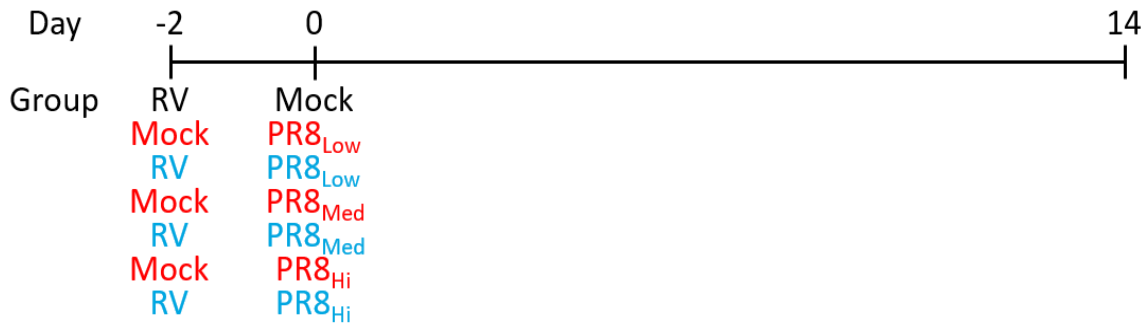


**Figure 4.7. Coinfection scheme with RV inoculation two days before a mild, medium, and severe PR8 infection.** $PR8_{Low}$ dose is a mild infection, $PR8_{Med}$ dose is a moderate infection, and $PR8_{Hi}$ dose is a severe infection.

As expected, RV-mediated disease attenuation was less effective as the severity of PR8 infection increased. Both single and coinfection with mild PR8 ($PR8_{Low}$) infection were explained above (Fig. 4.2), and further explanation will be omitted here, but data will be included in Fig. 4.8A-C for comparison. Inoculation of a moderate dose of PR8 (Mock/$PR8_{Med}$) resulted in a more lethal phenotype than a mild dose of PR8 infection, and 100% of mice succumbed to infection by day 8 (Fig. 4.8D). Mock/$PR8_{Med}$ infected mice lost weight on day 3, which progressed to day 8 until all mice reached the designated weight cutoff for humane euthanasia (Fig. 4.8E). Clinical signs were also elevated in Mock/$PR8_{Med}$ infected mice compared to a single infection. Signs first appeared on day 3 as minor ruffling and hunching and quickly progressed to moderate ruffling with minor lethargy, hunching, and labored breathing by day 6 (Fig. 4.8F). Coinfection with RV two days before moderate PR8 (RV/$PR8_{Med}$) still attenuated PR8 disease, but to a lesser extent compared to mild PR8 coinfection. RV/$PR8_{Med}$ coinfected mice were not completely protected from PR8-induced mortality and 70% (5 out of 7) of mice succumbed to PR8 infection by day 10 (Fig. 4.8D). Coinfected mice also exhibited increased weight loss compared to mild PR8 coinfection (RV/$PR8_{Low}$), closely resembling the Mock/$PR8_{Med}$ curve. RV/$PR8_{Med}$ coinfected mice lost weight on day 3 and progressed to day 8 before the remaining mice recovered and regained weight (Fig. 4.8E). Clinical signs were increased in RV/$PR8_{Med}$ coinfected mice compared to RV/$PR8_{Low}$ coinfected mice. Signs initially displayed as minor ruffling on day 3 and progressed to moderate ruffling with minor lethargy and hunching on days 6 and 7 in

RV/PR8$_{Med}$ coinfected mice (Fig. 4.8F). No differences in mortality, weight loss, or clinical signs were observed between mice infected with severe PR8 alone (Mock/PR8$_{Hi}$) and mice coinfected with RV and severe PR8 (RV/PR8$_{Hi}$). Both Mock/PR8$_{Hi}$ and RV/PR8$_{Hi}$ groups of mice experienced 100% mortality by day 7 and 6, respectively (Fig. 4.8G). Single and coinfected mice lost weight at identical rates, which began on day 3 and continued until each group reached the 75% weight cutoff (Fig. 4.8H). Clinical signs in Mock/PR8$_{Hi}$ infected mice appeared on day 2 as minor ruffling and reached the peak on day 7 with severe ruffling and hunching accompanied by moderate lethargy and labored breathing (Fig. 4.8I). RV/PR8$_{Hi}$ coinfected mice exhibited signs on day 3 as moderate ruffling and minor lethargy and labored breathing and peaked on day 5 as moderate ruffling and hunching with minor lethargy and labored breathing. These data demonstrate that RV-mediated disease attenuation is dependent upon the severity of the secondary PR8 infection.

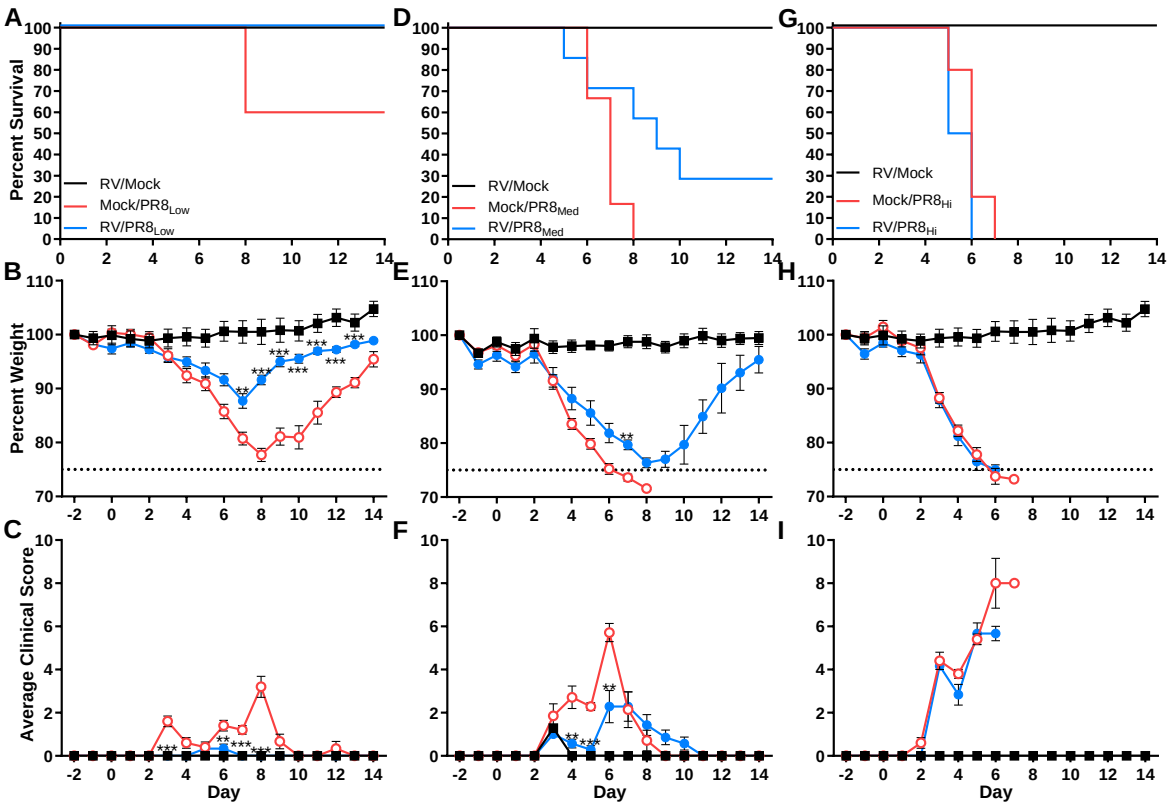


**Figure 4.8. RV-mediated disease attenuation was reduced as the severity of PR8 increased.** Groups of 5-6 BALB/c mice were inoculated with Mock (media) or RV ($7.6x10^6$ $TCID_{50}$/mouse) on day -2. On day 0, mice were inoculated with Mock (media) or PR8 (77.5 (low), 150 (medium), or $7.5x10^3$ (high) $TCID_{50}$/mouse). Mice were then monitored for mortality, weight loss, and clinical scores (lethargy, ruffled fur, hunched back, labored breathing) for 14 days after PR8 inoculation. (A-C) RV and low dose PR8 coinfection mortality (A), weight loss (B), and clinical scores (C). (D-F) RV and medium dose PR8 coinfection mortality (D), weight loss (E), and clinical scores (F). (G-I) RV and high dose PR8 coinfection mortality (G), weight loss (H), and clinical scores (I). RV/Mock (black lines, closed squares), Mock/PR8 (red lines, open circles), RV/PR8 (blue lines, closed circles). Survival curves were compared using log-rank Mantel-Cox curve comparison versus Mock/PR8. Weight loss and clinical score data were compared using multiple Student's *t*-tests versus Mock/PR8. P-values are shown as ** ≤ 0.01 or *** ≤ 0.001.

Next, we wanted to know how varying the severity of the primary infection would affect coinfection-mediated disease attenuation. Inoculation of a high dose of RV in mice elicits a rapid cytokine and chemokine response complemented by short neutrophil recruitment to the lungs. However, RV does not establish a strong, lasting infection and RV viral loads rapidly decrease post-inoculation (52). Given RV's poor infection in mice following a high dose of inoculation, we did not believe this would serve as a good model for varied infection severity. Instead, we decided to test varied doses of MHV during coinfection with PR8. We wanted to find a dose of MHV that attenuated PR8-induced

disease without inducing the dramatic weight loss seen in initial MHV/PR8 coinfection experiments (Fig. 4.6B).

Mice were either inoculated with Mock (media), $2x10^2$ $TCID_{50}$/mouse (mild), $1x10^3$ $TCID_{50}$/mouse (moderate), or $2x10^3$ $TCID_{50}$/mouse (severe) MHV infection two days before inoculating with either Mock (media) or PR8 (Fig. 4.9). Mice were monitored for mortality, weight loss, and clinical signs for 14 days following PR8-inoculation.


**Figure 4.9. Varied severity of MHV coinfected with PR8 scheme.** $MHV_{200}$ is a mild infection, $MHV_{1000}$ is a moderate infection, and $MHV_{2000}$ is a severe infection.

MHV-mediated attenuation of PR8 disease was dependent upon the initial severity of MHV infection. Mice infected with PR8 alone (Mock/PR8) all succumbed to infection by day 6 (Fig. 4.10A). Weight loss in Mock/PR8 infected mice began on day 3 and rapidly increased to the designated 75% cutoff for euthanasia on day 6 (Fig. 4.10B). Clinical signs in Mock/PR8 infected mice correlated with weight loss, and signs appeared on day 3 with minor lethargy, ruffling, and hunching and peaked on day 6 with severe ruffling, moderate breathing complications, and minor lethargy and hunching (Fig. 4.10C). Severe MHV-infection ($MHV_{2000}$/Mock) was 20% (1 of 5) lethal by day 3, while the remaining mice survived until day 14 (Fig. 4.10A). Mice that received a severe dose of MHV ($MHV_{2000}$/Mock) lost weight from days 0-2 before regaining weight on days 4-14 (Fig. 4.10A). $MHV_{2000}$/Mock infected mice also maintained peak signs from days 1-5, displayed as moderate ruffling with minor lethargy, hunching, and breathing complications before signs diminished by day 13 (Fig. 4.10C). Mortality and weight loss were similar between

severe MHV-infected mice and coinfected mice ($MHV_{2000}$/PR8). $MHV_{2000}$/PR8 coinfection was 20% lethal; 1 of 5 mice succumbed to the infection on day 5, two days later than severe MHV alone infection (Fig. 4.10A). Coinfected mice lost weight at the same rate as severe MHV-infected mice, but convalescence was delayed in coinfected mice until day 11 when coinfected and MHV/Mock-infected mice began to match in weight again (Fig. 4.10B). Initial clinical signs on days 1-5 in coinfected mice matched severe MHV infection alone, but coinfected mice maintained low-level signs until the end of the study (Fig. 4.10C).

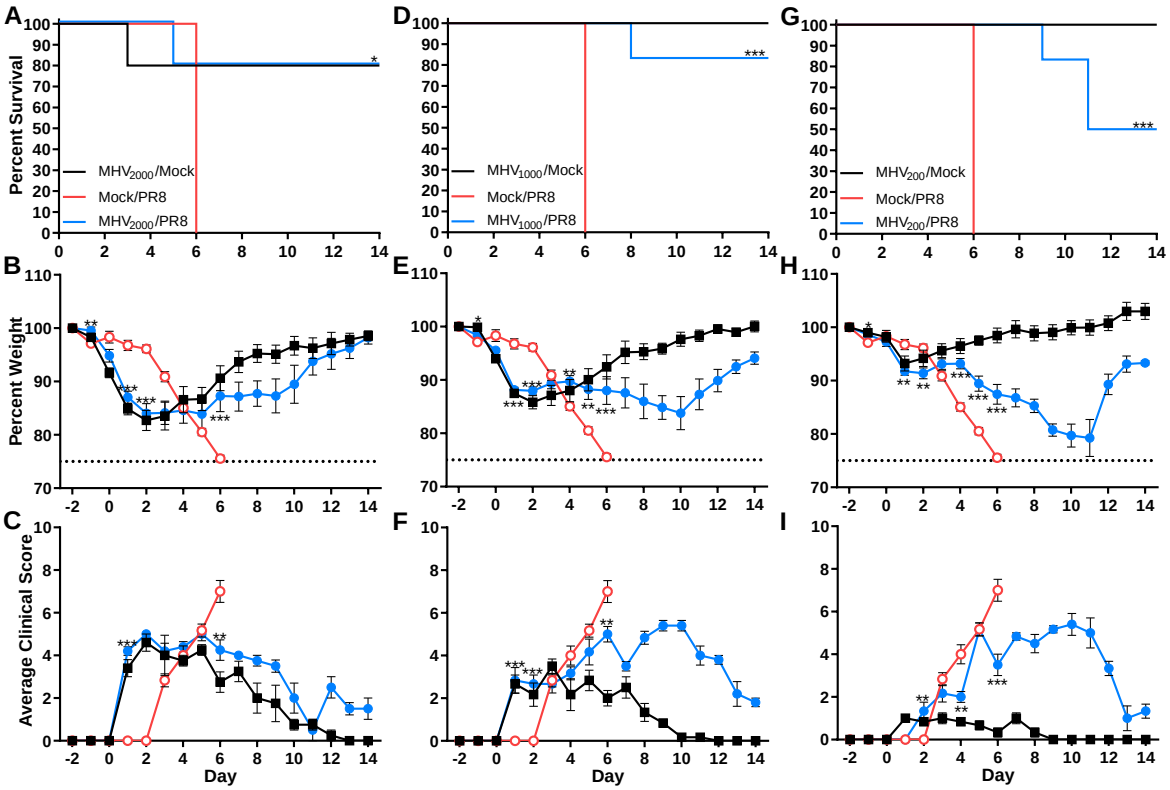


**Fig 4.10. MHV-mediated attenuation of PR8 disease was dependent on the severity of MHV infection.** Groups of 5-6 BALB/c mice were inoculated with Mock (media) or MHV ($2.0x10^3$ ($MHV_{2000}$), $1.0x10^3$ ($MHV_{1000}$), or $2.0x10^2$ ($MHV_{200}$) $TCID_{50}$/mouse) two days before PR8 (77.5 $TCID_{50}$/mouse). Mice were then monitored for mortality, weight loss, and clinical signs of disease (lethargy, ruffled fur, hunched back, labored breathing) for 14 days after PR8 inoculation. (A-C) $MHV_{2000}$ and PR8 coinfection mortality (A), weight loss (B), and clinical signs (C). (D-F) $MHV_{1000}$ and PR8 coinfection mortality (D), weight loss (E), and clinical scores (F). (G-I) $MHV_{200}$ and PR8 coinfection mortality (G), weight loss (H), and clinical scores (I). MHV/Mock (black lines, closed squares), Mock/PR8 (red lines, open circles), MHV/PR8 (blue lines, closed circles). Survival curves were compared using log-rank Mantel-Cox curve comparison versus Mock/PR8. Weight loss and clinical score data were compared using multiple Student's *t*-tests versus Mock/PR8. P-values shown as * ≤ 0.05, ** ≤ 0.01, or *** ≤0.001.

Coinfection using a moderate MHV dose still attenuated PR8-induced disease. However, the disease was more prolonged compared to coinfection with a severe MHV dose. Infection with moderate MHV alone ($MHV_{1000}$/Mock) was no longer lethal (Fig. 4.10D), but was associated with rapid weight loss. $MHV_{1000}$/Mock infected mice lost weight on day 0 until day 2 and then regained weight on day 3 until the end of the study (Fig. 4.10E). Clinical signs in moderate MHV-infection exhibited primarily as minor ruffling and hunching with sporadic minor lethargy and labored breathing from day 0 until day 8 before signs resolved (Fig. 4.10F). Although moderate MHV-infection was not lethal, coinfection with moderate MHV two days before PR8 ($MHV_{1000}$/PR8) was 17% lethal by day 8 (Fig. 4.10D). Weight loss during moderate MHV and PR8 coinfection had two discernable peaks. $MHV_{1000}$/PR8 coinfected mice initially lost weight from days 0-1 before weight plateaued on days 2-7 followed by a second weight loss peak around day 10 (Fig. 4.10E). Coinfected mice failed to fully recover their starting weight by the end of the study. Clinical signs in coinfected mice initially displayed on day 1 and progressed until days 9 and 10 before slowly diminishing (Fig. 4.10F). Clinical signs in coinfected mice presented as minor lethargy, ruffling, and hunching before they progressed to moderate lethargy and ruffling with minor hunching and labored breathing.

Finally, coinfection with a mild MHV infection and PR8 produced the poorest attenuation of PR8 disease. Mild MHV alone ($MHV_{200}$/Mock) was not lethal (Fig. 4.10G) and only induced transient, minor weight loss on days 0-1 (Fig. 4.10H). Clinical signs in mild MHV alone infection were limited to minor ruffling from days 0-7 before returning to baseline (Fig. 4.10I). Coinfection with a mild MHV infection two days before PR8 ($MHV_{200}$/PR8) resulted in 50% mortality by day 11 (Fig. 4.10G). Similar to moderate MHV coinfection, mice coinfected with a mild MHV infection also had two discernable weight loss peaks, but the second peak during coinfection with a mild MHV-infection was more pronounced and severe compared to coinfection with a moderate MHV infection. Mild MHV coinfected mice initially lost weight from days 1-2 before a small increase in weight on day 3 (Fig. 4.10H). Coinfected mice did not exhibit any clinical signs associated with initial weight loss on days 0-1, but signs appeared during the secondary weight loss peak on days 2-12 (Fig. 4.10I). Coinfected mice initially presented with minor lethargy, ruffling, and hunching. Signs quickly progressed to moderate lethargy and ruffling with minor hunching

and labored breathing during the second peak in weight loss. These experiments provide evidence for coinfection-mediated disease attenuation being dependent upon the severity of the initial viral infection.

### 4.2.5 Effects of coinfection are dependent upon the timing of virus inoculations

As stated above, clinical reports lack the ability to discern the level of initial virus exposure before admittance to a hospital. Similarly, if clinicians identify multiple viruses in a patient, they cannot determine when that patient contracted each virus. This ignorance could mask why some viral coinfection pairings are reported to exacerbate disease in one study, while another study reports no differences in disease severity. Using our murine model of viral coinfection, we were interested in whether the timing of each virus infection affected disease severity.

To test this, mice were either inoculated with Mock (media) or RV two days before, simultaneously with, or two days after inoculation with a low (mild) or medium (moderate) dose of PR8 or PVM (Fig 4.11). Mice were monitored daily for mortality, weight loss, and clinical signs for 14 days after PR8 or PVM inoculation.

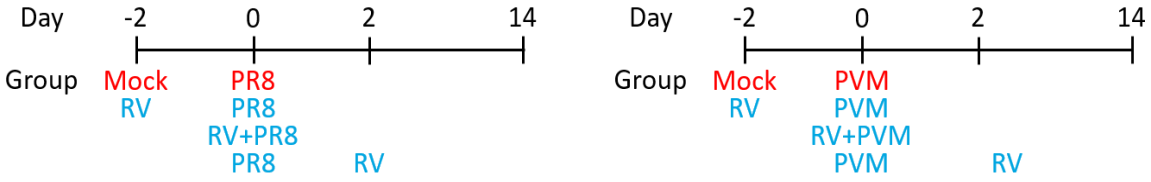


**Figure 4.11. Varied timings of coinfection inoculation scheme.** PR8 inoculations were given at both low (mild) and medium (moderate) doses for all timings.

All mice succumbed to a moderate PR8-infection (Mock/$PR8_{med}$) by day 8 (Fig. 4.12A). Rapid weight loss (Fig. 4.12B) and elevated clinical signs (Fig. 4.12C) began on day 3 and progressed until day 8. Coinfection with RV two days before moderate PR8 infection (RV/$PR8_{Med}$) was described above (Fig. 4.8) and will not be discussed here, but

mortality (Fig. 4.12A), weight loss (Fig. 4.12B), and clinical signs (Fig. 4.12C) data are shown for comparison. RV coinfected simultaneously with (RV+$PR8_{Med}$) and two days after ($PR8_{Med}$/RV) moderate PR8 infection did not attenuate PR8 disease in contrast to infection with RV two days before PR8 (RV/$PR8_{Med}$). Coinfection with RV simultaneously with and two days after PR8 were 100% lethal, and all mice succumbed to the infection on day 8 and day 7, respectively (Fig. 4.12A). There were no differences in weight loss observed between either RV+$PR8_{Med}$ or $PR8_{Med}$/RV and Mock/$PR8_{Med}$ (Fig. 4.12B). Mice simultaneously coinfected with RV and moderate PR8 exhibited similar levels of clinical signs as Mock/$PR8_{Med}$ infected mice from days 3 to 8 (Fig. 4.12C): intermittent moderate ruffling accompanied by minor lethargy, hunching, and sporadic labored breathing. However, coinfection with RV two days after $PR8_{Med}$ exhibited elevated signs from days 3 to 5, with a significant difference found on day 5 (Fig. 4.12C). Initial signs displayed by $PR8_{Med}$/RV coinfected mice were moderate ruffling with minor lethargy and ruffling before quickly rising to severe ruffling, moderate hunching, and minor lethargy and labored breathing.

RV-mediated disease attenuation was reduced as the timing between virus inoculations was shortened. Mice infected with a low dose of PR8 (Mock/$PR8_{Low}$) all succumbed to infection by day 9 (Fig. 4.12D) after continuous weight loss from day 3 on (Fig. 4.12E). Mock/$PR8_{Low}$ mice displayed minor ruffling on day 3, and signs increased to severe ruffling with moderate lethargy, hunching, and labored breathing by day 6 (Fig. 4.12F). In contrast to simultaneous coinfection with RV and moderate PR8 infection, RV still retained the ability to attenuate PR8 disease when coinfected simultaneously with a mild dose of PR8. RV+$PR8_{Low}$ coinfection was 33% lethal by day 9 (Fig. 4.12D). Simultaneously coinfected mice were not protected from PR8-induced weight loss and the weight loss curve matched Mock/$PR8_{Low}$ group until day 6. However, coinfected mice stopped losing weight by day 7 and began recovering on day 10 (Fig. 4.12E). Clinical signs were also similar between PR8 alone and simultaneously coinfected mice until day 8, when coinfected mice displayed fewer signs overall (Fig. 4.12F). Although the average clinical scores were similar between Mock/$PR8_{Low}$ and RV+$PR8_{Low}$, coinfected mice only exhibited moderate ruffling, whereas singly infected mice exhibited severe ruffling.

It is of particular importance to note that not only was PR8 disease attenuation lost when RV was inoculated two days after a mild PR8 infection (PR8/RV), but PR8 disease was exacerbated compared to mice infected with PR8 alone. PR8/RV coinfected mice initially succumbed to the infection on day 5, two days sooner than any other mild PR8 infection scheme (Fig. 4.12D). All PR8/RV coinfected mice succumbed to PR8 infection by day 7. Initial weight loss during PR8/RV coinfection occurred on the same day, day 3, as other coinfected and singly infected groups, however, the extent of weight loss was greater for PR8/RV mice than the other groups (Fig. 4.12E). Mice inoculated with RV two days after PR8 lost weight throughout the experiment and maintained a higher rate of weight loss than singly infected mice. Finally, PR8/RV mice began displaying higher average clinical scores than other coinfected and singly infected groups on day 3, and this trend continued throughout the experiment (Fig. 4.12F). Mice inoculated with RV two days after PR8 infection initially displayed moderate ruffling with some mild hunching on day 3, which rapidly progressed to severe ruffling and moderate lethargy, hunching, and breathing complications by day 4. This progressed to include moderate-severe lethargy and breathing complications by day 6. These data demonstrate that RV-mediated PR8 disease attenuation is dependent upon the timing between virus inoculations and the severity of the infection. For the most effective modulation of PR8 disease, RV requires at least two days before a subsequent challenge with a mild or moderate PR8 infection. However, more time could prove to be more effective than two days between inoculations, and more experiments will be needed to focus on further effects of inoculation timing.

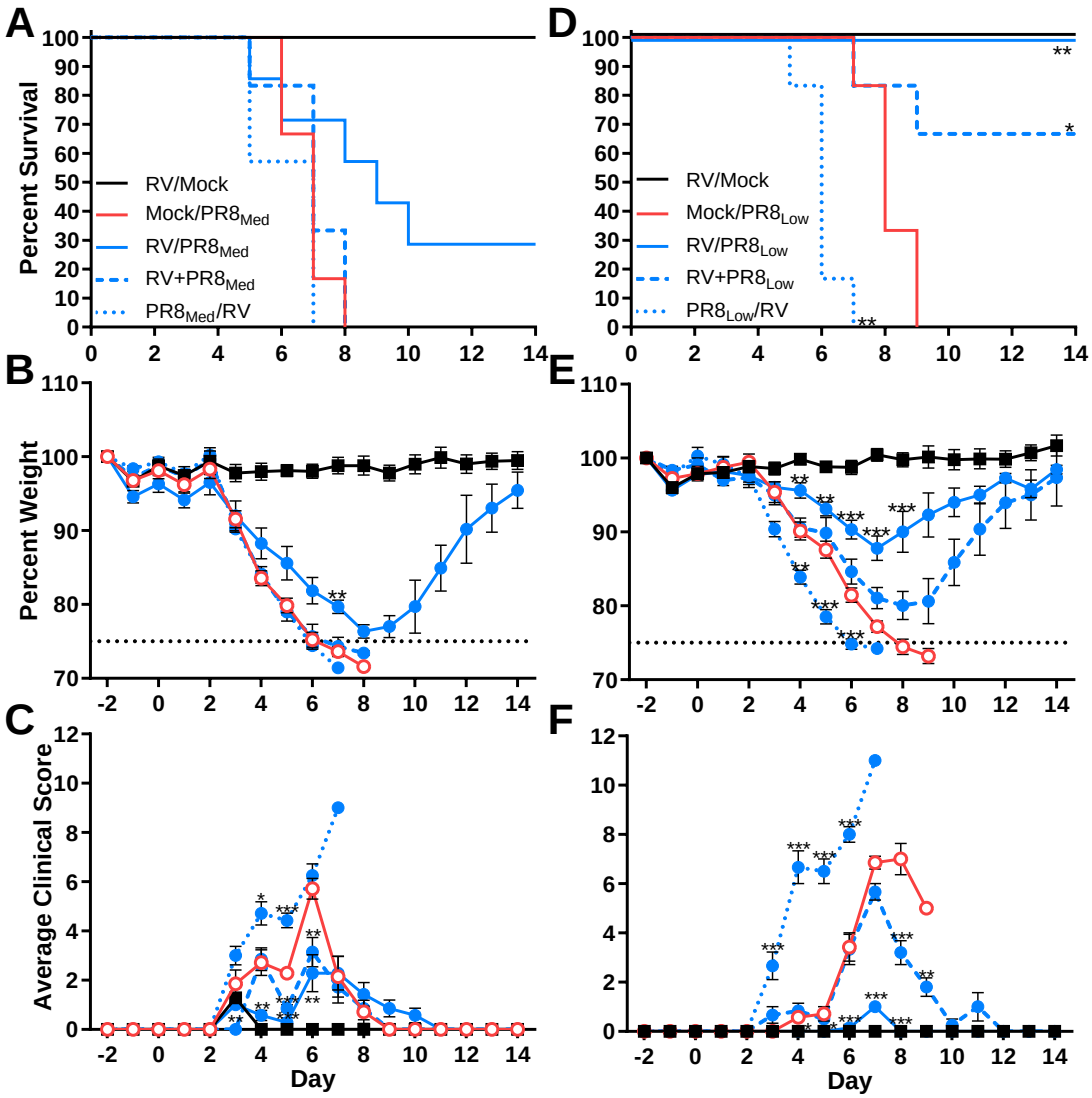


**Figure 4.12. Timing of virus inoculations affected RV-mediated attenuation of PR8 disease.** Groups of 6-7 BALB/c mice were inoculated with Mock (media) or RV ($7.6x10^6$ $TCID_{50}$/mouse) two days before (RV/PR8), simultaneously with (RV+PR8), or two days after (PR8/RV) PR8 (77.5 (low) or 150 (medium) $TCID_{50}$/mouse). Mice were then monitored for mortality, weight loss, and clinical signs (lethargy, ruffled fur, hunched back, labored breathing) for 14 days after PR8 inoculation. (A-C) RV and medium dose PR8 coinfection mortality (A), weight loss (B), and clinical signs (C). (D-F) RV and low dose PR8 coinfection mortality (D), weight loss (E), and clinical signs (F). Mock/PR8 (red lines, open circles), RV/PR8 (blue lines, closed circles), RV+PR8 (blue dashed lines, closed circles), PR8/RV (blue dotted lines, closed circles). Survival curves were compared using log-rank Mantel-Cox curve comparison versus Mock/PR8. Weight loss and clinical score data were compared using multiple Student's *t*-tests versus Mock/PR8. P-values are shown as * ≤ 0.05, ** ≤ 0.01, or *** ≤ 0.001.

Curiously, RV-mediated attenuation of PVM disease was less influenced by variations in the timing of inoculations. Infection with PVM alone (Mock/PVM) was 100%

lethal; all mice succumbed to infection by day 8 (Fig. 4.13A). Mock/PVM mice began losing weight on day 3 and steadily increased until day 8 when all mice had reached the designated 75% weight cutoff for euthanasia (Fig. 4.13B). PVM singly infected mice displayed minor ruffling on day 4 and progressed to severe lethargy, ruffling, labored breathing, and moderate hunching by day 6 (Fig. 4.13C). Coinfection with RV two days before PVM (RV/PVM) was detailed above and will not be discussed here, but mortality (Fig. 4.13A), weight loss (Fig. 4.13B), and clinical signs (Fig. 4.13C) data are shown for comparison. Interestingly, RV+PVM coinfected mice were all protected from mortality (Fig. 4.13A), weight loss (Fig. 4.13B), and clinical signs (Fig. 4.13C). All simultaneously coinfected mice survived until the end of the study and experienced minimal weight loss; the peak weight loss was 7% on day 7. Coinfected mice displayed no signs of infection except for day 4 when 3 of 7 mice exhibited mild ruffling. When mice were coinfected with RV two days after PVM (PVM/RV), coinfection no longer attenuated disease severity. RV coinfection two days after PVM (PVM/RV) was 100% lethal, and all coinfected mice succumbed to infection by day 8, similar to the Mock/PVM-infected group (Fig. 4.13A). Weight loss in PVM/RV coinfected mice was almost identical to that in Mock/PVM infected mice. PVM/RV coinfected mice began losing weight on day 3 and increased until reaching the 75% weight cutoff on day 8 (Fig. 4.13B). PVM/RV coinfected mice exhibited minor ruffling on day 3, followed by moderate ruffling and hunching with minor lethargy and labored breathing on day 6 (Fig. 1C). These signs increased to severe lethargy with moderate ruffling, hunching, and labored breathing on day 8.  (Fig. 4.13C).

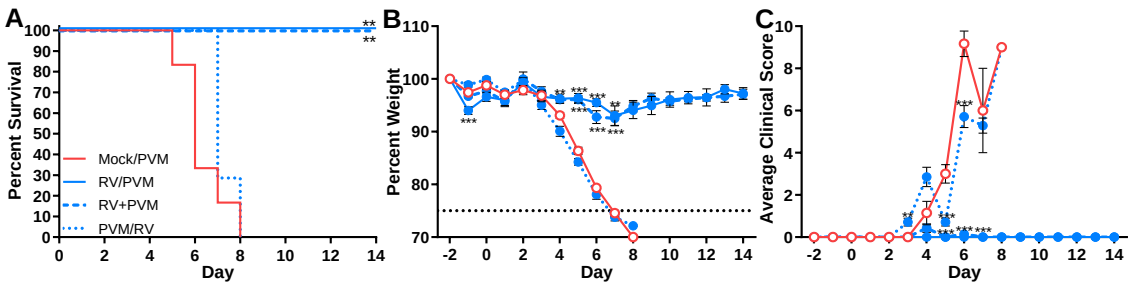


**Figure 4.13. Timing of virus inoculations affected RV-mediated attenuation of PVM disease.** Groups of 7 BALB/c mice were inoculated with Mock (media) or RV ($7.6x10^6$ $TCID_{50}$/mouse) two days before (RV/PVM), simultaneously with (RV+PVM), or two days after (PVM/RV) PVM ($1.0x10^4$ $TCID_{50}$/mouse). Mice were then monitored for mortality, weight loss, and clinical signs (lethargy, ruffled fur, hunched back, labored breathing) for 14 days after PVM inoculation. (A-C) RV and PVM coinfection mortality (A), weight loss (B), and clinical scores (C). Mock/PVM (red lines, open circles), RV/PVM (solid blue lines, closed circles), RV+PVM (blue dashed lines, closed circles), PVM/RV (blue dotted lines, closed circles). Survival curves were compared using log-rank Mantel-Cox curve comparison versus Mock/PVM. Weight loss and clinical score data were compared using multiple Student's *t*-tests versus Mock/PVM. P-values are shown as ** ≤ 0.01 or *** ≤ 0.001.

## 4.3 Discussion

Respiratory viral coinfections remain a metaphorical Pandora's box because there is the potential for many interactions within the host. Clinical data cannot inform when a person contracts each virus or the severity of each infection by itself. This may explain why some coinfections are reported to be beneficial versus detrimental to the host. Our murine model of respiratory viral coinfection provides evidence that the effects of coinfection are dependent on both the timing and severity of each infection, while variations in coinfection dynamics, e.g., rates of weight loss and mortality, are based on which viruses are used.

Our initial coinfection experiments determined that a minor group rhinovirus attenuated disease caused by multiple unrelated viruses: influenza A virus, pneumonia virus of mice, and mouse hepatitis virus. This fits with a trend observed by another group that found infection with HRV reduced the chances of infection by several other respiratory viruses, including IAV and RSV (50). Interestingly, when RV was inoculated two days after PVM, coinfection was not able to attenuate disease, and when given after PR8, the disease was exacerbated. Similarly, RV-mediated disease attenuation was reduced during coinfection with a moderate or severe PR8 infection. These data imply that RV induces an immune response capable of attenuating PR8 or PVM disease when given enough time

between inoculations. But when infection severity is increased, or timing before the secondary infection is reduced, RV-induced responses become overwhelmed, and attenuation is rendered less effective.

Rhinovirus infection could influence disease severity by stimulating the immune system in two main ways: antiviral response or cellular response. An antiviral response, mediated by production of interferon and inflammatory cytokines, interferes with replication and spread of viruses during an infection. The antiviral response is usually accompanied by the recruitment of immune cells by production of chemokines during infection. The immune system uses these mechanisms to control and clear virus infections within the host. Eliciting an antiviral response is mediated through recognition of viruses by pattern recognition receptors (e.g., toll-like receptors) leading to stimulation of type I IFNs, which can regulate protein synthesis or cell susceptibility to infections. RV induces production of type I IFN through stimulation of TLR3, RIG-I, and MDA-5 and type III IFN through stimulation of RIG-I and MDA-5 (66). This is important because Bartlett *et al*. reported that RV induced production of both types I and III IFN in a mouse model (52). Knockdown of interferon regulatory factor 7 during RV infection suppressed type I IFN production, which was associated with a reduction in macrophage and neutrophil numbers in the airways (142). This implies that coinfection could use a coupled antiviral and cellular response to control a secondary infection by producing early type I IFN, leading to downstream activation of immune cells. TLR4 deficiency has been implicated in mouse susceptibility to MHV-induced mortality (72). Recognition of RV by various PRRs may supplement MHV-dependent signaling mechanisms leading to stronger interferon production generating a protective antiviral response.

Type I and III IFNs are produced following IAV infection in mice (143, 144). Type I IFN production during IAV infection helps limit inflammation in the lungs (145). An increase in mortality and viral load is observed when type I IFN receptor (146) or interferon-β (147) is knocked out during IAV infection. Knockout of type I IFN receptor dysregulates downstream chemokine production and recruitment of neutrophils. Type I IFN produced by an initial virus infection could then lead to downstream production of chemokines to recruit neutrophils and macrophages, which would be able to respond to a subsequent infection.

Type I IFNs do not work alone but in conjunction with type III IFNs. Type III IFNs are produced faster than type I and are preferentially produced during a sublethal IAV infection and is sufficient to control infection (148). Although both types I and III IFNs are required for efficient control of IAV, excessive amounts of type I IFN can be detrimental and is associated with increased IAV disease (149). Type I IFNs are produced up to day 6 during PVM-infection in mice (150, 151) and contribute to reducing PVM pathogenesis (152). Type III IFNs are also produced following PVM infection of RAW macrophages (153). Knockout of type I IFN receptor during PVM infection slightly increases survival of mice, but viral clearance is delayed in knockout mice. Increased survival may be linked to decreased neutrophils in knockout mice and altered inflammatory responses. Type III IFN remains poorly understood in the context of PVM infection. MHV induces the production of type I IFN in multiple strains of mice (55, 83). De Albuquerque *et al*. found MHV-resistant mouse strains produced higher amounts of type I IFN transcript than susceptible mice. Further studies found type I IFN receptor knockout mice (MHV-resistant strains) are more susceptible to MHV-induced mortality and weight loss and reduced viral clearance following infection (154, 155).

This early induction of type I and III IFNs could limit inflammation when RV is inoculated two days before PVM or PR8. But when RV is inoculated two days after PVM, the protective effects of early interferon production are lost, and PVM-induced inflammation is no longer controlled, which fits our model of exacerbated disease observed when RV is inoculated two days after PR8. Another potential mechanism involved is an initial RV infection could be inducing recruitment of neutrophils and macrophages, which would be activated by type I IFN. These immune cells could then contribute to efficient control of a subsequent infection. This fits with the timing of infection experiments: coinfection-mediated disease attenuation is reduced or lost when RV is inoculated simultaneously with PR8 or two days after PR8 and PVM because there is no longer early recruitment of immune cells. Further, we observed variability in attenuation of PR8 disease when we tested multiple severities of initial MHV infections. Mild MHV infection may not induce a strong enough interferon response leading to impaired recruitment of immune cells. Thus coinfection-mediated disease attenuation is not as effective as a higher MHV infection severity.

RV infection in mice is known to induce mucin-5 subtypes A and C (Muc5AC) along with proinflammatory cytokines (52, 156, 157). While overexpression of Muc5AC in mice reduces both PR8 titers and recruitment of inflammatory cells (158), mucin genes are linked to pathogenesis during RSV (159) and IAV (34) infection. Since RV can induce mucin production, this could be involved in limiting early viral replication and spread, thereby limiting the overexpression of mucin genes associated with severe IAV and RSV infections. This hypothesis is supported by the finding that *Schistosoma mansoni* infection in mice induces early tumor necrosis factor alpha production and mucus secretion, which reduces PR8- and PVM-induced mortality during secondary challenge (160). But when RV is inoculated two days after PVM, this could help further exacerbate observed PVM disease. These responses can also work in conjunction with cellular responses of the immune system to help limit the spread of infection.

The *in vitro* experiments from chapter 3 determined that RV did not affect PR8 replication in lung epithelia. This implies that RV is stimulating an immune response partially dependent on cellular mechanisms, which help modulate secondary virus disease. Neutrophils are known to play a protective role against influenza infection, as evidenced by neutrophil depletion studies (53, 161). However, excessive neutrophil recruitment to the lungs damages alveolar architecture and increases the viral load (162). Initial infection with RV may be recruiting neutrophils, as Bartlett *et al.* report, leading to attenuation of PR8 disease. These early recruited neutrophils would already be at the site of infection and primed to respond to a secondary virus. However, when time is reduced between RV and PR8, the RV-recruited neutrophils become harmful by contributing to extensive inflammation in the lungs and increase PR8 disease severity. This presumption correlates with the release of tumor necrosis alpha, cytokine linked to mucus production, from neutrophils correlating with mucus plugs during RSV pathology (159).

Pre-infection with RV may prime alveolar macrophages, leading to protection from secondary virus infections. An initial rhinovirus infection in mice delays the clearance of a secondary bacterial infection (118). This delay is attributed to attenuating chemokine production from alveolar macrophages, which reducing neutrophil recruitment to the lungs. This study demonstrates that rhinovirus alters alveolar macrophage responses to a secondary

stimulus. Alveolar macrophages are susceptible to PVM and can produce infectious virions (163). One group reported that priming of alveolar macrophages with *Lactobacillus plantarum* reduced PVM infection of both alveolar macrophages and dendritic cells, and reduced the production of PVM virions from alveolar macrophages and promoted survival of infected mice (163). Alveolar macrophage depletion studies report an increase in mortality following influenza infections compared to healthy animals (164, 165). However, alveolar macrophage depletion improves survival during MHV infection in mice (166). Concomitantly, this RV priming effect may predispose alveolar macrophages to be less pro-inflammatory or could control alveolar macrophage responses to ameliorate their detrimental effects during MHV infection. Attenuation during RV coinfection is most likely a combination of several effects leading to a more controlled immune response and reducing immune-mediated cytopathic effects during infections.

Coinfection-mediated disease attenuation was not limited to RV but was also observed during coinfection with MHV and PR8 or PVM. Both coinfection of mice with MHV two days before PR8 or PVM disease kinetics mimicked kinetics observed in MHV/Mock infections. These data heavily imply that MHV infection is inducing an MHV-dominated immune response in mice, which can suppress immune responses normally induced by PR8 or PVM. MHV infection in mice generates diffuse inflammation and recruits a large percentage of lymphocytes followed by macrophages but only a small percentage of neutrophils (72). This small but limited inflammatory cell recruitment may provide the same protection conveyed during RV coinfection. T cells are necessary for PVM clearance from the lungs (167), but these lymphocytes are also implicated in PVM-induced weight loss and inflammation (150, 167). T cell recruitment has been reported to protect mice against PR8 infection and adoptive transfer of activated T cells one day before PR8 infection protected from PR8-induced mortality (168). These studies provide a potential role for early MHV-dependent recruitment of T cells contributing to control and clearance of both PR8 and PVM during coinfection. This early control could be limiting harmful effects induced by T cell responses observed at later time points in PVM and PR8 infection. We also discovered the degree of MHV-mediated reduction of PR8 disease was dependent upon the severity of MHV infection. This implies that if MHV does not establish a strong

infection, then recruited cells and inflammatory responses may also not be strong enough to reduce PR8-induced disease.

Together, these data demonstrate that coinfection-mediated disease attenuation is dependent upon certain infection parameters. The severity of primary and secondary infections, along with timing and order of viral inoculations, exhibit strong influences on the outcome of respiratory viral coinfection. Both RV and MHV attenuated disease from multiple viruses leading to the idea that viral pairings may not have a significant effect on coinfection outcomes, but a combination of infection severity and timing is critical. Coinfection with multiple viruses can alter immune responses due to the induction of different immune pathways unique to each virus. These changes have the potential to supplement ineffective responses or exacerbate disease by overexpressing inflammatory mediators. More directed studies are required to tease out which infection parameters contribute to disease outcome during coinfection and which mechanisms are essential for attenuating disease severity.

# CHAPTER 5

# Elucidation of Mechanisms that Contribute to Coinfection-Mediated Disease Attenuation

## 5.1 Overview

We previously found that both RV and MHV attenuated severe respiratory viral infections during coinfection. We also determined that RV- or MHV-mediated effects on disease severity during coinfection were unique to each virus pairing. The initial virus infection may heavily influence the immune responses during coinfection. Although RV and MHV are RNA viruses with respiratory tract tropisms, they are known to stimulate both common and unique immune responses during infection.

RV is a well-known pathogen in humans, but this virus also stimulates some minor immune responses in mice. Other studies observe that RV stimulates the PRRs RIG-I, MDA5, and TLR3 *in vitro* (65, 66) and *in vivo* (68). RV stimulation of MDA5 and TLR3 are required for maximum type I and III IFN and chemokine responses. Similar to RV, MDA5 is implicated in recognition of MHV in macrophages, resulting in the production of type I IFN (75, 169). Along with MDA5, activation of TLR4 is known to protect mice from lethal MHV infection (72). This early stimulation of MDA5 could be critical to control IAV. IAV recognition is thought to be dominated by RIG-I (170), but the NS1 protein of IAV silences MDA5 signaling, reducing type I IFN signaling (171). Early stimulation of PRRs could generate an antiviral state through the production of type I IFNs and downstream interferon-stimulated genes that could overwhelm NS1 silencing and help recruit and activate immune cells. However, disease attenuation mediated by early induction of type I IFN is unlikely during MHV infection because studies with other strains of MHV report that MHV inhibits type I IFN production by failing to activate nuclear factor kappa-light-chain-enhancer of activated B cells (NF-kB) and interferon regulatory factor (IRF) 3 for nuclear translocation (172, 173). Our laboratory has also shown that lung epithelial cells infected by MHV fail to differentially express many type I IFNs and IFN receptor genes *in vitro* (85). This limited

type I IFN response could be beneficial to coinfection because an excessive type I IFN response is associated with increased mortality and weight loss in mice infected with IAV (149). These experiments suggest that coinfection-mediated disease attenuation may involve early type I IFN production and recruitment of immune cells.

Recognition of infection is quickly followed by recruitment of inflammatory innate immune cells and then lymphocytes to the site of infection. Following the recognition of RV in a murine model, neutrophils are recruited to the lungs by the production of chemokines such as C-X-C motif chemokine ligand (CXCL) 1 and CXCL2 (52) in a C-X-C motif chemokine receptor (CXCR) 2-dependent manner (76). MHV is also known to rapidly recruit neutrophils to the lungs and peripheral organs during infection (169, 174, 175). Neutrophils are known to contribute to inflammation (162), but in the scope of IAV infection, they help limit IAV-induced peribronchiolar inflammation and alveolitis and promote survival of infected mice (176). Neutrophils recruited by RV and MHV may provide a strong frontline defense against subsequent PR8 infection and limit PR8-induced inflammation. Another mechanism for reduction of IAV-induced inflammation is seen during effector T cell infiltration. These infiltrating lymphocytes produce interleukin (IL)-10 to help ameliorate immune-mediated pulmonary damage (177). Following RV-mediated recruitment of neutrophils, lymphocytes are recruited via the production of interferon gamma-induced protein 10 (IP-10) and C-C motif chemokine ligand 5 (CCL5) (52). MHV infection also recruits macrophages and lymphocytes at later time points during infection (55, 72, 169). Recruitment of inflammatory macrophages can help limit the spread of a secondary virus while recruitment of lymphocytes can expedite viral clearance and resolution of inflammation.

Initial RV or MHV infection reduced the disease severity of a secondary lethal viral infection. Both RV and MHV induce shared immune responses through host recognition by PRRs, which lead to downstream production of type I IFNs and inflammatory mediators. However, our *in vitro* data suggest that coinfection-mediated disease attenuation is dependent upon a cellular immune response more than a type I IFN/antiviral state response. Here we use an *in vivo* model to determine the roles of recruited cells and cytokine/chemokine responses during RV or MHV coinfection with PR8 or PVM.

## 5.2 Results

### 5.2.1 RV and MHV effects on PR8 replication in the lungs are unique to each virus

Experiments from chapter 4 determined that coinfection with either RV or MHV two days before PR8 attenuated PR8-induced disease. We were then interested if disease attenuation were associated with inhibition of PR8 replication. To test this, we inoculated mice with either Mock (media), RV, or MHV two days before inoculation with PR8. Groups of mice were euthanized, and lungs were collected on days 2, 4, 7, and 10 for RV and PR8 coinfection or days 2 and 4 for MHV and PR8 coinfection. Lungs were homogenized, and PR8 was titrated by $TCID_{50}$ assay on MDCK cells.

PR8 replication was affected by coinfection with either RV or MHV. However, RV/PR8 and MHV/PR8 coinfections induced contrasting effects. RV inoculation two days before PR8 did not interfere with early PR8 replication but led to faster clearance of PR8 from the lungs compared to mice infected with PR8 alone. PR8 titers peaked on day 2 during both single infection (Mock/PR8) and coinfection (RV/PR8) (Fig. 5.1A). Although both groups shared comparable timings in peak viral titers, differences in PR8 clearance were observed. On day 7, PR8 singly infected mice retained PR8 titers around $10^4$ $TCID_{50}$ per gram of lung. Interestingly, all coinfected mice, except one, had cleared PR8 from the lungs by day 7. Mock/PR8 infected mice eventually cleared PR8 from the lungs by day 10, three days after RV/PR8 coinfected mice. Thus, it is not the immediate early response induced by RV that is important for controlling PR8, but some arm of the immune system that requires time to activate.

In contrast, pre-infection with MHV disrupted early, but not late, PR8 replication. PR8 titers in singly infected (Mock/PR8) mice were measured at about $10^6$ $TCID_{50}$ per gram of lung on day 2 (Fig. 5.1B). However, coinfected (MHV/PR8) mice had significantly lower titers on day 2 than Mock/PR8 mice. The delay in PR8 replication in coinfected mice was short-lived because, on day 4, both Mock/PR8 infected and coinfected mice had similar PR8 titers. MHV infection may be inducing an early immune response sufficient to delay PR8 replication, but not completely inhibit PR8 infection. Thus, early recognition of a primary virus infection does not prevent infection. Coinfection-mediated effects on PR8 replication

may be dependent upon unique immune responses or different levels of induction of shared immune responses to each virus.

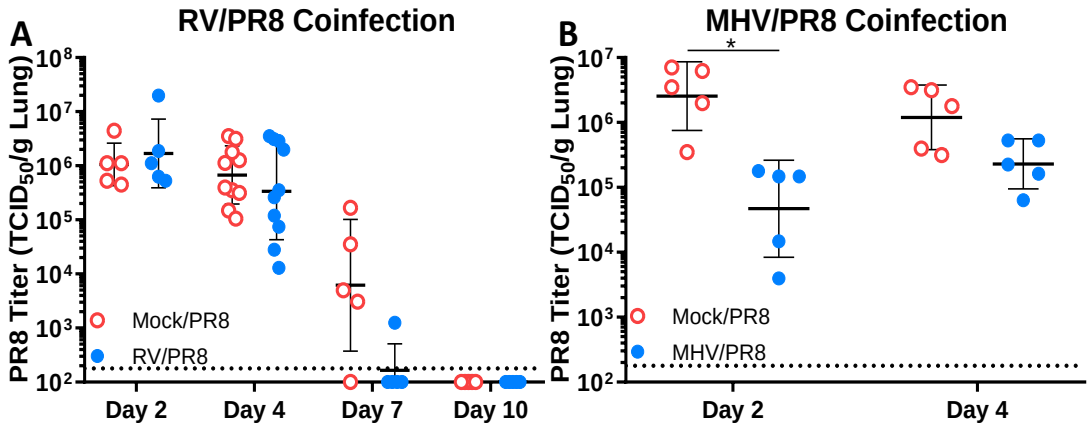


**Figure 5.1. Coinfection-mediated effects on PR8 replication were dependent upon which viruses were involved.** Groups of 5-10 mice were inoculated with Mock, RV ($7.6x10^6$ $TCID_{50}$/mouse), or MHV ($2.0x10^3$ PFU/mouse) on day -2. Two days later, on day 0, mice were inoculated with PR8 (77.5 $TCID_{50}$/mouse). Lungs were collected on days 2, 4, 7, and 10. PR8 was titrated by $TCID_{50}$ assay on MDCK cells A) PR8 titers from RV and PR8 coinfection. Mock/PR8 (red, open circles), RV/PR8 (blue, closed circles). B) PR8 titers from MHV and PR8 coinfection. Mock/PR8 (red, open circles), MHV/PR8 (blue, closed circles). Significance versus Mock/PR8 was determined by students *t*-test. P-values are shown as * ≤ 0.05.

### 5.2.2 Coinfection reduces PR8-induced inflammation in the lungs

RV infection did not interfere with early PR8 replication in the lungs. We were interested in visualizing the extent of inflammation in the lungs during coinfection with RV and PR8 compared to PR8 single infection. Mice were either inoculated with Mock or RV two days before inoculation with PR8. Lungs were harvested from mice on days 4, 7, and 10 after PR8 inoculation. Lungs were paraffin-embedded and sectioned then stained using hematoxylin and eosin. Staining was performed by Emmanuel Ijezie, and data analysis was spearheaded by Dr. Onesmo Balemba.

Coinfection with RV and PR8 induced immune cell infiltration early and limited inflammation at later time points. Mice singly infected with PR8 had no visible signs of infection on day 4 (Fig. 5.2). Day 4 histology sections showed large areas of white space, meaning gas exchange and respiration were not hindered. However, coinfection with RV

two days before PR8 (RV/PR8) showed evidence of immune cell infiltration on day 4. These immune cells were associated with a slight thickening of alveolar walls, but overall, these lungs remained relatively healthy. On day 7, diffuse inflammation was seen in the Mock/PR8 group along with a large number of immune cells. This disruption of the alveolar architecture could decrease the area available for gas exchange. RV/PR8 coinfected mice inflammation was not as severe as in Mock/PR8 infected mice on day 7. Coinfected mice also had increased immune cell recruitment into the airways, but this cellular recruitment left the alveoli relatively intact. By day 10, both groups of mice had resolved the majority of inflammation in the lungs, but focal areas of alveolar wall thickening, and immune cell infiltration were present in the singly infected mice. These lung sections revealed that coinfection generated a strong influx of immune cells, which were potentially controlling inflammatory responses seen in Mock/PR8 infected lungs.

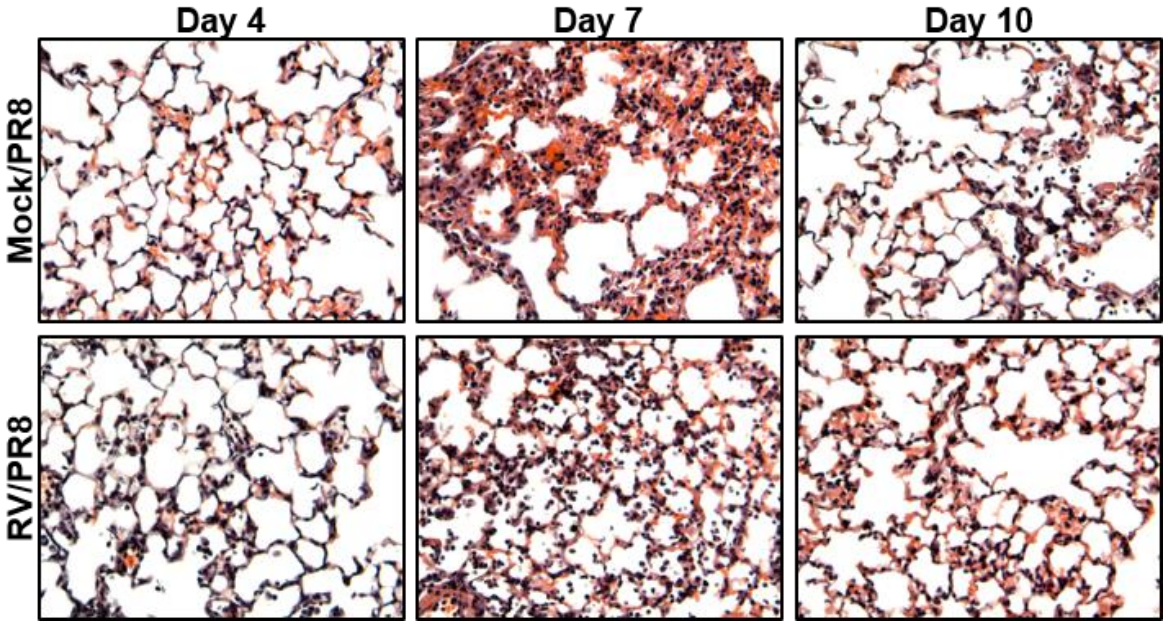


**Figure 5.2. Pre-infection with RV limited PR8-induced inflammation.** Mice were inoculated with Mock or RV ($7.6x10^6$ $TCID_{50}$/mouse) on day -2. On day 0, mice were inoculated with PR8 (77.5 $TCID_{50}$/mouse). Whole lungs were collected on days 4, 7, and 10 and stored in 10% formalin. Lungs were then paraffin embedded and sectioned before stained with hematoxylin and eosin. Images were taken using the 40X objective.

### 5.2.3 Coinfection-mediated disease attenuation is correlated with an early, but controlled, neutrophil response

Changes in immune responses during coinfection compared to single virus infections may be driving the differences in inflammation and PR8 clearance. These alterations can affect cell recruitment (e.g., type or number of cells) to sites of infection, thus influencing disease outcome and eventual viral clearance. To address this, we inoculated mice with Mock or RV two days before PR8 or PVM. Innate and T cell recruitment to the lungs were analyzed by flow cytometry on days 2, 4, and 6 after PR8 or PVM inoculation. Samples from mice inoculated with Mock or RV were also collected on day 0. Cells were identified by flow cytometry using the following markers: neutrophils (CD11b+Ly6G+), activated neutrophils (CD11b+Ly6G+CD64+), alveolar macrophages (CD11b-CD64+SiglecF+), interstitial macrophages (CD11b+Ly6G-CD64+), CD4+ T cells (CD3+CD4+), and CD8+ T cells (CD3+CD8+). Cells were initially gated on “Potential cells” to remove any debris and then gated on “Singlets” to select for single cells versus groups of cells (Fig. 5.3).

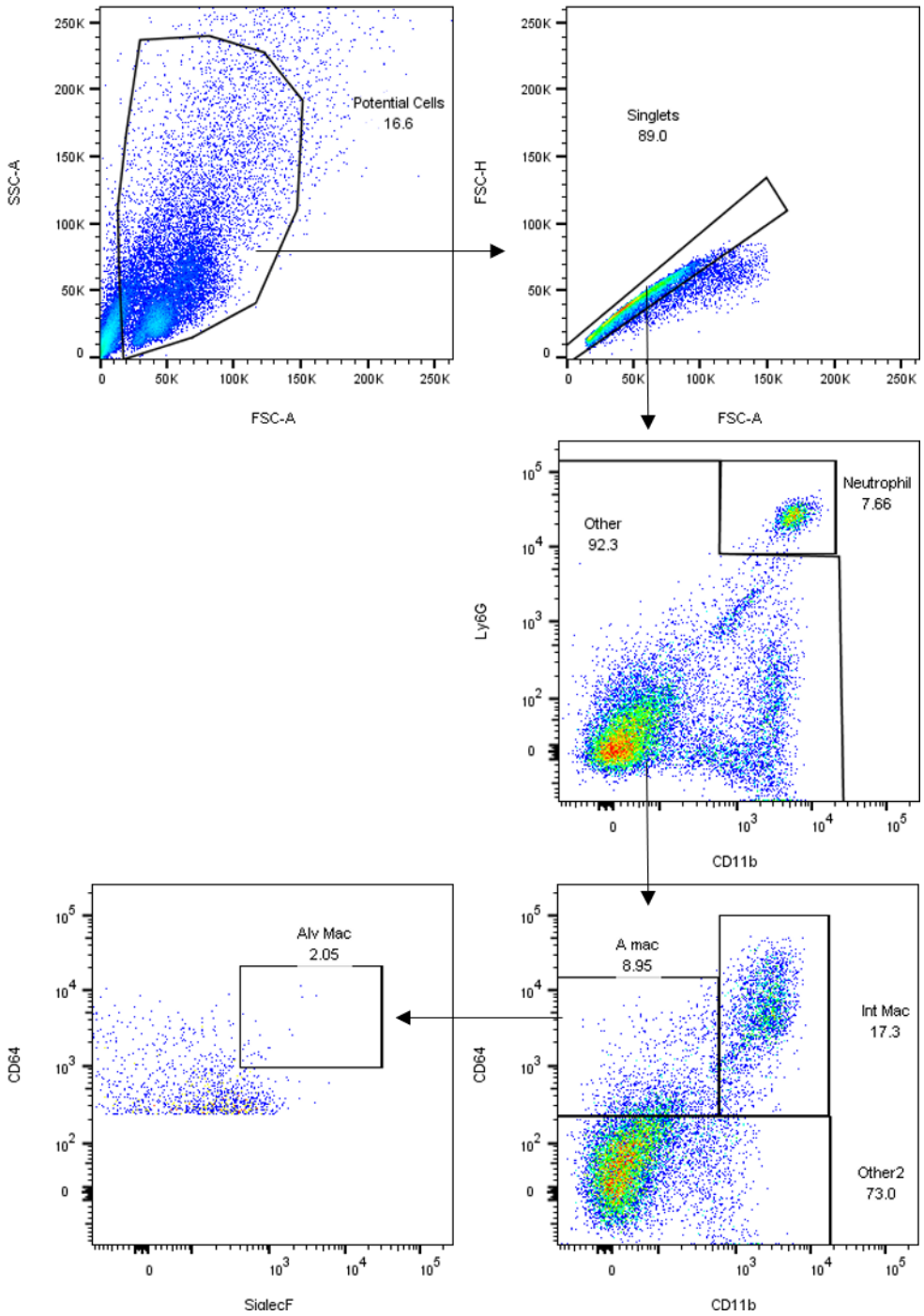


**Figure 5.3. Innate cell gating strategy.**

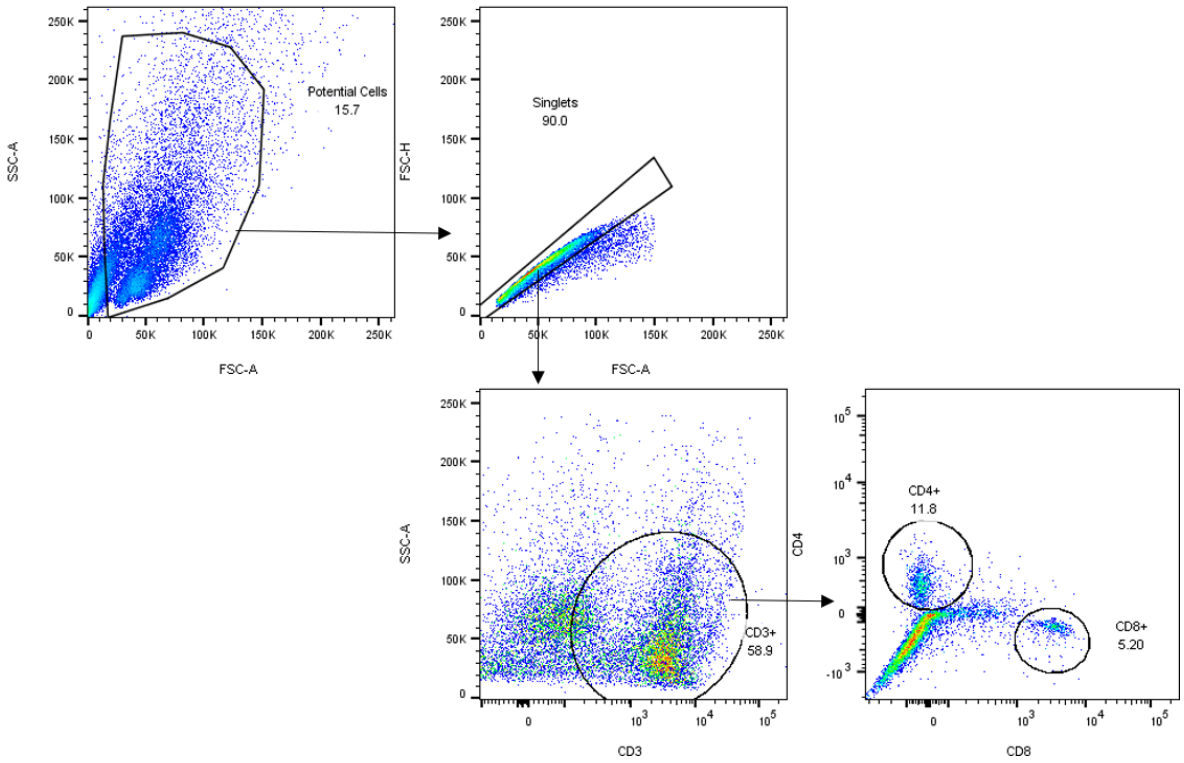


**Figure 5.4. T cell gating strategy.**

Pre-infection with RV limited neutrophil recruitment during coinfection compared to PR8 infection. Variable neutrophil numbers were recorded for PR8-infected mice on day 0, but minimal activated neutrophils were found as seen in both total cell count and percent cell graphs (Fig. 5.5A). Neutrophil numbers for Mock/PR8-infected mice increased on day 2 and were maintained until day 6 when neutrophil numbers decreased. Coinfection with RV and PR8 (RV/PR8) was marked by early neutrophil recruitment, similar to previous studies focused on RV infection (52, 76) (Fig. 5.5A). However, neutrophil numbers declined in RV/PR8 coinfected mice by day 2 and continued decreasing until day 6. Although neutrophil numbers were lower in coinfected versus Mock/PR8-infected mice on day 2, activated neutrophil numbers remained higher in the RV/PR8 coinfected group. On days 4 and 6, activated neutrophils in coinfected mice were reduced to levels below Mock/PR8-infected mice. These RV-activated neutrophils could respond faster to help control PR8 infection, leading to an earlier contraction in neutrophil accumulation, thereby limiting neutrophil-mediated damage to the lungs.

Fewer differences in macrophage populations were seen during Mock/PR8 versus coinfection. Pre-infection with RV two days before PR8 did not alter interstitial macrophage (IM) recruitment when compared to Mock/PR8 infection. Of note, coinfected mice had significantly more total IM than Mock/PR8-infected mice on day 2, but this was not significant when considering the percentage of all responding cell types (Fig. 5.5A). On day 4, the trend switched, and coinfected mice had fewer IM as a percentage of responding cell types compared to Mock/PR8-infected mice, but this was not significantly different for total IM between groups. Initial RV infection resulted in a reduction of total and percent alveolar macrophages (AM) on day 0 compared to Mock-inoculated mice (Fig. 5.5A). However, AM numbers and rate of decline were similar between Mock/PR8 and coinfected (RV/PR8) mice on days 2, 4, and 6.

T lymphocyte recruitment was also measured to monitor adaptive immune responses. We found no significant differences in either CD4 (Fig. 5.5B) or CD8 (Fig. 5.5B) T cell populations between Mock/PR8-infected mice and coinfection throughout the experiment. CD4 T cells declined early in both groups, but RV/PR8 coinfected mice sustained numbers slightly higher than Mock/PR8-infected mice from days 2 to 6. These data associated attenuation of PR8-induced disease severity with early neutrophil stimulation and limited neutrophil recruitment at later times with no major differences in other cell types.

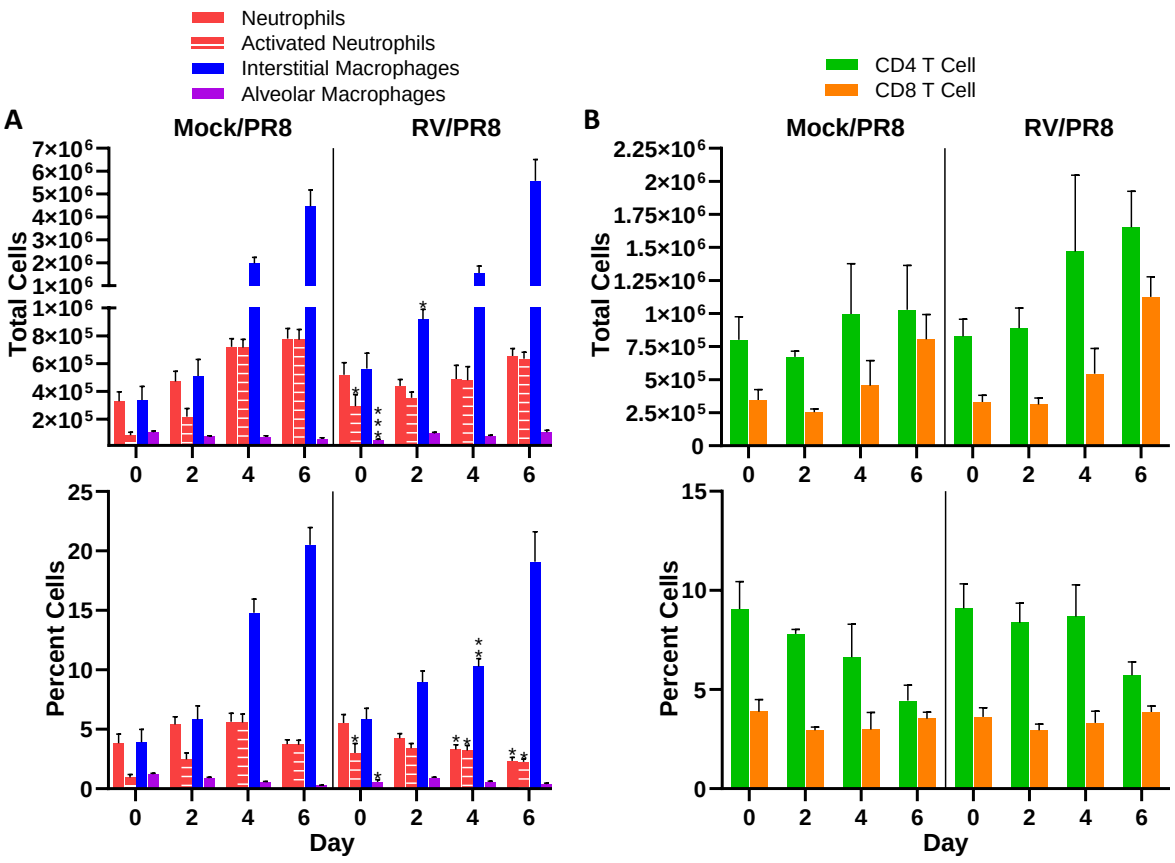


**Figure 5.5. Flow cytometry analyses of recruited cells to the lungs during RV and PR8 coinfection compared to PR8 single infection.** Groups of 5 mice were inoculated with Mock or RV ($7.6x10^6$ $TCID_{50}$/mouse) on day -2. Two days later on day 0, mice were inoculated with PR8 (77.5 $TCID_{50}$/mouse). Lungs were collected on days 0, 2, 4, and 6. Lungs were homogenized and single cell suspensions were stained for the following cell types: A) total and percent neutrophils (solid red bars; CD11b+Ly6G+), activated neutrophils (striped red bars lines; CD11b+Ly6G+CD64+), interstitial macrophages (blue bars; CD11b+Ly6G-CD64+), and alveolar macrophages (purple bars; CD11b-CD64+SiglecF+). B) total and percent CD4+ T cells (green bars; CD3+CD4+) and CD8+ T cells (orange bars; CD3+CD8+). Significance versus Mock/PR8 for each cell type was determined by students *t*-test. P-values are shown as * ≤ 0.05, ** ≤ 0.01, or *** ≤ 0.001.

RV and PVM coinfection limited neutrophil recruitment to a higher degree than coinfection with RV and PR8. Neutrophil recruitment and activation in Mock/PVM-infected mice began on day 4 and increased until day 6 (Fig. 5.6A). We did not observe an early increase in neutrophil numbers or activation on day 0 following RV infection (Fig. 5.6A). This implies that the dose we used may be at the limit of RV-induced cell recruitment in mice or specific to our mouse cohort used in this experiment. Interestingly, coinfection with RV two days before PVM (RV/PVM) severely limited neutrophil recruitment on days 4 and 6 compared to infection with Mock/PVM. Coinfection-mediated restriction of neutrophil

recruitment was also associated with a reduction in activated neutrophils on days 4 and 6. These data, in combination with RV/PR8 coinfection data, further support the idea that preventing excessive neutrophilic inflammation may be important for coinfection-mediated protection.

IM recruitment in PVM-infected mice increased on day 4 and continued until day 6 (Fig. 5.6A). Coinfected mice had higher IM accumulation on days 0 and 2 compared to PVM-infected mice (Fig. 5.6A). Although coinfected mice had increased IM recruitment on days 4 and 6, IM numbers did not reach levels comparable to PVM-infected mice on either day. RV and PVM coinfection also maintained AM populations. PVM (Mock/PVM) infection reduced AM numbers on day 4 and continued to decrease on day 6 (Fig. 5.6A). Pre-infection with RV did not affect AM populations on day 0, with numbers similar to mock-inoculated mice (Fig. 5.6A). Mock/PVM infected and RV/PVM coinfected mice had similar numbers of AM on days 0 and 2, but RV/PVM coinfected mice maintained AM levels on day 4. However, this maintenance was short-lived and AM populations in coinfected mice declined on day 6, but levels remained higher than PVM-infected mice.

Coinfection with RV not only limited neutrophil recruitment upon PVM infection but also helped sustain T lymphocyte numbers. For both CD4+ and CD8+ T cells, PVM infection resulted in a steady decrease in total T cell numbers from day 0-6, but a sharp decrease in the percentage of T cell was observed on day 4, which progressed through day 6 (Fig. 5.6B). However, total and percent CD4+ and CD8+ T cell populations did not decrease as dramatically in coinfected mice compared to PVM-infected mice (Fig. 5.6B). The percentages of CD4+ and CD8+ T cells were only slightly reduced in RV/PVM coinfected mice on both days 4 and 6. Similar to RV and PR8 coinfection, coinfection-mediated attenuation of PVM disease was associated with limited recruitment of neutrophils, but RV and PVM coinfection also limited IM recruitment and prevented the decline in CD4+ and CD8+ T lymphocyte populations.

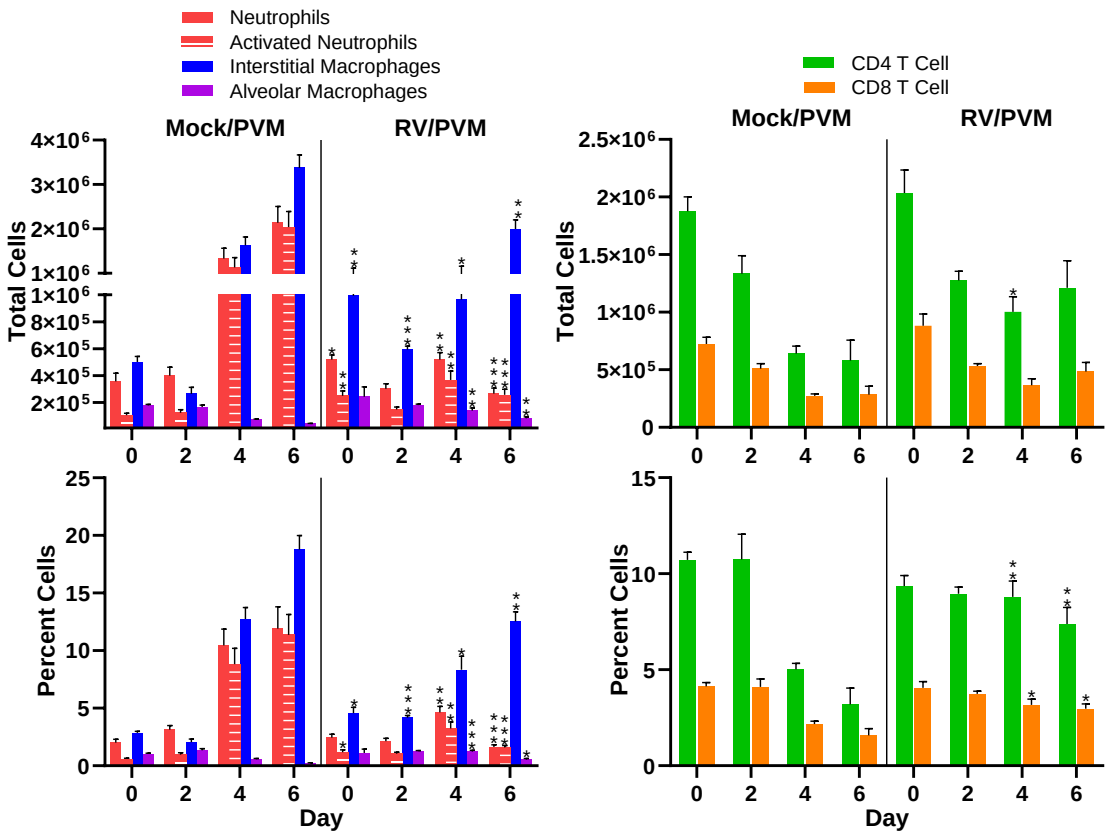


**Figure 5.6. Flow cytometry analyses of recruited cells to the lungs during RV and PVM coinfection compared to PVM single infection.** Groups of 5 mice were inoculated with Mock or RV ($7.6x10^6$ $TCID_{50}$/mouse) on day -2. Two days later on day 0, mice were inoculated with PVM ($1.0x10^4$ $TCID_{50}$/mouse). Lungs were collected on days 0, 2, 4, and 6. Lungs were homogenized, and single cell suspensions were stained for the following cell types: A) total and percent neutrophils (solid red bars; CD11b+Ly6G+), activated neutrophils (striped red bars lines; CD11b+Ly6G+CD64+), interstitial macrophages (blue bars; CD11b+Ly6G-CD64+), and alveolar macrophages (purple bars; CD11b-CD64+SiglecF+). B) total and percent CD4+ T cells (green bars; CD3+CD4+) and CD8+ T cells (orange bars; CD3+CD8+). Significance versus Mock/PVM for each cell type was determined by students *t*-test. P-values are shown as * ≤ 0.05, ** ≤ 0.01, or *** ≤ 0.001.

Coinfection with RV prevented a robust neutrophil response, regardless of which virus was coinfected with RV. Coinfection-mediated disease attenuation was reduced during simultaneous coinfection with RV and PR8 and disease was exacerbated when RV was inoculated two days after either PR8 or PVM. We were therefore interested if the disease attenuation associated with the timing of viral inoculations would correlate with neutrophil recruitment. To test this, we analyzed neutrophil recruitment when RV was inoculated two days before, simultaneously with, or two days after PR8 or PVM (Fig. 5.7). Both total and activated neutrophils were analyzed on day 6 after PR8 or PVM inoculation by flow cytometry.

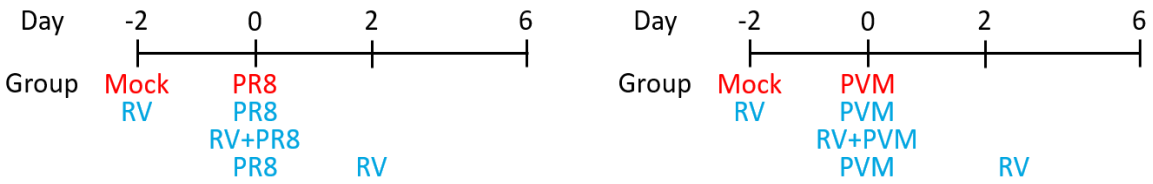


**Figure 5.7. Varied timings of coinfection inoculation scheme.**

Increased neutrophil recruitment correlated with more severe disease phenotypes for both PR8 and PVM coinfections. RV coinfected two days before PR8 (RV/PR8) attenuated PR8-induced mortality and weight loss (Fig. 4.12D, E). RV/PR8 coinfected mice also had fewer neutrophils compared to PR8 (Mock/PR8) infection (Fig. 5.6A). Simultaneous coinfection with RV and PR8 (RV+PR8) had increased PR8-induced disease compared to RV/PR8, but RV+PR8 coinfection still attenuated PR8-induced mortality and weight loss compared to PR8 infection (Fig. 4.12D, E). RV coinfected two days after PR8 (PR8/RV) exacerbated PR8-induced mortality and weight loss compared to Mock/PR8 infection (Fig. 4.12D, E). Interestingly, total (Fig. 5.8A) and activated (Fig. 5.8B) neutrophil numbers were similar between RV+PR8 and PR8/RV coinfected mice, regardless of the degree of disease attenuation. Similar correlations between neutrophil recruitment and disease severity were seen in PVM coinfected mice. RV coinfected two days before (RV/PVM) and simultaneously with (RV+PVM) PVM both completely attenuated PVM disease, while RV coinfected two days after PVM (PVM/RV) did not affect PVM-induced disease (Fig. 4.13A-C). Although both RV/PVM and RV+PVM coinfections attenuated PVM-induced disease, only RV/PVM coinfection significantly reduced neutrophil accumulation (Fig. 5.8C) and activation (Fig. 5.8D) compared to PVM infection (Mock/PVM). Although the data were not significant, RV+PVM coinfected mice had slightly reduced neutrophil recruitment and activation compared to Mock/PVM infection. PVM/RV coinfected mice recruited more total and activated neutrophils (Fig. 5.8C, D), which correlated with increased of PVM-disease. These data support the hypothesis that higher levels of neutrophils correlate with increased disease.

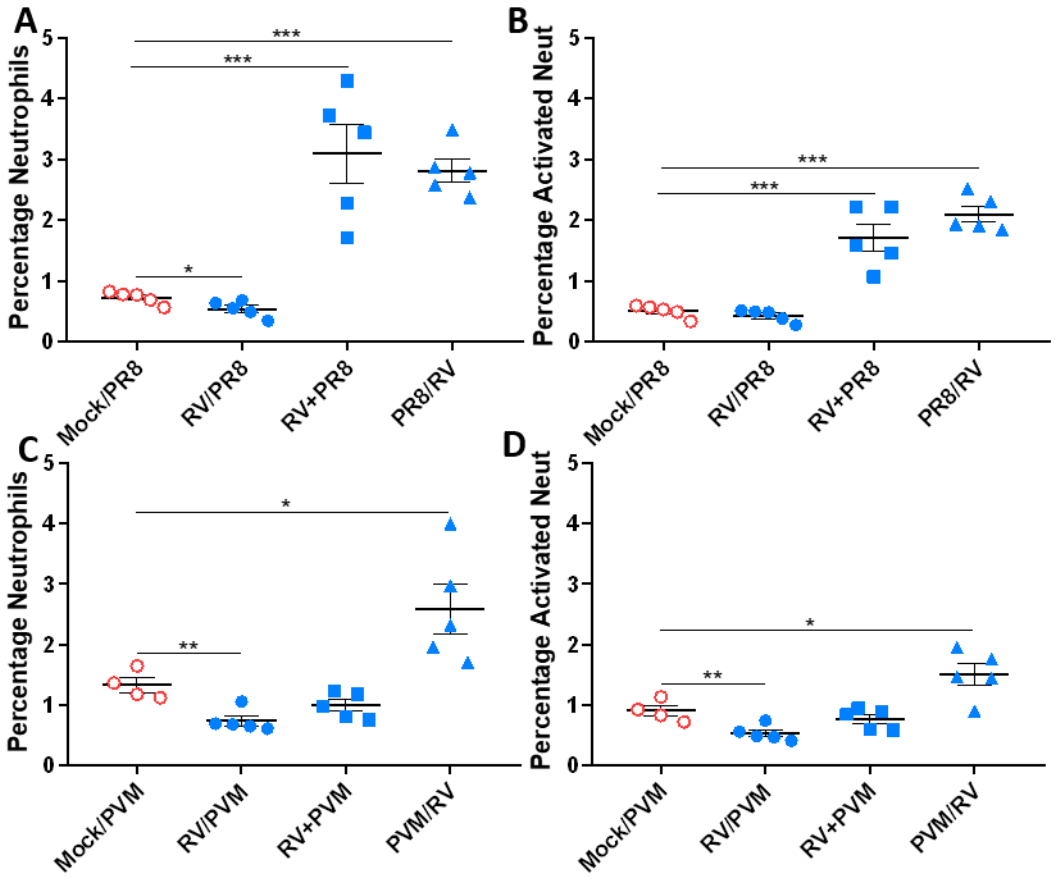


**Figure 5.8. Increased neutrophil recruitment mirrors increased PR8 and PVM disease states during coinfection.** Groups of 5 mice were inoculated with Mock or RV ($7.6x10^6$ $TCID_{50}$/mouse) on day -2. Two days later on day 0, mice were inoculated with PR8 (77.5 $TCID_{50}$/mouse) or PVM ($1.0x10^4$ $TCID_{50}$/mouse). Lungs were collected on day 6. Lungs were homogenized, and single cell suspensions were stained for total neutrophils (CD11b+Ly6G+) and activated neutrophils (CD11b+Ly6G+CD64+). A-B) RV and PR8 coinfection. A) Total neutrophils and B) activated neutrophils. C-D) RV and PVM coinfection. C) Total neutrophils and D) activated neutrophils. Significance determined by students *t*-test versus Mock/PR8 or Mock/PVM. P-values are shown as * ≤ 0.05, ** ≤ 0.01, or *** ≤ 0.001.

### 5.2.4 Coinfection alters interferon and inflammatory mediator expression

RV was most effective at reducing PR8-induced disease when mice were inoculated with RV two days before PR8. We were interested if the initial RV infection altered downstream IFN and inflammatory mediator responses. To test this, mice were either Mock-inoculated (media) or inoculated with RV two days before PR8 inoculation. Groups of mice were euthanized on days 2, 4, 7, and 10 and lungs were collected for homogenization (day 2) or bronchoalveolar lavage (BAL) fluid was collected (days 4, 7, and 10). Type I IFN was

analyzed using an IFN bioassay, and the potent inflammatory mediator TNF-α was analyzed using enzyme-linked immunosorbent assay (ELISA). The IFN bioassay quantifies type I IFN levels using an IFN-sensitive cell line and virus. In short, cells are exposed to homogenized lung samples before being inoculated with vesicular stomatitis virus (VSV) expressing green fluorescent protein (GFP). GFP is then quantified using a plate reader, and high GFP readings equate to high VSV infection, which means low IFN levels and vice versa.

Coinfection increased type I IFN early in infection. On day 2, Mock/PR8-infected mice had reduced type I IFN levels compared to mice coinfected with RV two days before PR8 (RV/PR8), as evidenced by higher fluorescence readings (Fig. 5.9). However, on day 4, the trend flipped, and mice coinfected with RV and PR8 had reduced type I IFN levels compared to Mock/PR8 infected mice (Fig. 5.9). This trend continued into day 7, where coinfected mice still expressed lower levels of type I IFN (Fig. 5.9). Lower expression of type I IFN on day 7 in coinfected mice may be explained by PR8 already being cleared in coinfected mice (Fig. 5.1A). Coinfection elicits a stronger, but limited, type I IFN response compared to PR8 alone infection.

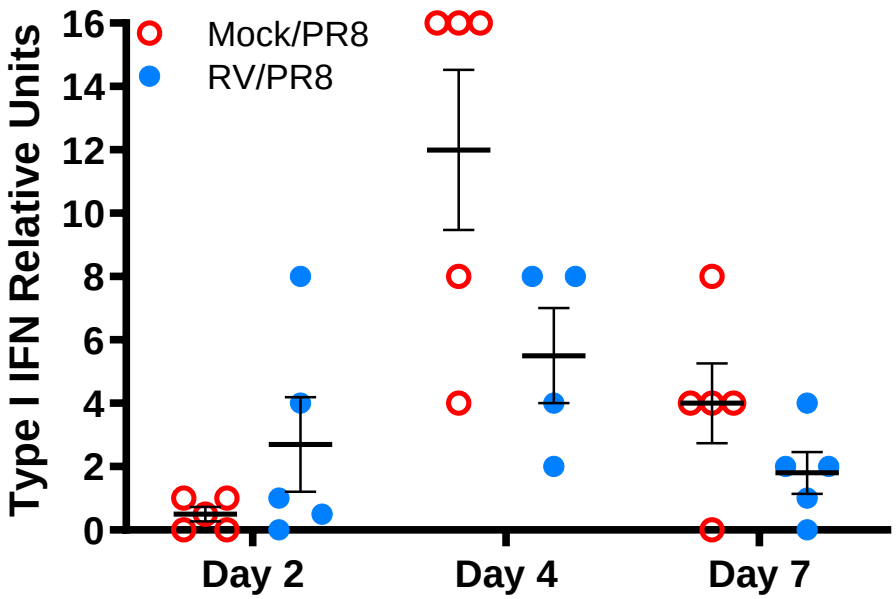


**Figure 5.9. Coinfection induced type I interferon early in infection.** Groups of 5 mice were inoculated with Mock or RV ($7.6x10^6$ $TCID_{50}$/mouse) on day -2. Two days later, on day 0, mice were inoculated with PR8 (77.5 $TCID_{50}$/mouse). On day 2, lungs were collected and homogenized, and cells were removed from samples. On days 4 and 7, lungs were inflated with 1 mL PBS, and then the PBS was aspirated and stored at -80°C. Samples were diluted in a 96-well plate and UV-inactivated before the addition of a type I IFN-sensitive cell line. Green fluorescent protein-expressing vesicular stomatitis virus was added, and fluorescence was quantified after 24 hours post-inoculation. Data are expressed as the reciprocal of the highest dilution that mediated a 50% reduction in fluorescence, defined as one unit of type I IFN. Significance versus Mock/PR8 was determined by students *t*-test.

We also measured interferon-β (IFN-β), a type I IFN, transcript levels by qPCR during coinfection with either MHV or RV two days before PR8. Lungs were collected on days 2 and 4 after PR8 inoculation for MHV coinfection and days 0, 2, 4, and 6 after PR8 inoculation for RV coinfection. Lungs were saved in RNAlater for qPCR analysis. Data collection and analysis was performed by Dr. Tanya Miura.

IFN-β transcript levels were upregulated early during both MHV and RV coinfection. IFN-β transcripts were highly elevated in mice inoculated with MHV (MVH/Mock) on day 2 (Fig. 5.10A). This elevation was also mirrored in mice coinfected with MHV two days before PR8 (MHV/PR8), signifying that early responses were dominated by MHV infection and any contribution by PR8 was negligible. Further support for this idea was lent by IFN-β transcript levels in PR8-infected mice (Mock/PR8), where

transcript levels were still minimal on day 2 (Fig. 5.10A). However, on day 4, this trend flipped, and transcript levels for Mock/PR8 infected mice increased to levels greater than coinfected mice. No samples from MHV-infected mice were collected on day 4. It is important to note that interferon transcripts increase from day 2 to day 4 in PR8-infected mice, whereas transcript levels in coinfected mice decrease from days 2 to 4.

A similar trend was observed when IFN-β transcripts were evaluated during RV coinfection. IFN-β transcripts were upregulated in coinfected mice (RV/PR8) on day 2 compared to the Mock/PR8 group (Fig. 5.10B). On day 4, IFN-β transcript levels increased for both PR8-infected and coinfected mice. Although not significant, transcript levels were lower in RV/PR8 compared to Mock/PR8-infected mice. By day 6, IFN-β expression decreased in both Mock/PR8 and RV/PR8 groups. RV induced IFN-β expression was not as dramatic as MHV induction on day 2. We expect this because RV-induced IFN-β expression is rapid in mice with peak levels one day after RV inoculation before decreasing by day 2 (52). Our measurement was taken on day 2 after PR8 inoculation, which was actually day 4 after RV inoculation. This means our measurement would be during the contraction phase. However, we did not observe increased levels of IFN-β on day 0, two days after RV inoculation. It is interesting to see increased IFN-β levels on day 2 in coinfected animals. This could be evidence of re-stimulation of RV-recruited innate immune cells in the lungs, allowing for a more rapid/stronger induction of IFN-β expression following subsequent inoculation with PR8.

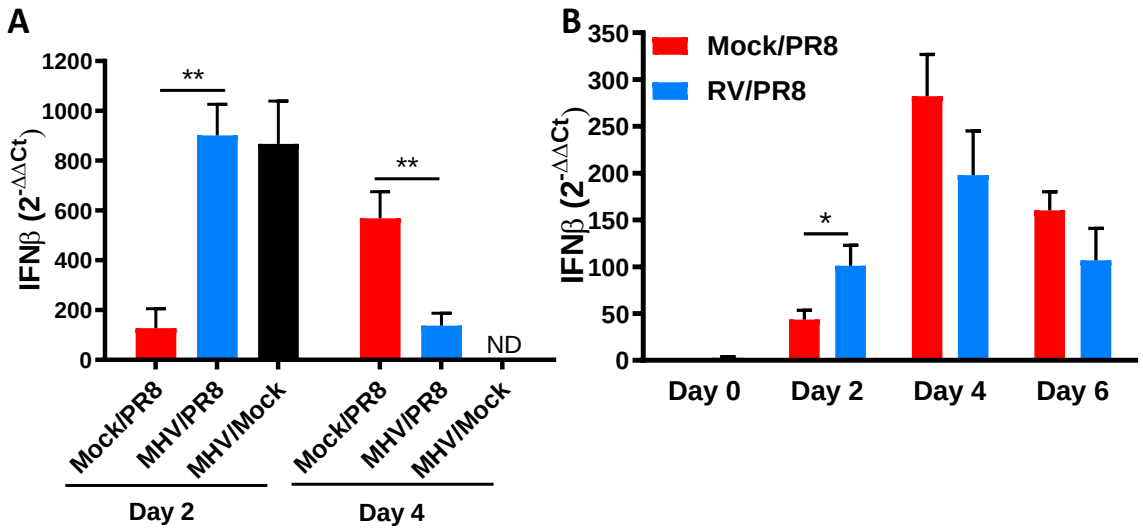


**Figure 5.10. Interferon-β expression was upregulated early following pre-infection with both RV and MHV.** Groups of 5 mice were inoculated with Mock, RV ($7.6x10^6$ $TCID_{50}$/mouse), or MHV ($2.0x10^3$ PFU/mouse) on day -2. Two days later on day 0, mice were inoculated with PR8 (77.5 $TCID_{50}$/mouse). Lungs were collected on days 2 and 4 for A) MHV/PR8 coinfection and days 0, 2, 4, and 6 for B) RV/PR8 coinfection. Right lobes of the lungs were stored in RNAlater and processed for qPCR at a later date. IFN-β transcript levels were determined by RT-qPCR. Threshold cycle (Ct) data were normalized to housekeeping gene (GAPDH) values and then fold change versus Mock-inoculated mice was calculated. Significance versus Mock/PR8 was determined by students *t*-test. P-values are shown as * ≤ 0.05, ** ≤ 0.01, or ND not determined.

RV coinfection reduced expression of TNF-α during PR8 infection. PR8 (Mock/PR8) infection was associated with a sustained TNF-α response throughout the study, which peaked on day 10 (Fig. 5.11). However, RV coinfected two days before PR8 (RV/PR8) reduced early expression of TNF-α on day 4 compared to Mock/PR8 infected mice (Fig. 5.11). TNF-α levels in RV/PR8 coinfected mice peaked on day 7 with comparable levels to PR8 single infection. Then, on day 10, TNF-α levels during coinfection contracted while levels in PR8-infected mice continued to increase. Coinfection helps limit PR8-induced inflammation, which may contribute to disease attenuation.

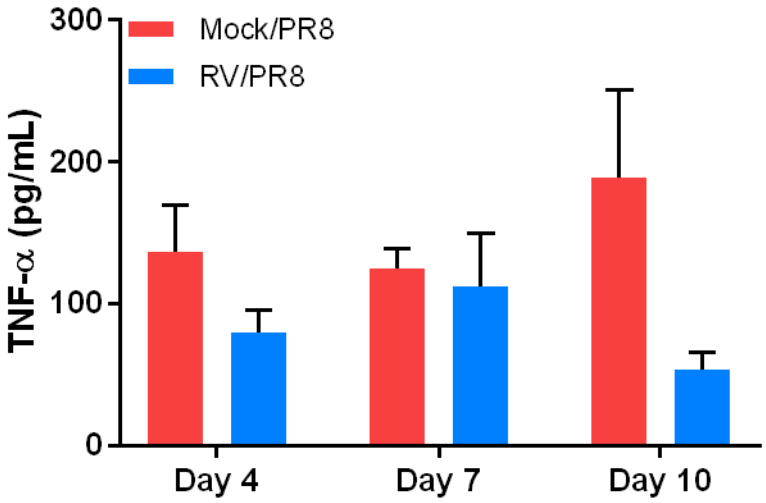


**Figure 5.11. Coinfection limited PR8-induced TNF-α expression.** Groups of 5 mice were inoculated with Mock or RV ($7.6x10^6$ $TCID_{50}$/mouse) on day -2. Two days later on day 0, mice were inoculated with PR8 (77.5 $TCID_{50}$/mouse). Lungs were collected on days 4, 7, and 10. BAL fluid was collected and processed for measurement of TNF-α using an enzyme-linked immunosorbent assay.

### 5.2.5 Neutrophil depletion did not affect coinfection-mediated disease attenuation

Coinfection with RV two days before PR8 was associated with an early neutrophil response evidenced by our flow cytometry experiments (Fig. 5.5A). We were interested if PR8 disease attenuation would be reduced during coinfection if neutrophils were depleted early during infection. To test this, we Mock- or RV-inoculated mice two days before PR8. We depleted neutrophils by using the antibody against Ly6G clone 1A8, which specifically binds to $Ly6G^{high}$ neutrophils (53, 176). We administered 1A8 intraperitoneally (i.p.) on days -3, -1, 1, and 3. Mice also received an intranasal dose of 1A8 antibody on day -2. Control mice were inoculated similarly, but instead of receiving 1A8, control mice received an isotype-matched non-specific control antibody. Mice were then monitored for mortality, weight loss, and clinical signs of infection for 14 days after PR8 inoculation.

Mice inoculated with either PR8 alone (Mock/PR8 – Ctl) or RV two days before PR8 (RV/PR8 – Ctl) and isotype control antibody experienced mortality, weight loss, and clinical scores similar to previously reported in chapter 4. However, when PR8 infected mice received 1A8 (Mock/PR8 – 1A8), no mortality was observed with PR8 infection (Fig.

5.12A). Mock/PR8 – 1A8 mice initially lost weight on day 3, and peak weight loss was reached on day 7 before complete recovery by day 14 (Fig. 5.12B). Mock/PR8 – 1A8 mice began displaying clinical signs on day 4 as mild ruffling and hunched posture, but signs increased to moderate ruffling and mild lethargy, hunching, and labored breathing by day 6 (Fig. 5.12C). No mortality was seen in RV/PR8 coinfected mice treated with 1A8 (Fig. 5.12A). Weight loss also began on day 3 for coinfected, neutrophil-depleted mice (Fig. 5.12B). Weight loss then peaked on day 7 at 13%, before recovering completely by day 11. Clinical signs recorded for coinfected, neutrophil-depleted mice were mild ruffling on day 4, and signs then increased to include mild hunching with sporadic lethargy and labored breathing over days 5 to 7 before returning to baseline by day 9 (Fig. 5.12C). It seems, from these data, that early neutrophilic infiltration does not contribute to disease attenuation during coinfection.

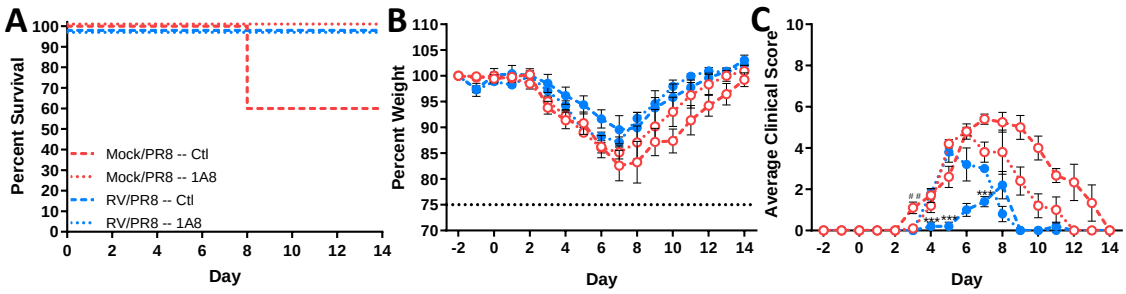


**Figure 5.12. Neutrophils were not required to attenuate PR8-induced disease during coinfection.** Groups of 5 mice were inoculated with Mock or RV ($7.6x10^6$ $TCID_{50}$/mouse) on day -2. Two days later on day 0, mice were inoculated with PR8 (77.5 $TCID_{50}$/mouse). Mice were also administered either isotype control antibody or anti-Ly6G clone 1A8 antibody intraperitoneally on days -3, -1, 1, and 3 and then intranasally on day -2. Mice were then monitored for A) mortality, B) weight loss, and C) clinical signs. Mock/PR8 is red lines, open circles and RV/PR8 is blue lines, closed circles while the control antibody is thick dashed lines and anti-Ly6G clone 1A8 is dotted lines. Survival curves were compared using log-rank Mantel-Cox curve comparison. Weight loss and clinical score data were compared using multiple Student's *t*-tests. Isotype control antibody treatment was compared to 1A8 treatment for Mock/PR8 and RV/PR8 groups. P-values are shown as ** ≤ 0.01 or *** ≤ 0.001.

We wanted to ensure that neutrophil depletion was occurring during treatment with anti-Ly6G clone 1A8. We took BAL fluid samples from mice inoculated with PR8 (Mock/PR8) during both control and 1A8 antibody treatments on day 4 after PR8 inoculation. Samples were centrifuged, and cells were spun onto a slide for counting. Cell

types counted were expressed as a percentage of total cells counted. About 60% of cells counted from BAL fluid were neutrophils in the control treated group (Mock/PR8 – Ctl) (Fig. 5.13). Neutrophils were reduced to about 5% of cells in the BAL fluid from mice treated with 1A8 antibody (Mock/PR8 – 1A8). These data confirmed that we sufficiently depleted recruited neutrophils during PR8 infection using 1A8 antibody.

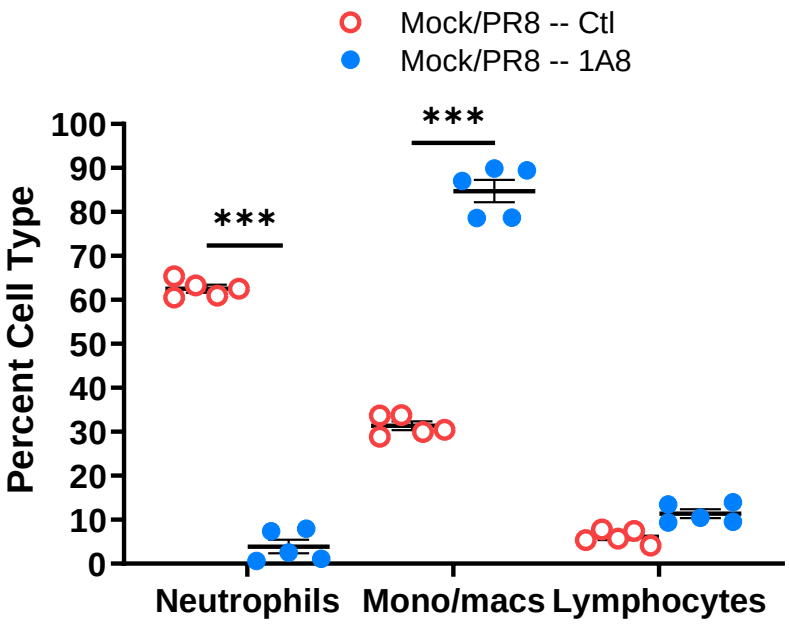


**Figure 5.13. Anti-Ly6G clone 1A8 antibody treatment reduced neutrophils in pulmonary airways on day 4.** Groups of 5 mice were inoculated with Mock on day -2. Two days later on day 0, mice were inoculated with PR8 (77.5 $TCID_{50}$/mouse). Mice were also administered either isotype control antibody or anti-Ly6G clone 1A8 antibody intraperitoneally on days -3, -1, 1, and 3 and then intranasally on day -2. On day 4, lungs were inflated with 1 mL PBS then the PBS was aspirated and collected for cell counts. After spinning cells onto a slide, total cells were counted, and each cell type is expressed as a percentage of total cells. Control treated mice are open red circles and 1A8 treated mice are closed blue circles. Significance versus Mock/PR8 -- Ctl was determined by students *t*-test. P-values are shown as *** ≤ 0.001.

After concluding that early neutrophil depletion did not affect PR8 disease severity, we were interested if these neutrophils were able to control early PR8 replication. Mice were either Mock- or RV-inoculated two days before PR8. Once again, either isotype control or 1A8 antibody was administered on days -3, -2, -1, 1, and 3. Lungs were collected on day 2 after PR8 inoculation, and tissues were homogenized and PR8 titrated by $TCID_{50}$ assay on MDCK cells. We found no difference in early PR8 replication between control and neutrophil-depleted groups (Fig. 5.14). We also measured PR8 titers for Mock/PR8 control and 1A8 treated groups on day 4, and no differences were found between the groups (data

not shown). These data further bolster the idea that early neutrophil recruitment is not required for control of PR8 or attenuation of PR8 disease.

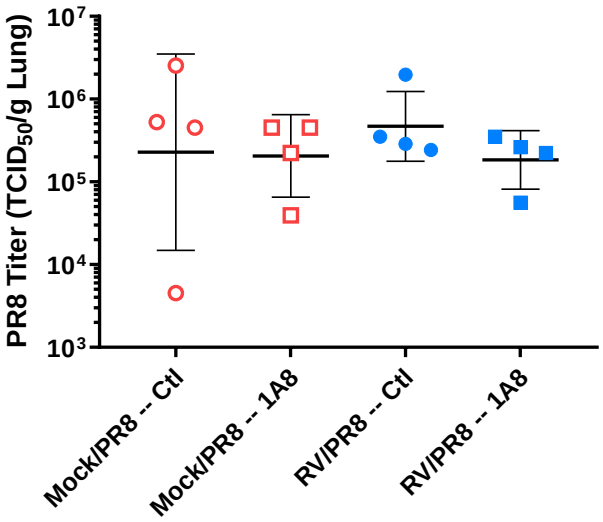


**Figure 5.14. Early neutrophil depletion did not affect PR8 replication on day 2.** Groups of 5 mice were inoculated with Mock or RV ($7.6x10^6$ $TCID_{50}$/mouse) on day -2. Two days later on day 0, mice were inoculated with PR8 (77.5 $TCID_{50}$/mouse). Mice were also administered either isotype control antibody or anti-Ly6G clone 1A8 antibody intraperitoneally on days -3, -1, 1, and 3 and then intranasally on day -2. Lungs were collected on day 2 and homogenized for PR8 titration. PR8 titer was quantified by $TCID_{50}$ assay on MDCK cells. Significance was determined by students *t*-test.

### 5.2.6 Blocking of type I interferon signaling did not affect coinfection-mediated disease attenuation

Since neutrophil depletion did not affect disease severity, we were curious if coinfection-mediated disease attenuation was dependent upon early interferon induction. To test this, mice were either Mock- or RV-inoculated two days before PVM. We blocked type I IFN signaling with the use of an antibody specific to the type I interferon α/β receptor (IFNAR) clone MAR1-5A3 (178). IFNAR-specific antibody was intranasally (i.n.) administered on days -2 and 0. Control groups of Mock/PVM and RV/PVM infected mice received either an isotype control antibody. Mice were then monitored for mortality, weight loss, and clinical signs of infection for 14 days after PR8 inoculation.

Mice inoculated with either PVM alone or RV two days before PVM had similar mortality, weight loss, and clinical signs as described earlier in chapter 4. Mice inoculated with PVM and treated with anti-IFNAR (Mock/PVM – IFNAR) had disease kinetics similar to PVM-infected mice treated with isotype control antibody (Mock/PVM – Ctl). These mice all succumbed to infection by day 8 (Fig. 5.15A), rapidly lost weight from days 5 to 8 (Fig.

5.15B), and displayed mild ruffling on day 4 before signs peaked on day 7 with severe ruffling and moderate hunching, lethargy, and labored breathing (Fig. 5.15C). Surprisingly, one of five coinfected mice treated with anti-IFNAR (RV/PVM – IFNAR) succumbed to the infection on day 6, but the rest survived until the end of the study (Fig. 5.15A). Coinfected mice were protected from PVM-induced weight loss and only displayed a short dip in weight loss on days 6-8 (Fig. 5.15B). Weight loss for anti-IFNAR treated coinfected mice (RV/PVM – IFNAR) weight loss mirrored coinfected mice treated with isotype control antibody (RV/PVM – Ctl). RV/PVM – IFNAR treated mice displayed sporadic ruffling and hunching between days 5 to 10, but signs remained mild except for one mouse that succumbed to infection (Fig. 5.15C).

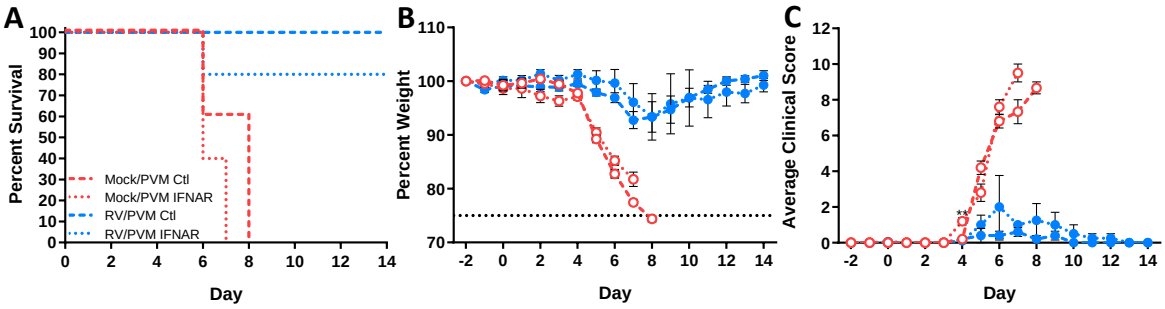


**Figure 5.15. Type I interferon was not critical for protection from PVM disease during coinfection.** Groups of 5 mice were inoculated with Mock or RV ($7.6x10^6$ $TCID_{50}$/mouse) on day -2. Two days later on day 0, mice were inoculated with PVM ($1.0x10^4$ $TCID_{50}$/mouse). Mice were also administered either isotype control or anti-IFNAR antibody intranasally on day -2 and 0. Mice were then monitored for A) mortality, B) weight loss, and C) clinical signs. Mock/PVM is red lines, open circles and RV/PVM is blue lines, closed circles; isotype control antibody treatment is solid lines and anti-IFNAR treatment is solid lines. Survival curves were compared using log-rank Mantel-Cox curve comparison. Weight loss and clinical score data were compared using multiple Student's *t*-tests. Isotype control antibody treatment was compared to anti-IFNAR treatment for Mock/PVM and RV/PVM groups. P-values are shown as ** ≤ 0.01.

To verify if type I IFN signaling was blocked during the early time points of the study, we collected lungs from Mock/PVM and RV/PVM mice treated with either isotype control or anti-IFNAR antibody on days -1, 2, and 4 after PVM inoculation. Lungs were stored in RNAlater before RNA isolation. We performed qPCR with primers specific for Mx1, a gene induced by type I IFN signaling. The expression of Mx1 is entirely dependent on IFNAR signaling, as evidenced by IFNAR knockout mice (149). Anti-IFNAR treatment

for both Mock/PVM – IFNAR and RV/PVM – IFNAR groups of mice resulted in decreased Mx1 transcript levels compared to mice treated with control antibody (Fig. 5.16). Mx1 transcripts were reduced on both day -1 and day 2 for anti-IFNAR groups compared to control groups (Ctl). However, transcript levels were lower, but not statistically significant on day 4 in the anti-IFNAR groups. This proved that we impaired type I IFN signaling early in infection while letting it return to normal levels later. Early type I IFN was not critical for attenuation of PVM-induced disease during coinfection.

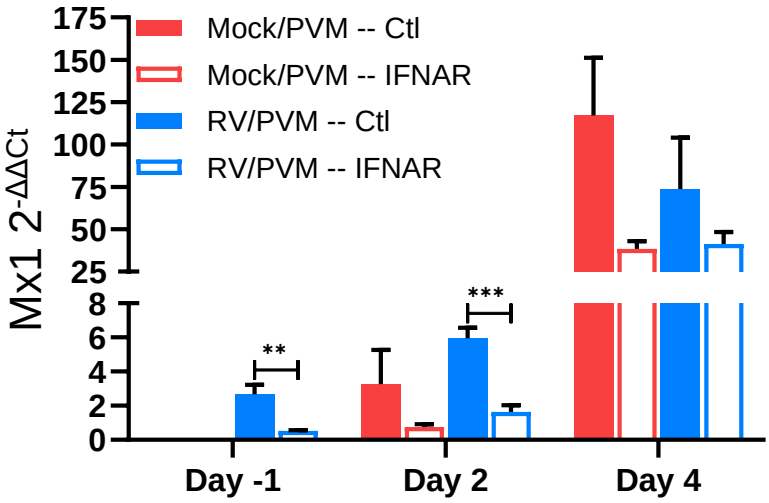


**Figure 5.16. Intranasal administration of anti-IFNAR reduced Mx1 expression for early time points.** Groups of 5 mice were inoculated with Mock or RV ($7.6x10^6$ $TCID_{50}$/mouse) on day -2. Two days later on day 0, mice were inoculated with PVM ($1.0x10^4$ $TCID_{50}$/mouse). Mice were also administered either isotype control or anti-IFNAR antibody intranasally on day -2 and 0. Lungs were collected on days -1, 2, and 4 and stored in RNAlater. RNA was isolated, and Mx1 was quantified using RT-qPCR. Data are expressed as $2^{-\Delta\Delta Ct}$ normalized to Mock-treated samples. Significance determined by students *t*-test. P-values are shown as ** ≤ 0.01 or *** ≤ 0.001.

### 5.2.7 Gene expression during coinfection

Following the conclusions that both early type I IFN signaling and neutrophil responses are not necessary for coinfection-mediated disease attenuation, it is critical to determine another pathway active during coinfection. RNA samples from one mouse inoculated with PR8 (Mock/PR8) and one mouse coinfected with RV two days before PR8

(RV/PR8) were collected on day 2 and stored in RNAlater. We tested the RNA expression of inflammatory genes using Qiagen's $RT^2$ Profiler PCR Array as a screening tool for potential genes of interest. Table 5.1 displays the genes that were 2-fold up- or down-regulated in coinfected mice (RV/PR8) normalized to the Mock/PR8 group. Numbers in blue denote up-regulated genes, while numbers in red denote down-regulated genes.

The genes in Table 5.1 represent a diverse array of functions. Many of these up-regulated genes are involved in macrophage/monocyte signaling and chemotaxis: *Ccl1, Ccl12, Ccl2, Ccl4, Ccl7, Crp, Cxcl10, Ifng,* and *Il3*. Although coinfection did not drastically alter macrophage recruitment, these genes could be important in regulating key functions during infection. Of note, *Ifng* (interferon gamma) is involved in macrophage activation and increased phagocytosis, and this gene is the fourth highest induced gene in coinfection compared to a single infection. Another pathway of up-regulated genes from Table 5.1 is genes involved in regulating anti-inflammatory and repair mechanisms: *IL10, IL10ra, IL11, IL13, IL20, IL4,* and *Lta*. These genes are involved in controlling immune cell activity, restructuring the extracellular matrix, and promoting cell survival. Upregulation of these genes during coinfection matches the decreased inflammation seen in our H&E stained lung sections in coinfected groups (Fig. 5.2). *Il10* (interleukin-10) and *IL13* (interleukin-13) are highly upregulated in coinfected mice, suggesting that coinfection induces an immunosuppressive response, thus limiting inflammatory responses. The last set of up-regulated genes of interest is related to T cell function and chemotaxis: *Ccl1, Ccl4, Ccl8, Ccr8, Cxcl10, Cxcl11, Cxcl9, Cxcr3, Ifng,* and *Cd40lg*. These genes are either involved in T cell chemotaxis and activation or are secreted by activated T cell for further regulation of innate immune cells. Flow cytometric analysis of PR8 single and coinfection did not reveal any significant differences for T cell accumulation (Fig 5.3D, E). However, T cell responses can still be altered during coinfection regardless of actual T cell numbers. Several of these T cell-related genes are involved in the activation and recruitment of professional antigen presenting cells. This strong interplay between T cells and macrophages can contribute to more effective control of PR8 infection by increasing the presentation of antigen to adaptive cells. More information is needed to tease apart which genes are critical for coinfection-mediated disease attenuation.

| Gene | Fold Regulation | Gene | Fold Regulation |
|---|---|---|---|
| *Ccl1* | 17.15 | *Il11* | 3.01 |
| *Il10* | 10.22 | *Cxcl10* | 2.99 |
| *Il13* | 9.74 | *Ccr8* | 2.79 |
| *Ifng* | 7.95 | *Ccl22* | 2.77 |
| *Il3* | 6.15 | *Il20* | 2.67 |
| *Cxcl11* | 5.92 | *Tnf* | 2.61 |
| *Ccl4* | 5.73 | *Cxcr3* | 2.57 |
| *Ccl7* | 5.19 | *Il2rb* | 2.4 |
| *Ccl2* | 4.37 | *Ccl12* | 2.39 |
| *Ccr4* | 4.36 | *Il1f6* | 2.34 |
| *Ccl8* | 4.35 | *Cd40lg* | 2.33 |
| *Ccr5* | 4.09 | *IL10ra* | 2.26 |
| *Ccl3* | 3.87 | *Ccl11* | 2.15 |
| *Crp* | 3.58 | *Il4* | 2.14 |
| *Cxcl9* | 3.52 | *Ccr1* | 2.12 |
| *Cxcl13* | 3.1 | *Lta* | 2.04 |
| *Ccr3* | 3.07 | *Ccl20* | -2.44 |
| *Cxcl1* | 3.06 | | |

**Table 5.1 Genes 2-fold or greater differentially expressed during coinfection.**

The effects of coinfection can be vast and most likely involve interactions on many fronts. We wanted to know how coinfection changed gene expression in response to PR8 and PVM infection compared to single virus infections. Mice were Mock- or RV inoculated two days before PR8- or PVM-inoculation. Lungs were collected on days 2, 4, and 6 after PR8 or PVM inoculation. Lungs were stored in RNAlater and prepared for RNAseq. Data collection and processing was done by Dr. Tanya Miura and data analysis performed by Dr. JT Van Leuven.

RNAseq data can be overwhelming and a lifetime can be spent analyzing every pathway that might be differentially expressed. For the sake of simplicity and digestibility, I have only included a small snapshot of genes that could provide a possible mechanism for disease attenuation (Table 5.2). These data are expressed as log2 fold change compared to Mock (uninfected) mice.

One major distinction between single infection and coinfection, whether it be PR8 or PVM, is the expression of lymphocyte-related genes. *Ifng* is responsible for activation of macrophages (179, 180), cytotoxic T-lymphocyte-associated protein 4 (*Ctla4*) is involved in immunosuppressive activities (181, 182), and granzyme b (*Gzmb*) is a serine protease involved in inducing inflammation and cellular apoptosis (183). An interesting trend is coinfection limits expression of both Ifng and Gzmb while increasing early expression of Ctla4. These differences could result in reducing inflammation from macrophage activation and cell apoptosis while also regulating early cytokine production.

Pre-infection with RV can increase PRRs through initial recognition of RV and then cyclical feedback. These increases in PRRs could then increase the likelihood and sensitivity of recognizing subsequent infections and stimulating the production of molecules that interfere with viral replication. No obvious trends in PRR expression were elucidated from RNAseq. Coinfection with RV and PR8 did increase *Mx1* (involved in interfering with IAV replication (184, 185))and *TLR9* (endosomal toll-like receptor) transcripts on day 2, but differences were negligible on day 4 before coinfection decreased expression on day 6 compared to single infections. Coinfection with RV and PVM had overall lower transcript levels for PRRs compared to single infections. This could help limit overproduction of cytokines and chemokines leading to a more controlled response to PVM infection, but this is currently unclear. Another approach would be to look into pathway components of PRRs to determine if there are any alterations in PRR signaling during coinfection.

The next set of genes belongs to antiviral responses and pathogen clearance. *Muc5ac* (mucin 5AC) is involved in mucus hypersecretion by goblet cells and used to protect pulmonary epithelia from infection by trapping pathogens (186, 187); *Clca1* (chloride channel accessory 1) is linked to muc5ac production (188, 189). Tumor necrosis factor (*Tnf*) is a superfamily of proteins involved in a plethora of actions including inducing

inflammation, fever, mobilization of adipocytes, etc. (190, 191). Interferon regulatory factor 7 (*Irf7*) is a transcriptional activator of antiviral genes and plays a major role in type I IFN expression (192). *Muc5ac* and its associated chloride channel were dramatically increased in coinfection of both PR8 and PVM, compared to single infections. This could increase mucin production in the lungs and help prevent the spread of PR8 and PVM. Both PR8 and PVM coinfection reduced *Tnf* transcript levels at later time points during infection, which could be related to reducing inflammation and clinical signs in the mice. Both PR8 and PVM coinfection also reduced *Irf7* transcripts on days 4 and 6, but day 2 transcript expression was increased for coinfection with RV and PR8. This fits with Fig. 5.8, which show an increase in type I IFN on day 2 compared to a single infection.

The last set of genes in the table is related to neutrophil chemotaxis. Both *Cxcl1*, chemokine (C-X-C) ligand 1 or KC in mice, and *Il1b*, interleukin 1 beta, are potent neutrophil attractants following infection (193-195). RV and PR8 coinfection increased transcript expression of both *Cxcl1* and *Il1b*, which correlated with the increased number of neutrophils observed at early time points during coinfection in Fig. 5.5. Then on days 4 and 6, both PR8 and PVM coinfection reduced *Cxcl1* and *Il1b* expression compared to respective single infections. Although early neutrophil depletion does not affect disease attenuation, Fig. 5.12, it is still a possibility that neutrophils during later time points of infection could be a culprit in contributing to PR8 and PVM disease, which are down-regulated by coinfection.

| Gene | Mock/PR8 | | | RV/PR8 | | | Mock/PVM | | | RV/PVM | | |
|---|---|---|---|---|---|---|---|---|---|---|---|---|
| **Day** | **2** | **4** | **6** | **2** | **4** | **6** | **2** | **4** | **6** | **2** | **4** | **6** |
| **T Cell Function** | | | | | | | | | | | | |
| *Ifng* | 2.85 | 2.83 | 5.31 | 2.85 | 2.99 | 4.81 | **ND** | 3.37 | 4.95 | **ND** | 2.13 | 4.63 |
| *Ctla4* | **ND** | 1.60 | 3.93 | 2.81 | 2.30 | 3.66 | **ND** | 1.30 | 3.30 | 2.49 | 1.70 | 3.30 |
| *Gzmb* | 1.22 | 2.54 | 5.14 | 2.45 | 2.75 | 4.63 | **ND** | 2.74 | 3.89 | **ND** | 1.76 | 3.86 |
| **Antiviral Defense** | | | | | | | | | | | | |
| *Mx1* | 3.95 | 4.83 | 4.94 | 4.52 | 4.71 | 4.00 | **ND** | 5.00 | 4.73 | **ND** | 4.23 | 4.23 |
| *Oas1b* | 1.49 | 2.51 | **ND** | 1.98 | 2.43 | 1.87 | **ND** | 2.52 | 2.39 | **ND** | 2.10 | 2.11 |
| *Tlr2* | 0.84 | 1.50 | 1.56 | 0.98 | 1.43 | 1.26 | **ND** | 1.54 | 1.18 | **ND** | 0.95 | 1.19 |
| *Tlr6* | **ND** | 0.80 | 1.00 | **ND** | 0.79 | 0.86 | **ND** | **ND** | 0.78 | **ND** | ND | 0.78 |
| *Tlr9* | 1.27 | 2.97 | 2.79 | 2.04 | 2.94 | 2.46 | **ND** | 2.29 | 2.41 | **ND** | 1.77 | 2.47 |
| **Pathogen clearance** | | | | | | | | | | | | |
| *Muc5ac* | **ND** | 1.01 | -1.10 | 1.42 | 1.87 | 2.22 | **ND** | **ND** | **ND** | **ND** | 2.72 | 2.06 |
| *Clca1* | **ND** | 1.25 | **ND** | 4.48 | 3.40 | 5.03 | **ND** | **ND** | **ND** | 5.01 | 6.59 | 5.55 |
| *Tnf* | 2.12 | 3.22 | 3.38 | 2.64 | 3.11 | 2.88 | **ND** | 3.21 | 2.77 | **ND** | 2.31 | 2.65 |
| *Irf7* | 2.52 | 4.06 | 4.06 | 3.26 | 3.98 | 3.57 | **ND** | 4.02 | 4.08 | **ND** | 3.18 | 3.84 |
| **Neutrophil chemotaxis** | | | | | | | | | | | | |
| *Cxcl1* | 2.73 | 3.20 | 2.90 | 2.95 | 2.96 | 1.66 | **ND** | 4.81 | 3.50 | **ND** | 3.24 | 3.27 |
| *Il1b* | 1.36 | 2.08 | 2.00 | 1.65 | 2.02 | 1.43 | **ND** | 2.15 | 2.09 | **ND** | 1.71 | 1.97 |

**Table 5.2 Snapshot of important genes from RNAseq.** ND, not detected.

## 5.3 Discussion

We discovered that pre-infection with RV attenuated multiple, unrelated pathogenic respiratory virus diseases. We also found the degree of disease attenuation by RV was dependent upon which viruses were coinfected with it: RV and PVM coinfection was associated with minimal weight loss while RV and PR8 coinfection sustained higher weight loss before recovery. The timing of virus inoculations also contributed to the degree of disease attenuation conveyed by coinfection. We inferred from these data that RV was most likely eliciting an immune response that was coordinating or supplementing PR8- and PVM-induced responses. But the immune response contributions from RV infection become

harmful when RV is inoculated after PR8 or ineffective after PVM. It is essential to understand the mechanisms behind coinfection to understand which components are necessary for disease attenuation and which are responsible for disease exacerbation or shared between both.

Initial experiments were focused on learning if coinfection interfered with PR8 replication. We tested two coinfection schemes: RV two days before PR8 (RV/PR8) and MHV two days before PR8 (MHV/PR8) (Fig. 5.1). RV/PR8 coinfection did not interfere with early PR8 replication but instead led to faster clearance of PR8 compared to single virus infection. However, MHV/PR8 coinfection did delay early PR8 replication on day 2 compared to single infection, but by day 4 coinfected and single infected groups had similar PR8 titers. Reduction in PR8 titers on day 2 during MHV/PR8 coinfection correlated with elevated IFN-β levels (Fig. 5.10A). However, the elevated IFN-β levels on day 2 during RV/PR8 coinfection did not correlate with decreased PR8 titers. This was surprising because studies have reported that exogenous treatment with IFN-α, another type I IFN, reduced IAV titers in rhesus macaques (196) and ferrets (197). One explanation for this is MHV induces about a 9-fold increase in IFN-β compared to RV infection. A certain threshold of IFN may be required to interfere with PR8 replication. This is not entirely surprising because PR8 is known to have mechanisms for inhibiting IFN responses through its NS1 protein (121) and polymerase (198). This specific threshold of IFN would then be required to overwhelm the antagonistic mechanisms of PR8. Although early IFN levels did not correlate with the interference of PR8 replication during RV and PR8 coinfection, we did observe that coinfected mice had lower levels of type I IFN transcripts (Fig. 5.10B) later in infection compared to single virus-infected mice. This contraction of IFN response may be beneficial to coinfection and help reduce disease severity. Different groups have reported that highly pathogenic influenza strains induce higher transcription of IFN-β (199) and susceptible strains of mice also typically produce higher amounts of type I IFN compared to resistant strains when challenged with the same influenza virus (149). We then wanted to know if early type I IFN was necessary for coinfection-mediated disease attenuation. After blocking type I IFN signaling on days -2 and 0, we observed minimal deviation in disease severity for coinfection compared to coinfected mice that received a control antibody (Fig. 5.15). One mouse succumbed to PVM-induced disease, and there was slightly more weight loss

observed in coinfection-IFNAR treated animals. It seems that early type-I IFN signaling is not essential to PVM-disease attenuation, but it may play a minor role instead. No difference in Mock/PVM disease severity was observed between control and IFNAR treated groups, which is supported by Heinze *et al.* (153). Heinze *et al.* did not observe differences in weight loss during PVM infection in wild-type or IFNAR-knockout mice. These results provide support for the role of reduced type I IFN being a larger contributor to disease attenuation than the early interferon response.

We next investigated immune cell infiltration into the lungs to see if this could explain the effects of coinfection. Histological analyses of single and coinfected mouse lungs revealed increased cellular infiltration into the airways for coinfected mice on day 4 compared to single infected mice (Fig. 5.2). We also observed faster clearance of immune cells from the airways in coinfected mice compared to single infected mice. We then used flow cytometry to phenotype these immune cells to gauge if there were a predominant population responding during coinfection. We observed increased neutrophil influx at early time points in mice coinfected with RV two days before PR8, which rapidly contracted by day 6 (Fig. 5.5A). PR8-infected mice maintained higher neutrophil numbers on days 2 to 6 compared to coinfected animals, which reflected neutrophil infiltration seen in other studies after influenza infection (200-202). A similar trend was seen during coinfection with RV two days before PVM. Coinfection dramatically reduced neutrophil recruitment on days 4 and 6 compared to single infected mice, similar to other studies with PVM (203) (Fig. 5.6A). Excessive neutrophil accumulation and responses, e.g., myeloperoxidase, nitric oxides, and neutrophil extracellular traps, have been implicated in causing both IAV (162, 200, 204) and RSV (41, 205) disease. To further support this claim, when pre-infection timing of RV relative to PR8 or PVM was shortened, RV-mediated disease attenuation was reduced. Correlating with this reduction was increased neutrophil infiltration into the lungs for RV+PR8, PR8/RV, and PVM/RV coinfections (Fig. 5.8). We also observed a reduction in neutrophil chemotactic transcripts (*Cxcl1* and *Il1b*) at later time points during coinfection with either PR8 or PVM compared to respective single virus-infections (Table 5.2). A similar reduction of neutrophil chemoattractant signaling was observed upon bacterial stimulation of RV-infected alveolar macrophages (118). Initial RV infection attenuated production of neutrophil chemokines in response to a secondary bacterial infection, which

resulted in reduced neutrophil infiltration. This provided a role for an early neutrophil infiltration combined with reducing neutrophil infiltration at later times of infection contributing to disease attenuation during coinfection. We then depleted neutrophils at early time points during coinfection with RV two days before PR8 using an antibody specific to the neutrophil Ly6G surface protein. Neutrophil depletion did not create any noticeable effects during coinfection compared to control antibody-treated mice (Fig. 5.12). PR8 replication was also unaffected by neutrophil depletion, and PR8 titers in depleted animals matched those of control-treated animals (Fig. 5.12). The mortality and weight loss data from the neutrophil depleted and control groups of mice in our experiment were a little surprising since previous reports of neutrophil depletion during influenza infection increased disease severity (53, 176). These studies determined that neutrophil depletion increased the disease of the less pathogenic IAV strains while also causing PR8 infected mice to reach peak weight loss one day sooner. The deviations may be due to limiting neutrophil depletion to earlier time points, whereas Tate *et al.* continued neutrophil depletion throughout the experiment. These effects may be mouse dependent since they were performed in C57BL/6 mice and we use BALB/c mice. The effects may also be virus strain-dependent because neutrophil depletion increased the severity of less virulent strains of influenza virus. Another study reported that neutrophil depletion in PR8-infected mice exhibited mild PR8 pathology (162). In contrast, PR8 infection in macrophage-depleted mice resulted in high neutrophil infiltration, accompanied by elevated levels of matrix metalloproteinase-9 and myeloperoxidase, which contributed to alveolar damage within the lungs. Coinfection reduced accumulation of neutrophils at later time points during infection, which would reduce the production of these neutrophil-related proteins, thus reduce damage to the lungs. This could mean that it is not the early recruitment of neutrophils but reduced late-stage neutrophil infiltration that is required for disease attenuation.

Flow cytometry analysis of coinfected mouse lungs revealed similar numbers of interstitial and alveolar macrophages between PR8-infection and RV/PR8 coinfection (Fig. 5.5A). RV and PVM coinfected mice had reduced interstitial macrophage numbers and increased alveolar macrophage numbers on days 4 and 6 compared to PVM-infected mice (Fig. 5.6A). One study reported that depletion of alveolar macrophages before PVM challenge slightly improved survival despite increasing viral replication (206). This does not

seem to be the mechanism here if alveolar macrophage populations are maintained during RV and PVM coinfection compared to PVM infection. One alternative explanation is that RV coinfection may be predisposing macrophage populations to being less inflammatory compared to single virus infection. Primed alveolar macrophages had attenuated neutrophil chemokine responses following bacterial or TLR stimulation (118). Our RNAseq data did not identify any dramatic differences in PRR expression or antiviral genes (Table 5.2). This would reflect that pre-infection with RV did not increase the chance to recognize a secondary viral pathogen, but instead altered how immune cells respond to a secondary infection. *In vitro*, PVM infection of murine macrophages upregulates expression of inflammatory cytokines such as TNF-α, IFN-β, macrophage inflammatory protein-1 alpha (MIP-1α), macrophage inflammatory protein-1 beta (MIP-1β), and macrophage inflammatory protein-2 (MIP-2) (207). A similar study using influenza found that alveolar macrophages produced inflammatory proteins at early times post-infection, but at later times responses were more anti-inflammatory (208). Cheung *et al.* also reported that influenza infection of macrophages induced higher gene expression of TNF-α and IFN-β (199). Our initial TNF-α ELISA (Fig. 5.11) and RNAseq data (Table 5.2) showed coinfection with RV and PR8 had lower TNF-α and *Tnf* levels, respectively, compared to PR8-infected mice (Fig. 5.11). Decreased TNF-α and IFN-β expression seen in our experiments may reflect a transition of macrophage populations away from an inflammatory response to an anti-inflammatory response. Alveolar macrophages may be directing the immune response during coinfection, and further research will be needed to understand their contribution.

Another potential mechanism could be altered T cell responses during coinfection. Once again, our flow cytometry data showed no difference in T cell infiltration for RV/PR8 coinfection compared to PR8-infection (Fig. 5.5B). But coinfection with RV/PVM maintained higher numbers of both CD4+ and CD8+ T cells at later time points compared to PVM-infection (Fig. 5.6B). Functional CD8+ T cell responses are required for survival and influenza clearance (209), and RAG knockout mice challenged with influenza have increased mortality, weight loss, and sustained inflammation (210). T cells play a more pathogenic role during PVM infection in C57BL/6 mice by producing inflammatory cytokines leading to the classic cytokine storm (211, 212). These studies found that T cells were associated with PVM-induced weight loss and mortality, but T cells were also required

for clearance of PVM. Our pilot qPCR array showed mice coinfected with RV two days before PR8 had increased levels of genes associated with T cell activation and recruitment on day 2, e.g., *Cxcl9, Cxcl10,* and *Ifng* (Table 5.1). Interestingly, the RNAseq study showed decreased *Ifng* and *Gzmb* at later time points in infection, related to reduced cytotoxic T cell responses. Interferon-gamma knockout mice have increased survival following challenge with influenza compared to mice with intact interferon-gamma responses, with survival dependent upon IL-5 expression (213). Interferon-gamma knockout may be excessive, and reduction in transcript expression seen in our study could be sufficient to promote survival in our model. More studies need to be directed at T cell responses to fully tease out their contribution to respiratory viral coinfection.

We did not assess natural killer (NK) cell recruitment to the lungs during coinfection. However, RNAseq data imply that coinfection may recruit this cell type. Granzyme B was elevated on day 2 in RV and PR8 coinfected mice compared to PR8-infected mice (Table 5.2). NK cells are known to produce granzyme B (214). This NK cell protein is involved in the cytotoxic killing of virally infected cells. NK cells are implicated in controlling IAV infection in mice (215, 216), and NK cell depletion increases IAV-induced disease (217). Increased levels of *Gzmb* during RV/PR8 coinfection and the presence of *Ifng* could improve NK responses against a PR8 infection and be critical for coinfection-mediated disease attenuation. NK cells can also play a pathogenic role during PVM infection. The mouse strain C57BL/6 is less susceptible to PVM infection than BALB/c (88). C57BL/6 mice produce higher levels of interferon-gamma at early time points, but reduced levels at later time points compared to BALB/c mice. Our RNAseq data show reduced interferon-gamma transcript levels at later time points during RV/PVM coinfection compared to PVM-infected mice (Table 5.2). This suggests that coinfection may have reduced NK cell activity at later time points, thus reducing NK cytotoxic killing of pulmonary cells. More work will need to address NK cell recruitment and cytokine production during coinfection to determine their role during disease attenuation.

Finally, the last mechanism could be a more rapid induction of repair processes in the lungs. Our pilot qPCR array identified a set of genes associated with anti-inflammatory and wound repair processes upregulated in RV and PR8 coinfection compared to single

infection (Table 5.1). These data fit other published results that identified a set of wound repair genes upregulated during RV infection *in vitro* (85, 218). These groups identified RV-induced genes directed at repair of the extracellular matrix, apoptotic pathways, and tissue remodeling that could contribute to reduced disease during coinfection within an animal model. We have also observed increased cellular proliferation and alveolar architecture repair in histological lung sections from RV and PR8 coinfected mice compared to PR8-infected mice (data not shown). Further studies are required to elucidate which pathways are being upregulated, or downregulated, during coinfection that can contribute to repair of pulmonary architecture.

Respiratory viral coinfection remains a complicated mixing pot of immune responses. We observed significant differences in type I IFN expression and neutrophil recruitment during coinfection compared to a single infection. However, depletion studies determined that early neutrophil depletion was not required for attenuation of PR8 disease, and early block of type I IFN signaling was not required for attenuation of PVM disease. In all likelihood, coinfection effects will not be binary and dominated by one single, obvious response and differences will be dependent upon virus pairs. It will likely involve multiple facets of the immune response and subtle changes between each arm with coinfection supplementing or downregulating responses as needed to reduce disease severity. More work is needed to elucidate which portions are required for disease attenuation.

# CHAPTER 6

## Summary and Conclusions

Respiratory viral coinfections are a common occurrence in clinical cases, but viral coinfections remain understudied within the lab. Using our murine model, we have further contributed to the understanding of coinfections, both *in vitro* and *in vivo*. This work expanded upon the field of coinfection to include the model viruses: PVM, a model for severe respiratory syncytial virus infections, and MHV, a model for severe coronavirus infections. We can conclude that respiratory viral coinfection with a mild respiratory pathogen can reduce the disease severity of a more severe respiratory pathogen. Clinical data cannot determine: 1) the amount of time between each viral infection, 2) the order in which each virus was contracted, and 3) the severity of each virus infection. Our work discovered that all three of these parameters were critical for determining how coinfection affected disease severity (Chapter 4). Further work found effects of viral interference were minimal during *in vitro* coinfection with a minor group rhinovirus RV and PR8 (Chapter 3). Finally, we determined that early neutrophil recruitment was not required for attenuation of PR8 disease, and early type I IFN signaling was not required for attenuation of PVM disease (Chapter 5). These experiments provide a foundation to study respiratory viral coinfection that can be further expanded by other investigators. Although we were not able to isolate a single mechanism that was crucial to disease attenuation by coinfection, we were able to exclude some likely candidates. Coinfection creates a complex network for potential interactions and manipulations of immune responses in the host. In all likelihood, the mechanism of action will not be dependent upon one arm of the immune response but on multiple.

Viruses are known to induce a type I interferon response upon recognition by target or immune cells (219). This initiates an antiviral response, which limits the extent of virus infections by reducing intake of extracellular material, termination of protein synthesis, etc. We believed this to be a key mechanism during coinfection because RV induced a rapid production of type I interferon in mice, which could then prevent the establishment of a

secondary infection. However, after inhibition of type I interferon signaling, we still observed coinfection-mediated disease attenuation. One possible explanation for this is type I and III interferons have redundant effects during respiratory infection, and we only inhibited type I interferon signaling. Pre-treatment of type I interferon receptor knockout mice with type III interferon before influenza infection protected mice from mortality and limited viral replication (220). In a similar study, clearance of severe acute respiratory syndrome-associated coronavirus is reduced when type I and III interferon signaling is inhibited (221). Double knockout of type I and III interferon receptors in mice increases influenza-induced mortality compared to infection in individual receptor knockout mice (222). Double receptor knockout in mice also enhances respiratory syncytial virus replication, which is not seen in individual receptor knockout mice. These data support a redundant function between type I and III interferons during respiratory virus infection. Viruses have mechanisms for circumventing both types I and III interferon responses. The nonstructural proteins NS1 and NS2 from pneumonia virus of mice inhibit the production of both type I and III interferons in mice (153). IAV nonstructural protein NS1 is well documented to interfere with the activation of interferon regulatory factor 3 and downstream production of type I interferon (223, 224). IAV polymerase inhibits type I interferon production by inhibiting activation of the interferon-beta promoter (198). Rhinovirus infection is known to induce higher production of type III interferon compared to its type I counterpart in mice (52, 77). Pre-infection with rhinovirus could help control secondary virus infections through stimulation of type I and III interferon responses before the secondary virus has a chance to circumvent them. Further experiments would need to focus on how coinfection-mediated disease attenuation is affected when type III interferon signaling is blocked or using a type I and III interferon receptor double knockout mouse model.

We initially believed that coinfection-mediated disease attenuation was reliant upon early neutrophil recruitment followed by rapid clearance of neutrophils from the lungs at later time points. However, we found depleting neutrophils early in infection did not affect disease attenuation. We did not evaluate the effect of decreased neutrophils at later time points, and this could be a potential mechanism coinfection-mediated disease attenuation. The early recruitment of neutrophils may have been a red herring and distracted us from

another important cell type: alveolar macrophages. Alveolar macrophages are a frontline defense in the respiratory tract, but they also tend to play a pathogenic role during some infections. Interestingly, depletion of alveolar macrophages prolongs mouse survival following pneumonia virus of mice infection (206, 225). Increases in survival are associated with a decrease in IL-6 production and an increase in interferon-gamma production. Another study reports that priming alveolar macrophages with *Lactobacillus plantarum* increases survival following pneumonia virus of mice infection and limits release of virions from alveolar macrophages (163). Depletion of alveolar macrophages during mouse hepatitis virus strain 1 infection improves mouse survival compared to non-depleted infected mice (166). Depletion of alveolar macrophages has the opposite effect during IAV infections and mortality is increased (164, 226). Depletion is linked to increased inflammation and virus replication in the lungs during influenza infection. Similar to bacterial priming during pneumonia virus of mice infection, priming of mice with *Staphylococcus aureus* reduces influenza-induced mortality, and this phenotype is lost when alveolar macrophages are depleted (227). These studies portray a need for alveolar macrophages during respiratory virus infection, while also noting they are involved in increased pathogenesis. Our model did not focus on the depletion of alveolar macrophage but focused more on the potential priming of alveolar macrophages by pre-infection with rhinovirus. Initial rhinovirus infection has been shown to modulate cytokine and chemokine production following secondary bacterial infections in human alveolar macrophages (134) and mice (118). Primed alveolar macrophages were associated with a reduction in neutrophil accumulation. Initial infection with rhinovirus may be priming alveolar macrophages to dampen subsequent responses and decrease neutrophil recruitment, thus creating our red herring. Future experiments would need to identify the role of alveolar macrophages during coinfection. Depletion of alveolar macrophages during coinfection could elucidate a key role for this cell type in our model. Evaluation of alveolar macrophage-related cytokines and chemokines would further confirm the contributions of this cell type.

We focused on innate immune responses during coinfection because we observed disease attenuation effects early during infection. This does not rule out the possibility for an adaptive immune response to participate in coinfection mediated effects. Rhinovirus infection in mice recruits lymphocytes four days post-infection (52, 77). Our best model of

coinfection-mediated disease attenuation was inoculating rhinovirus two days before a secondary virus. This means lymphocytes would be recruited to the lungs two days after inoculation with the second virus. These early lymphocytes could be involved in the clearance of secondary viral infections or coordinating further immune responses while also contributing to pathology (154, 167, 228). Our flow cytometry data do not agree with this idea because we did not see an increase in T lymphocytes at early time points on either day 2 or 4 after secondary virus inoculation (Figs. 5.5B and 5.6B). However, we did not assess activation states of T cells recruited during coinfection versus single infection. Initial rhinovirus infection could differentially activate T cells to be less pathogenic during a subsequent infection. Coinfection could be tested using Rag1 knockout mice or nude mice as the model organism. Nude mice are athymic and lack T cells, and Rag1 knockout mice lack mature T and B cells. These mice would allow us to determine if disease attenuation mediated by coinfection is dependent upon adaptive immune responses or if it is mediated solely by the innate immune response. If cell-mediated immune responses are required for disease attenuation, further work would need to focus on the role of CD4 and CD8 T cells during coinfection using their respective knockout mouse models.

Our model of coinfection attenuated disease for multiple, unrelated viruses in individual mice. We also used a large enough inoculation volume to ensure all viruses reached the lower respiratory tract. This is a little manufactured for infections because it is an atypical route for infection. Respiratory tract infections typically initiate in the upper respiratory tract before more severe infections progress to lower airways. We could expand our model to use a more realistic transmission model by using ferrets. Ferrets replicate influenza pathology similar to humans (229) and have been used to study transmission dynamics of IAV (230-232). Ferrets are not the best model host for respiratory syncytial virus, but ferrets have been used to study viral interference between influenza and respiratory syncytial virus (94). One group used immunocompromised ferrets as a transmission model for respiratory syncytial virus and found that immunocompromised ferrets could transmit the virus to immunocompetent ferrets (233). Ferrets have also been used to study severe acute respiratory syndrome-associated coronavirus with some efficacy (234, 235). It is unclear whether the ferret is a susceptible host for rhinovirus, but it may be worth investigating. Ferrets inoculated with rhinovirus could be co-housed with ferrets

inoculated with an unrelated virus and virus transmission could be monitored. This could inform if rhinovirus can prevent infection in a primed host through normal means of transmission.

We determined that a less pathogenic virus can attenuate the disease of a more pathogenic virus using a mouse model. This disease attenuation was not limited to one specific pairing of viruses but was replicated in multiple unique pairings of viruses. Timing of virus inoculations and severity of virus infections did affect the degree of disease attenuation. We found that coinfection-mediated attenuation of influenza disease did not rely on early neutrophil recruitment using neutrophil depletion studies. We also found that early type I interferon signaling was not crucial for attenuation of PVM disease by blocking type I interferon receptor during coinfection. Many facets of the immune system may be manipulated during coinfection due to multiple viruses coinhabiting a single host. It is imperative to elucidate which arms of the immune system are critical to disease attenuation during coinfection to understand how coinfection alters disease severity in humans.

# References


1. **Lim YK, Kweon OJ, Kim HR, Kim TH, Lee MK.** 2019. Impact of bacterial and viral coinfection in community-acquired pneumonia in adults. Diagn Microbiol Infect Dis **94:**50-54.

2. **Franz A, Adams O, Willems R, Bonzel L, Neuhausen N, Schweizer-Krantz S, Ruggeberg JU, Willers R, Henrich B, Schroten H, Tenenbaum T.** 2010. Correlation of viral load of respiratory pathogens and co-infections with disease severity in children hospitalized for lower respiratory tract infection. J Clin Virol **48:**239-245.

3. **Baroudy NRE, Refay ASE, Hamid TAA, Hassan DM, Soliman MS, Sherif L.** 2018. Respiratory Viruses and Atypical Bacteria Co-Infection in Children with Acute Respiratory Infection. Open Access Maced J Med Sci **6:**1588-1593.

4. **Sung CC, Chi H, Chiu NC, Huang DT, Weng LC, Wang NY, Huang FY.** 2011. Viral etiology of acute lower respiratory tract infections in hospitalized young children in Northern Taiwan. J Microbiol Immunol Infect **44:**184-190.

5. **Mazur NI, Bont L, Cohen AL, Cohen C, von Gottberg A, Groome MJ, Hellferscee O, Klipstein-Grobusch K, Mekgoe O, Naby F, Moyes J, Tempia S, Treurnicht FK, Venter M, Walaza S, Wolter N, Madhi SA, South African Severe Acute Respiratory Illness Surveillance G.** 2017. Severity of Respiratory Syncytial Virus Lower Respiratory Tract Infection With Viral Coinfection in HIV-Uninfected Children. Clin Infect Dis **64:**443-450.

6. **Hassan DA, Rachid SK, Ziebuhr J.** 2018. A Single-Center Study of Viral Respiratory Tract Infections in Hospitalized Children From the Kurdistan Region of Iraq. Glob Pediatr Health **5:**2333794X18784996.

7. **Gill JR, Sheng Z-M, Ely SF, Guinee DG, Beasley MB, Suh J, Deshpande C, Mollura DJ, Morens DM, Bray M, Travis WD, Taubenberger JK.** 2010. Pulmonary Pathologic Findings of Fatal 2009 Pandemic Influenza A/H1N1 Viral Infections. Archives of Pathology & Laboratory Medicine **134:**235-243.

8. **Martin ET, Kuypers J, Wald A, Englund JA.** 2012. Multiple versus single virus respiratory infections: viral load and clinical disease severity in hospitalized children. Influenza Other Respi Viruses **6:**71-77.

9. **Stempel HE, Martin ET, Kuypers J, Englund JA, Zerr DM.** 2009. Multiple viral respiratory pathogens in children with bronchiolitis. Acta Paediatr **98:**123-126.

10. **Drews AL, Atmar RL, Glezen WP, Baxter BD, Piedra PA, Greenberg SB.** 1997. Dual respiratory virus infections. Clinical Infectious Diseases **25:**1421-1429.

11. **Nolan VG, Arnold SR, Bramley AM, Ampofo K, Williams DJ, Grijalva CG, Self WH, Anderson EJ, Wunderink RG, Edwards KM, Pavia AT, Jain S, McCullers JA.** 2018. Etiology and Impact of Coinfections in Children Hospitalized With Community-Acquired Pneumonia. J Infect Dis **218:**179-188.

12. **Cebey-Lopez M, Herberg J, Pardo-Seco J, Gomez-Carballa A, Martinon-Torres N, Salas A, Martinon-Sanchez JM, Gormley S, Sumner E, Fink C, Martinon-Torres F, network G.** 2015. Viral Co-Infections in Pediatric Patients Hospitalized with Lower Tract Acute Respiratory Infections. PLoS One **10:**e0136526.

13. **Martinez-Roig A, Salvado M, Caballero-Rabasco MA, Sanchez-Buenavida A, Lopez-Segura N, Bonet-Alcaina M.** 2015. Viral coinfection in childhood respiratory tract infections. Arch Bronconeumol **51:**5-9.

14. **Chu HY, Kuypers J, Renaud C, Wald A, Martin E, Fairchok M, Magaret A, Sarancino M, Englund JA.** 2013. Molecular epidemiology of respiratory syncytial virus transmission in childcare. J Clin Virol **57:**343-350.

15. **Tanner H, Boxall E, Osman H.** 2012. Respiratory viral infections during the 2009-2010 winter season in Central England, UK: incidence and patterns of multiple virus co-infections. Eur J Clin Microbiol Infect Dis **31:**3001-3006.

16. **Achten NB, Wu P, Bont L, Blanken MO, Gebretsadik T, Chappell JD, Wang L, Yu C, Larkin EK, Carroll KN, Anderson LJ, Moore ML, Sloan CD, Hartert TV.** 2017. Interference Between Respiratory Syncytial Virus and Human Rhinovirus Infection in Infancy. J Infect Dis **215:**1102-1106.

17. **Zhang SF, Tuo JL, Huang XB, Zhu X, Zhang DM, Zhou K, Yuan L, Luo HJ, Zheng BJ, Yuen KY, Li MF, Cao KY, Xu L.** 2018. Epidemiology characteristics of human coronaviruses in patients with respiratory infection symptoms and phylogenetic analysis of HCoV-OC43 during 2010-2015 in Guangzhou. PLoS One **13:**e0191789.

18. **Lepiller Q, Barth H, Lefebvre F, Herbrecht R, Lutz P, Kessler R, Fafi-Kremer S, Stoll-Keller F.** 2013. High incidence but low burden of coronaviruses and preferential associations between respiratory viruses. J Clin Microbiol **51:**3039-3046.

19. **Jevsnik M, Ursic T, Zigon N, Lusa L, Krivec U, Petrovec M.** 2012. Coronavirus infections in hospitalized pediatric patients with acute respiratory tract disease. BMC Infect Dis **12:**365.

20. **Goka E, Vallely P, Mutton K, Klapper P.** 2013. Influenza A viruses dual and multiple infections with other respiratory viruses and risk of hospitalisation and mortality. Influenza Other Respir Viruses **7:**1079-1087.

21. **Grondahl B, Ankermann T, von Bismarck P, Rockahr S, Kowalzik F, Gehring S, Meyer C, Knuf M, Puppe W.** 2014. The 2009 pandemic influenza A(H1N1) coincides with changes in the epidemiology of other viral pathogens causing acute respiratory tract infections in children. Infection **42:**303-308.

22. **Pascalis H, Temmam S, Turpin M, Rollot O, Flahault A, Carrat F, de Lamballerie X, Gerardin P, Dellagi K.** 2012. Intense co-circulation of non-influenza respiratory viruses during the first wave of pandemic influenza pH1N1/2009: a cohort study in Reunion Island. PLoS One **7:**e44755.

23. **Cilla G, Onate E, Perez-Yarza EG, Montes M, Vicente D, Perez-Trallero E.** 2008. Viruses in community-acquired pneumonia in children aged less than 3 years old: High rate of viral coinfection. J Med Virol **80:**1843-1849.

24. **Ahn JG, Choi SY, Kim DS, Kim KH.** 2014. Human bocavirus isolated from children with acute respiratory tract infections in Korea, 2010-2011. J Med Virol **86:**2011-2018.

25. **Venter M, Lassauniere R, Kresfelder TL, Westerberg Y, Visser A.** 2011. Contribution of common and recently described respiratory viruses to annual hospitalizations in children in South Africa. J Med Virol **83:**1458-1468.

26. **Fathima S, Lee BE, May-Hadford J, Mukhi S, Drews SJ.** 2012. Use of an Innovative Web-Based Laboratory Surveillance Platform to Analyze Mixed Infections Between Human Metapneumovirus (hMPV) and Other Respiratory Viruses Circulating in Alberta (AB), Canada (2009-2012). Viruses-Basel **4:**2754-2765.

27. **Kuypers J, Wright N, Corey L, Morrow R.** 2005. Detection and quantification of human metapneumovirus in pediatric specimens by real-time RT-PCR. J Clin Virol **33:**299-305.

28. **Xiao NG, Zhang B, Xie ZP, Zhou QH, Zhang RF, Zhong LL, Ding XF, Li J, Song JR, Gao HC, Hou YD, Duan ZJ.** 2013. Prevalence of human metapneumovirus in children with acute lower respiratory infection in Changsha, China. J Med Virol **85:**546-553.

29. **Syrmis MW, Whiley DM, Thomas M, Mackay IM, Williamson J, Siebert DJ, Nissen MD, Sloots TP.** 2004. A sensitive, specific, and cost-effective multiplex reverse transcriptase-PCR assay for the detection of seven common respiratory viruses in respiratory samples. J Mol Diagn **6:**125-131.

30. **Freymuth F, Vabret A, Cuvillon-Nimal D, Simon S, Dina J, Legrand L, Gouarin S, Petitjean J, Eckart P, Brouard J.** 2006. Comparison of multiplex PCR assays and conventional techniques for the diagnostic of respiratory virus infections in children admitted to hospital with an acute respiratory illness. J Med Virol **78:**1498-1504.

31. **Beckmann C, Hirsch HH.** 2016. Comparing Luminex NxTAG-Respiratory Pathogen Panel and RespiFinder-22 for multiplex detection of respiratory pathogens. J Med Virol **88:**1319-1324.

32. **Brunstein JD, Cline CL, McKinney S, Thomas E.** 2008. Evidence from multiplex molecular assays for complex multipathogen interactions in acute respiratory infections. J Clin Microbiol **46:**97-102.

33. **Jartti T, Lehtinen P, Vuorinen T, Koskenvuo M, Ruuskanen O.** 2004. Persistence of rhinovirus and enterovirus RNA after acute respiratory illness in children. J Med Virol **72:**695-699.

34. **Keeler SP, Agapov EV, Hinojosa ME, Letvin AN, Wu K, Holtzman MJ.** 2018. Influenza A Virus Infection Causes Chronic Lung Disease Linked to Sites of Active Viral RNA Remnants. J Immunol **201:**2354-2368.

35. **Hamelin ME, Prince GA, Gomez AM, Kinkead R, Boivin G.** 2006. Human metapneumovirus infection induces long-term pulmonary inflammation associated with airway obstruction and hyperresponsiveness in mice. J Infect Dis **193:**1634-1642.

36. **Estripeaut D, Torres JP, Somers CS, Tagliabue C, Khokhar S, Bhoj VG, Grube SM, Wozniakowski A, Gomez AM, Ramilo O, Jafri HS, Mejias A.** 2008. Respiratory syncytial virus persistence in the lungs correlates with airway hyperreactivity in the mouse model. J Infect Dis **198:**1435-1443.

37. **Papadopoulos NG, Moustaki M, Tsolia M, Bossios A, Astra E, Prezerakou A, Gourgiotis D, Kafetzis D.** 2002. Association of rhinovirus infection with increased disease severity in acute bronchiolitis. Am J Respir Crit Care Med **165:**1285-1289.

38. **Aberle JH, Aberle SW, Pracher E, Hutter HP, Kundi M, Popow-Kraupp T.** 2005. Single versus dual respiratory virus infections in hospitalized infants: impact on clinical course of disease and interferon-gamma response. Pediatr Infect Dis J **24:**605-610.

39. **Paranhos-Baccala G, Komurian-Pradel F, Richard N, Vernet G, Lina B, Floret D.** 2008. Mixed respiratory virus infections. J Clin Virol **43:**407-410.

40. **Semple MG, Cowell A, Dove W, Greensill J, McNamara PS, Halfhide C, Shears P, Smyth RL, Hart CA.** 2005. Dual infection of infants by human metapneumovirus and human respiratory syncytial virus is strongly associated with severe bronchiolitis. J Infect Dis **191:**382-386.

41. **Marguet C, Lubrano M, Gueudin M, Le Roux P, Deschildre A, Forget C, Couderc L, Siret D, Donnou MD, Bubenheim M, Vabret A, Freymuth F.** 2009. In very young infants severity of acute bronchiolitis depends on carried viruses. PLoS One **4:**e4596.

42. **Esper FP, Spahlinger T, Zhou L.** 2011. Rate and influence of respiratory virus co-infection on pandemic (H1N1) influenza disease. J Infect **63:**260-266.

43. **Peng D, Zhao D, Liu J, Wang X, Yang K, Xicheng H, Li Y, Wang F.** 2009. Multipathogen infections in hospitalized children with acute respiratory infections. Virol J **6:**155.

44. **Huang JJ, Huang TY, Huang MY, Chen BH, Lin KH, Jeng JE, Wu JR, Dai ZK.** 1998. Simultaneous multiple viral infections in childhood acute lower respiratory tract infections in southern Taiwan. J Trop Pediatr **44:**308-311.

45. **Martin ET, Kuypers J, Wald A, Englund JA.** 2012. Multiple versus single virus respiratory infections: viral load and clinical disease severity in hospitalized children. Influenza Other Respir Viruses **6:**71-77.

46. **Suryadevara M, Cummings E, Bonville CA, Bartholoma N, Riddell S, Kiska D, Rosenberg HF, Domachowske JB.** 2011. Viral etiology of acute febrile respiratory illnesses in hospitalized children younger than 24 months. Clin Pediatr (Phila) **50:**513-517.

47. **Yoshida LM, Suzuki M, Nguyen HA, Le MN, Dinh Vu T, Yoshino H, Schmidt WP, Nguyen TT, Le HT, Morimoto K, Moriuchi H, Dang DA, Ariyoshi K.** 2013. Respiratory syncytial virus: co-infection and paediatric lower respiratory tract infections. Eur Respir J **42:**461-469.

48. **Camargo C, Guatura SB, Bellei N.** 2012. Respiratory viral coinfection among hospitalized patients with H1N1 2009 during the first pandemic wave in Brazil. Braz J Infect Dis **16:**180-183.

49. **Anestad G, Nordbo SA.** 2011. Virus interference. Did rhinoviruses activity hamper the progress of the 2009 influenza A (H1N1) pandemic in Norway? Med Hypotheses **77:**1132-1134.

50. **Greer RM, McErlean P, Arden KE, Faux CE, Nitsche A, Lambert SB, Nissen MD, Sloots TP, Mackay IM.** 2009. Do rhinoviruses reduce the probability of viral co-detection during acute respiratory tract infections? J Clin Virol **45:**10-15.

51. **Dominguez SR, Shrivastava S, Berglund A, Qian Z, Goes LG, Halpin RA, Fedorova N, Ransier A, Weston PA, Durigon EL, Jerez JA, Robinson CC, Town CD, Holmes KV.** 2014. Isolation, propagation, genome analysis and epidemiology of HKU1 betacoronaviruses. J Gen Virol **95:**836-848.

52. **Bartlett NW, Walton RP, Edwards MR, Aniscenko J, Caramori G, Zhu J, Glanville N, Choy KJ, Jourdan P, Burnet J, Tuthill TJ, Pedrick MS, Hurle MJ, Plumpton C, Sharp NA, Bussell JN, Swallow DM, Schwarze J, Guy B, Almond JW, Jeffery PK, Lloyd CM, Papi A, Killington RA, Rowlands DJ, Blair ED, Clarke NJ, Johnston SL.** 2008. Mouse models of rhinovirus-induced disease and exacerbation of allergic airway inflammation. Nat Med **14:**199-204.

53. **Tate MD, Ioannidis LJ, Croker B, Brown LE, Brooks AG, Reading PC.** 2011. The role of neutrophils during mild and severe influenza virus infections of mice. PLoS ONE **6:**e17618.

54. **Shrivastava P, Sarkar I, Atanley E, Gomis S, van Drunen Littel-van den Hurk S.** 2016. IL-12p40 gene-deficient BALB/c mice exhibit lower weight loss, reduced lung pathology and decreased sensitization to allergen in response to infection with pneumonia virus of mice. Virology **497:**1-10.

55. **De Albuquerque N, Baig E, Ma X, Zhang J, He W, Rowe A, Habal M, Liu M, Shalev I, Downey GP, Gorczynski R, Butany J, Leibowitz J, Weiss SR, McGilvray ID, Phillips MJ, Fish EN, Levy GA.** 2006. Murine hepatitis virus strain 1 produces a clinically relevant model of severe acute respiratory syndrome in A/J mice. J Virol **80:**10382-10394.

56. **Diebold SS, Kaisho T, Hemmi H, Akira S, Reis e Sousa C.** 2004. Innate antiviral responses by means of TLR7-mediated recognition of single-stranded RNA. Science **303:**1529-1531.

57. **Lund JM, Alexopoulou L, Sato A, Karow M, Adams NC, Gale NW, Iwasaki A, Flavell RA.** 2004. Recognition of single-stranded RNA viruses by Toll-like receptor 7. Proc Natl Acad Sci U S A **101:**5598-5603.

58. **Pang IK, Pillai PS, Iwasaki A.** 2013. Efficient influenza A virus replication in the respiratory tract requires signals from TLR7 and RIG-I. Proc Natl Acad Sci U S A **110:**13910-13915.

59. **Cervantes-Barragan L, Zust R, Weber F, Spiegel M, Lang KS, Akira S, Thiel V, Ludewig B.** 2007. Control of coronavirus infection through plasmacytoid dendritic-cell-derived type I interferon. Blood **109:**1131-1137.

60. **Davidson S, Kaiko G, Loh Z, Lalwani A, Zhang V, Spann K, Foo SY, Hansbro N, Uematsu S, Akira S, Matthaei KI, Rosenberg HF, Foster PS, Phipps S.** 2011. Plasmacytoid dendritic cells promote host defense against acute pneumovirus infection via the TLR7-MyD88-dependent signaling pathway. J Immunol **186:**5938-5948.

61. **Saba TG, Chung Y, Hong JY, Sajjan US, Bentley JK, Hershenson MB.** 2014. Rhinovirus-induced macrophage cytokine expression does not require endocytosis or replication. Am J Respir Cell Mol Biol **50:**974-984.

62. **Jacques A, Bleau C, Turbide C, Beauchemin N, Lamontagne L.** 2009. Macrophage interleukin-6 and tumour necrosis factor-alpha are induced by coronavirus fixation to Toll-like receptor 2/heparan sulphate receptors but not carcinoembryonic cell adhesion antigen 1a. Immunology **128:**e181-192.

63. **Wu W, Zhang W, Duggan ES, Booth JL, Zou MH, Metcalf JP.** 2015. RIG-I and TLR3 are both required for maximum interferon induction by influenza virus in human lung alveolar epithelial cells. Virology **482:**181-188.

64. **Kandasamy M, Suryawanshi A, Tundup S, Perez JT, Schmolke M, Manicassamy S, Manicassamy B.** 2016. RIG-I Signaling Is Critical for Efficient Polyfunctional T Cell Responses during Influenza Virus Infection. PLoS Pathog **12:**e1005754.

65. **Wang Q, Nagarkar DR, Bowman ER, Schneider D, Gosangi B, Lei J, Zhao Y, McHenry CL, Burgens RV, Miller DJ, Sajjan U, Hershenson MB.** 2009. Role of double-stranded RNA pattern recognition receptors in rhinovirus-induced airway epithelial cell responses. J Immunol **183:**6989-6997.

66. **Slater L, Bartlett NW, Haas JJ, Zhu J, Message SD, Walton RP, Sykes A, Dahdaleh S, Clarke DL, Belvisi MG, Kon OM, Fujita T, Jeffery PK, Johnston SL, Edwards MR.** 2010. Co-ordinated role of TLR3, RIG-I and MDA5 in the innate response to rhinovirus in bronchial epithelium. PLoS Pathog **6:**e1001178.

67. **Dhar J, Barik S.** 2016. Unique nonstructural proteins of Pneumonia Virus of Mice (PVM) promote degradation of interferon (IFN) pathway components and IFN-stimulated gene proteins. Sci Rep **6:**38139.

68. **Wang Q, Miller DJ, Bowman ER, Nagarkar DR, Schneider D, Zhao Y, Linn MJ, Goldsmith AM, Bentley JK, Sajjan US, Hershenson MB.** 2011. MDA5 and TLR3 initiate pro-inflammatory signaling pathways leading to rhinovirus-induced airways inflammation and hyperresponsiveness. PLoS Pathog **7:**e1002070.

69. **Triantafilou K, Vakakis E, Richer EA, Evans GL, Villiers JP, Triantafilou M.** 2011. Human rhinovirus recognition in non-immune cells is mediated by Toll-like receptors and MDA-5, which trigger a synergetic pro-inflammatory immune response. Virulence **2:**22-29.

70. **Benitez AA, Panis M, Xue J, Varble A, Shim JV, Frick AL, Lopez CB, Sachs D, tenOever BR.** 2015. In Vivo RNAi Screening Identifies MDA5 as a Significant Contributor to the Cellular Defense against Influenza A Virus. Cell Rep **11:**1714-1726.

71. **Kurt-Jones EA, Popova L, Kwinn L, Haynes LM, Jones LP, Tripp RA, Walsh EE, Freeman MW, Golenbock DT, Anderson LJ, Finberg RW.** 2000. Pattern recognition receptors TLR4 and CD14 mediate response to respiratory syncytial virus. Nat Immunol **1:**398-401.

72. **Khanolkar A, Hartwig SM, Haag BA, Meyerholz DK, Harty JT, Varga SM.** 2009. Toll-like receptor 4 deficiency increases disease and mortality after mouse hepatitis virus type 1 infection of susceptible C3H mice. J Virol **83:**8946-8956.

73. **Faisca P, Tran Anh DB, Thomas A, Desmecht D.** 2006. Suppression of pattern-recognition receptor TLR4 sensing does not alter lung responses to pneumovirus infection. Microbes Infect **8:**621-627.

74. **Bleau C, Filliol A, Samson M, Lamontagne L.** 2016. Mouse Hepatitis Virus Infection Induces a Toll-Like Receptor 2-Dependent Activation of Inflammatory Functions in Liver Sinusoidal Endothelial Cells during Acute Hepatitis. J Virol **90:**9096-9113.

75. **Roth-Cross JK, Bender SJ, Weiss SR.** 2008. Murine coronavirus mouse hepatitis virus is recognized by MDA5 and induces type I interferon in brain macrophages/microglia. J Virol **82:**9829-9838.

76. **Nagarkar DR, Wang Q, Shim J, Zhao Y, Tsai WC, Lukacs NW, Sajjan U, Hershenson MB.** 2009. CXCR2 is required for neutrophilic airway inflammation and hyperresponsiveness in a mouse model of human rhinovirus infection. J Immunol **183:**6698-6707.

77. **Newcomb DC, Sajjan US, Nagarkar DR, Wang Q, Nanua S, Zhou Y, McHenry CL, Hennrick KT, Tsai WC, Bentley JK, Lukacs NW, Johnston SL, Hershenson MB.** 2008. Human rhinovirus 1B exposure induces phosphatidylinositol 3-kinase-dependent airway inflammation in mice. Am J Respir Crit Care Med **177:**1111-1121.

78. **Bochkov YA, Gern JE.** 2016. Rhinoviruses and Their Receptors: Implications for Allergic Disease. Curr Allergy Asthma Rep **16:**30.

79. **Belser JA, Wadford DA, Pappas C, Gustin KM, Maines TR, Pearce MB, Zeng H, Swayne DE, Pantin-Jackwood M, Katz JM, Tumpey TM.** 2010. Pathogenesis of Pandemic Influenza A (H1N1) and Triple-Reassortant Swine Influenza A (H1) Viruses in Mice. Journal of Virology **84:**4194-4203.

80. **Fukushi M, Ito T, Oka T, Kitazawa T, Miyoshi-Akiyama T, Kirikae T, Yamashita M, Kudo K.** 2011. Serial histopathological examination of the lungs of mice infected with influenza A virus PR8 strain. PLoS One **6:**e21207.

81. **Allen IC, Scull MA, Moore CB, Holl EK, McElvania-TeKippe E, Taxman DJ, Guthrie EH, Pickles RJ, Ting JP.** 2009. The NLRP3 inflammasome mediates in vivo innate immunity to influenza A virus through recognition of viral RNA. Immunity **30:**556-565.

82. **Hufford MM, Richardson G, Zhou H, Manicassamy B, Garcia-Sastre A, Enelow RI, Braciale TJ.** 2012. Influenza-infected neutrophils within the infected lungs act as antigen presenting cells for anti-viral CD8(+) T cells. PLoS One **7:**e46581.

83. **Leibowitz JL, Srinivasa R, Williamson ST, Chua MM, Liu M, Wu S, Kang H, Ma XZ, Zhang J, Shalev I, Smith R, Phillips MJ, Levy GA, Weiss SR.** 2010. Genetic determinants of mouse hepatitis virus strain 1 pneumovirulence. J Virol **84:**9278-9291.

84. **Kebaabetswe LP, Haick AK, Miura TA.** 2013. Differentiated phenotypes of primary murine alveolar epithelial cells and their susceptibility to infection by respiratory viruses. Virus Res **175:**110-119.

85. **VanLeuven JT, Ridenhour BJ, Gonzalez AJ, Miller CR, Miura TA.** 2017. Lung epithelial cells have virus-specific and shared gene expression responses to infection by diverse respiratory viruses. PLoS One **12:**e0178408.

86. **Dyer KD, Garcia-Crespo KE, Glineur S, Domachowske JB, Rosenberg HF.** 2012. The Pneumonia Virus of Mice (PVM) model of acute respiratory infection. Viruses **4:**3494-3510.

87. **Cook PM, Eglin RP, Easton AJ.** 1998. Pathogenesis of pneumovirus infections in mice: detection of pneumonia virus of mice and human respiratory syncytial virus mRNA in lungs of infected mice by in situ hybridization. J Gen Virol **79 ( Pt 10):**2411-2417.

88. **Watkiss ER, Shrivastava P, Arsic N, Gomis S, van Drunen Littel-van den Hurk S.** 2013. Innate and adaptive immune response to pneumonia virus of mice in a resistant and a susceptible mouse strain. Viruses **5:**295-320.

89. **Hori T, Kiyoshima J, Shida K, Yasui H.** 2001. Effect of intranasal administration of Lactobacillus casei Shirota on influenza virus infection of upper respiratory tract in mice. Clin Diagn Lab Immunol **8:**593-597.

90. **Kawase M, He F, Kubota A, Harata G, Hiramatsu M.** 2010. Oral administration of lactobacilli from human intestinal tract protects mice against influenza virus infection. Lett Appl Microbiol **51:**6-10.

91. **Li R, Lim A, Phoon MC, Narasaraju T, Ng JK, Poh WP, Sim MK, Chow VT, Locht C, Alonso S.** 2010. Attenuated Bordetella pertussis protects against highly pathogenic influenza A viruses by dampening the cytokine storm. J Virol **84:**7105-7113.

92. **Carrano VA, Barthold SW, Beck DS, Smith AL.** 1984. Alteration of viral respiratory infections of mice by prior infection with mouse hepatitis virus. Lab Anim Sci **34:**573-576.

93. **Ayegbusi OT, Ajagbe OA, Afowowe TO, Aransi AT, Olusola BA, Awogbindin IO, Ogunsemowo OO, Faneye AO, Odaibo GN, Olaleye DO.** 2019. Virus genes and host correlates of pathology are markedly reduced during respiratory syncytial and influenza virus co-infection in BALB/c mice. Heliyon **5:**e01094.

94. **Chan KF, Carolan LA, Korenkov D, Druce J, McCaw J, Reading PC, Barr IG, Laurie KL.** 2018. Investigating Viral Interference Between Influenza A Virus and Human Respiratory Syncytial Virus in a Ferret Model of Infection. J Infect Dis **218:**406-417.

95. **Jung K, Renukaradhya GJ, Alekseev KP, Fang Y, Tang Y, Saif LJ.** 2009. Porcine reproductive and respiratory syndrome virus modifies innate immunity and alters disease outcome in pigs subsequently infected with porcine respiratory coronavirus: implications for respiratory viral co-infections. J Gen Virol **90:**2713-2723.

96. **Szretter KJ, Balish AL, Katz JM.** 2006. Influenza: propagation, quantification, and storage. Curr Protoc Microbiol **Chapter 15:**Unit 15G 11.

97. **Sommereyns C, Paul S, Staeheli P, Michiels T.** 2008. IFN-lambda (IFN-lambda) is expressed in a tissue-dependent fashion and primarily acts on epithelial cells in vivo. PLoS Pathog **4:**e1000017.

98. **Jones PH, Mehta HV, Maric M, Roller RJ, Okeoma CM.** 2012. Bone marrow stromal cell antigen 2 (BST-2) restricts mouse mammary tumor virus (MMTV) replication in vivo. Retrovirology **9:**10.

99. **Pazos MA, Kraus TA, Munoz-Fontela C, Moran TM.** 2012. Estrogen Mediates Innate and Adaptive Immune Alterations to Influenza Infection in Pregnant Mice. Plos One **7**.

100. **Livak KJ, Schmittgen TD.** 2001. Analysis of relative gene expression data using real-time quantitative PCR and the 2(-Delta Delta C(T)) Method. Methods **25:**402-408.

101. **Beale AJ.** 1963. Viral interference and interferon. Annu Rev Med **14:**133-140.

102. **Yewdell JW, Bennink JR.** 1999. Mechanisms of viral interference with MHC class I antigen processing and presentation. Annu Rev Cell Dev Biol **15:**579-606.

103. **Landi A, Iannucci V, Nuffel AV, Meuwissen P, Verhasselt B.** 2011. One protein to rule them all: modulation of cell surface receptors and molecules by HIV Nef. Curr HIV Res **9:**496-504.

104. **Zheng X, Song Z, Li Y, Zhang J, Wang XL.** 2017. Possible interference between seasonal epidemics of influenza and other respiratory viruses in Hong Kong, 2014-2017. BMC Infect Dis **17:**772.

105. **Casalegno JS, Ottmann M, Duchamp MB, Escuret V, Billaud G, Frobert E, Morfin F, Lina B.** 2010. Rhinoviruses delayed the circulation of the pandemic influenza A (H1N1) 2009 virus in France. Clin Microbiol Infect **16:**326-329.

106. **Linde A, Rotzen-Ostlund M, Zweygberg-Wirgart B, Rubinova S, Brytting M.** 2009. Does viral interference affect spread of influenza? Euro Surveill **14**.

107. **Bodewes R, Nieuwkoop NJ, Verburgh RJ, Fouchier RA, Osterhaus AD, Rimmelzwaan GF.** 2012. Use of influenza A viruses expressing reporter genes to assess the frequency of double infections in vitro. J Gen Virol **93:**1645-1648.

108. **Goto H, Ihira H, Morishita K, Tsuchiya M, Ohta K, Yumine N, Tsurudome M, Nishio M.** 2016. Enhanced growth of influenza A virus by coinfection with human parainfluenza virus type 2. Med Microbiol Immunol **205:**209-218.

109. **Laurie KL, Guarnaccia TA, Carolan LA, Yan AW, Aban M, Petrie S, Cao P, Heffernan JM, McVernon J, Mosse J, Kelso A, McCaw JM, Barr IG.** 2015. Interval Between Infections and Viral Hierarchy Are Determinants of Viral Interference Following Influenza Virus Infection in a Ferret Model. J Infect Dis **212:**1701-1710.

110. **Schaller T, Appel N, Koutsoudakis G, Kallis S, Lohmann V, Pietschmann T, Bartenschlager R.** 2007. Analysis of hepatitis C virus superinfection exclusion by using novel fluorochrome gene-tagged viral genomes. J Virol **81:**4591-4603.

111. **Webster B, Ott M, Greene WC.** 2013. Evasion of superinfection exclusion and elimination of primary viral RNA by an adapted strain of hepatitis C virus. J Virol **87:**13354-13369.

112. **Huang IC, Li W, Sui J, Marasco W, Choe H, Farzan M.** 2008. Influenza A virus neuraminidase limits viral superinfection. J Virol **82:**4834-4843.

113. **Karpf AR, Lenches E, Strauss EG, Strauss JH, Brown DT.** 1997. Superinfection exclusion of alphaviruses in three mosquito cell lines persistently infected with Sindbis virus. J Virol **71:**7119-7123.

114. **Folimonova SY.** 2012. Superinfection exclusion is an active virus-controlled function that requires a specific viral protein. J Virol **86:**5554-5561.

115. **Bergua M, Zwart MP, El-Mohtar C, Shilts T, Elena SF, Folimonova SY.** 2014. A viral protein mediates superinfection exclusion at the whole-organism level but is not required for exclusion at the cellular level. J Virol **88:**11327-11338.

116. **Tuthill TJ, Papadopoulos NG, Jourdan P, Challinor LJ, Sharp NA, Plumpton C, Shah K, Barnard S, Dash L, Burnet J, Killington RA, Rowlands DJ, Clarke NJ, Blair ED, Johnston SL.** 2003. Mouse respiratory epithelial cells support efficient replication of human rhinovirus. J Gen Virol **84:**2829-2836.

117. **Tate MD, Schilter HC, Brooks AG, Reading PC.** 2011. Responses of mouse airway epithelial cells and alveolar macrophages to virulent and avirulent strains of influenza A virus. Viral Immunol **24:**77-88.

118. **Unger BL, Faris AN, Ganesan S, Comstock AT, Hershenson MB, Sajjan US.** 2012. Rhinovirus attenuates non-typeable Hemophilus influenzae-stimulated IL-8 responses via TLR2-dependent degradation of IRAK-1. PLoS Pathog **8:**e1002969.

119. **Brenner TA, Rice TA, Anderson ED, Percopo CM, Rosenberg HF.** 2016. Immortalized MH-S cells lack defining features of primary alveolar macrophages and do not support mouse pneumovirus replication. Immunol Lett **172:**106-112.

120. **Shinjoh M, Omoe K, Saito N, Matsuo N, Nerome K.** 2000. In vitro growth profiles of respiratory syncytial virus in the presence of influenza virus. Acta Virol **44:**91-97.

121. **Haye K, Burmakina S, Moran T, Garcia-Sastre A, Fernandez-Sesma A.** 2009. The NS1 protein of a human influenza virus inhibits type I interferon production and the induction of antiviral responses in primary human dendritic and respiratory epithelial cells. J Virol **83:**6849-6862.

122. **Mangeat B, Cavagliotti L, Lehmann M, Gers-Huber G, Kaur I, Thomas Y, Kaiser L, Piguet V.** 2012. Influenza virus partially counteracts restriction imposed by tetherin/BST-2. J Biol Chem **287:**22015-22029.

123. **Anastasina M, Le May N, Bugai A, Fu Y, Soderholm S, Gaelings L, Ohman T, Tynell J, Kyttanen S, Barboric M, Nyman TA, Matikainen S, Julkunen I, Butcher SJ, Egly JM, Kainov DE.** 2016. Influenza virus NS1 protein binds cellular DNA to block transcription of antiviral genes. Biochim Biophys Acta **1859:**1440-1448.

124. **Xia C, Vijayan M, Pritzl CJ, Fuchs SY, McDermott AB, Hahm B.** 2015. Hemagglutinin of Influenza A Virus Antagonizes Type I Interferon (IFN) Responses by Inducing Degradation of Type I IFN Receptor 1. J Virol **90:**2403-2417.

125. **Hewson CA, Jardine A, Edwards MR, Laza-Stanca V, Johnston SL.** 2005. Toll-like receptor 3 is induced by and mediates antiviral activity against rhinovirus infection of human bronchial epithelial cells. J Virol **79:**12273-12279.

126. **Foxman EF, Storer JA, Fitzgerald ME, Wasik BR, Hou L, Zhao H, Turner PE, Pyle AM, Iwasaki A.** 2015. Temperature-dependent innate defense against the common cold virus limits viral replication at warm temperature in mouse airway cells. Proc Natl Acad Sci U S A **112:**827-832.

127. **Frensing T, Kupke SY, Bachmann M, Fritzsche S, Gallo-Ramirez LE, Reichl U.** 2016. Influenza virus intracellular replication dynamics, release kinetics, and particle morphology during propagation in MDCK cells. Appl Microbiol Biotechnol **100:**7181-7192.

128. **Fuchs R, Blaas D.** 2010. Uncoating of human rhinoviruses. Rev Med Virol **20:**281-297.

129. **Rehwinkel J, Tan CP, Goubau D, Schulz O, Pichlmair A, Bier K, Robb N, Vreede F, Barclay W, Fodor E, Reis e Sousa C.** 2010. RIG-I detects viral genomic RNA during negative-strand RNA virus infection. Cell **140:**397-408.

130. **Iwasaki A, Pillai PS.** 2014. Innate immunity to influenza virus infection. Nat Rev Immunol **14:**315-328.

131. **Londrigan SL, Short KR, Ma J, Gillespie L, Rockman SP, Brooks AG, Reading PC.** 2015. Infection of Mouse Macrophages by Seasonal Influenza Viruses Can Be Restricted at the Level of Virus Entry and at a Late Stage in the Virus Life Cycle. J Virol **89:**12319-12329.

132. **Wells MA, Albrecht P, Daniel S, Ennis FA.** 1978. Host defense mechanisms against influenza virus: interaction of influenza virus with murine macrophages in vitro. Infect Immun **22:**758-762.

133. **Reading PC, Whitney PG, Pickett DL, Tate MD, Brooks AG.** 2010. Influenza viruses differ in ability to infect macrophages and to induce a local inflammatory response following intraperitoneal injection of mice. Immunol Cell Biol **88:**641-650.

134. **Oliver BG, Lim S, Wark P, Laza-Stanca V, King N, Black JL, Burgess JK, Roth M, Johnston SL.** 2008. Rhinovirus exposure impairs immune responses to bacterial products in human alveolar macrophages. Thorax **63:**519-525.

135. **Gern JE, Dick EC, Lee WM, Murray S, Meyer K, Handzel ZT, Busse WW.** 1996. Rhinovirus enters but does not replicate inside monocytes and airway macrophages. J Immunol **156:**621-627.

136. **Brand HK, de Groot R, Galama JM, Brouwer ML, Teuwen K, Hermans PW, Melchers WJ, Warris A.** 2012. Infection with multiple viruses is not associated with increased disease severity in children with bronchiolitis. Pediatr Pulmonol **47:**393-400.

137. **Gaunt ER, Hardie A, Claas EC, Simmonds P, Templeton KE.** 2010. Epidemiology and clinical presentations of the four human coronaviruses 229E, HKU1, NL63, and OC43 detected over 3 years using a novel multiplex real-time PCR method. J Clin Microbiol **48:**2940-2947.

138. **Morris DE, Cleary DW, Clarke SC.** 2017. Secondary Bacterial Infections Associated with Influenza Pandemics. Front Microbiol **8:**1041.

139. **Morens DM, Taubenberger JK, Fauci AS.** 2008. Predominant role of bacterial pneumonia as a cause of death in pandemic influenza: implications for pandemic influenza preparedness. J Infect Dis **198:**962-970.

140. **MacIntyre CR, Chughtai AA, Barnes M, Ridda I, Seale H, Toms R, Heywood A.** 2018. The role of pneumonia and secondary bacterial infection in fatal and serious outcomes of pandemic influenza a(H1N1)pdm09. BMC Infect Dis **18:**637.

141. **Youn HN, Lee DH, Lee YN, Park JK, Yuk SS, Yang SY, Lee HJ, Woo SH, Kim HM, Lee JB, Park SY, Choi IS, Song CS.** 2012. Intranasal administration of live Lactobacillus species facilitates protection against influenza virus infection in mice. Antiviral Res **93:**138-143.

142. **Girkin J, Hatchwell L, Foster P, Johnston SL, Bartlett N, Collison A, Mattes J.** 2015. CCL7 and IRF-7 Mediate Hallmark Inflammatory and IFN Responses following Rhinovirus 1B Infection. J Immunol **194:**4924-4930.

143. **Crotta S, Davidson S, Mahlakoiv T, Desmet CJ, Buckwalter MR, Albert ML, Staeheli P, Wack A.** 2013. Type I and type III interferons drive redundant amplification loops to induce a transcriptional signature in influenza-infected airway epithelia. PLoS Pathog **9:**e1003773.

144. **Stifter SA, Bhattacharyya N, Pillay R, Florido M, Triccas JA, Britton WJ, Feng CG.** 2016. Functional Interplay between Type I and II Interferons Is Essential to Limit Influenza A Virus-Induced Tissue Inflammation. PLoS Pathog **12:**e1005378.

145. **Arimori Y, Nakamura R, Yamada H, Shibata K, Maeda N, Kase T, Yoshikai Y.** 2013. Type I interferon limits influenza virus-induced acute lung injury by regulation of excessive inflammation in mice. Antiviral Res **99:**230-237.

146. **Seo SU, Kwon HJ, Ko HJ, Byun YH, Seong BL, Uematsu S, Akira S, Kweon MN.** 2011. Type I interferon signaling regulates Ly6C(hi) monocytes and neutrophils during acute viral pneumonia in mice. PLoS Pathog **7:**e1001304.

147. **Koerner I, Kochs G, Kalinke U, Weiss S, Staeheli P.** 2007. Protective role of beta interferon in host defense against influenza A virus. J Virol **81:**2025-2030.

148. **Galani IE, Triantafyllia V, Eleminiadou EE, Koltsida O, Stavropoulos A, Manioudaki M, Thanos D, Doyle SE, Kotenko SV, Thanopoulou K, Andreakos E.** 2017. Interferon-lambda Mediates Non-redundant Front-Line Antiviral Protection against Influenza Virus Infection without Compromising Host Fitness. Immunity **46:**875-890 e876.

149. **Davidson S, Crotta S, McCabe TM, Wack A.** 2014. Pathogenic potential of interferon alphabeta in acute influenza infection. Nat Commun **5:**3864.

150. **Walsh KB, Teijaro JR, Brock LG, Fremgen DM, Collins PL, Rosen H, Oldstone MB.** 2014. Animal model of respiratory syncytial virus: CD8+ T cells cause a cytokine storm that is chemically tractable by sphingosine-1-phosphate 1 receptor agonist therapy. J Virol **88:**6281-6293.

151. **Garvey TL, Dyer KD, Ellis JA, Bonville CA, Foster B, Prussin C, Easton AJ, Domachowske JB, Rosenberg HF.** 2005. Inflammatory responses to pneumovirus infection in IFN-alpha beta R gene-deleted mice. J Immunol **175:**4735-4744.

152. **Glineur SF, Bowen AB, Percopo CM, Garcia-Crespo KE, Dyer KD, Ochkur SI, Lee NA, Lee JJ, Domachowske JB, Rosenberg HF.** 2014. Sustained inflammation and differential expression of interferons type I and III in PVM-infected interferon-gamma (IFNgamma) gene-deleted mice. Virology **468-470:**140-149.

153. **Heinze B, Frey S, Mordstein M, Schmitt-Graff A, Ehl S, Buchholz UJ, Collins PL, Staeheli P, Krempl CD.** 2011. Both nonstructural proteins NS1 and NS2 of pneumonia virus of mice are inhibitors of the interferon type I and type III responses in vivo. J Virol **85:**4071-4084.

154. **Khanolkar A, Hartwig SM, Haag BA, Meyerholz DK, Epping LL, Haring JS, Varga SM, Harty JT.** 2009. Protective and pathologic roles of the immune response to mouse hepatitis virus type 1: implications for severe acute respiratory syndrome. J Virol **83:**9258-9272.

155. **Channappanavar R, Fehr AR, Vijay R, Mack M, Zhao J, Meyerholz DK, Perlman S.** 2016. Dysregulated Type I Interferon and Inflammatory Monocyte-Macrophage Responses Cause Lethal Pneumonia in SARS-CoV-Infected Mice. Cell Host Microbe **19:**181-193.

156. **Singanayagam A, Glanville N, Walton RP, Aniscenko J, Pearson RM, Pinkerton JW, Horvat JC, Hansbro PM, Bartlett NW, Johnston SL.** 2015. A short-term mouse model that reproduces the immunopathological features of rhinovirus-induced exacerbation of COPD. Clin Sci (Lond) **129:**245-258.

157. **Han M, Hong JY, Jaipalli S, Rajput C, Lei J, Hinde JL, Chen Q, Hershenson NM, Bentley JK, Hershenson MB.** 2017. IFN-gamma Blocks Development of an Asthma Phenotype in Rhinovirus-Infected Baby Mice by Inhibiting Type 2 Innate Lymphoid Cells. Am J Respir Cell Mol Biol **56:**242-251.

158. **Ehre C, Worthington EN, Liesman RM, Grubb BR, Barbier D, O'Neal WK, Sallenave JM, Pickles RJ, Boucher RC.** 2012. Overexpressing mouse model demonstrates the protective role of Muc5ac in the lungs. Proc Natl Acad Sci U S A **109:**16528-16533.

159. **Stokes KL, Currier MG, Sakamoto K, Lee S, Collins PL, Plemper RK, Moore ML.** 2013. The respiratory syncytial virus fusion protein and neutrophils mediate the airway mucin response to pathogenic respiratory syncytial virus infection. J Virol **87:**10070-10082.

160. **Scheer S, Krempl C, Kallfass C, Frey S, Jakob T, Mouahid G, Mone H, Schmitt-Graff A, Staeheli P, Lamers MC.** 2014. S. mansoni bolsters anti-viral immunity in the murine respiratory tract. PLoS One **9:**e112469.

161. **Fujisawa H.** 2008. Neutrophils play an essential role in cooperation with antibody in both protection against and recovery from pulmonary infection with influenza virus in mice. J Virol **82:**2772-2783.

162. **Narasaraju T, Yang E, Samy RP, Ng HH, Poh WP, Liew AA, Phoon MC, van Rooijen N, Chow VT.** 2011. Excessive neutrophils and neutrophil extracellular traps contribute to acute lung injury of influenza pneumonitis. Am J Pathol **179:**199-210.

163. **Dyer KD, Drummond RA, Rice TA, Percopo CM, Brenner TA, Barisas DA, Karpe KA, Moore ML, Rosenberg HF.** 2016. Priming of the Respiratory Tract with Immunobiotic Lactobacillus plantarum Limits Infection of Alveolar Macrophages with Recombinant Pneumonia Virus of Mice (rK2-PVM). J Virol **90:**979-991.

164. **Tate MD, Pickett DL, van Rooijen N, Brooks AG, Reading PC.** 2010. Critical role of airway macrophages in modulating disease severity during influenza virus infection of mice. J Virol **84:**7569-7580.

165. **Kim HM, Lee YW, Lee KJ, Kim HS, Cho SW, van Rooijen N, Guan Y, Seo SH.** 2008. Alveolar macrophages are indispensable for controlling influenza viruses in lungs of pigs. J Virol **82:**4265-4274.

166. **Hartwig SM, Holman KM, Varga SM.** 2014. Depletion of alveolar macrophages ameliorates virus-induced disease following a pulmonary coronavirus infection. PLoS One **9:**e90720.

167. **Frey S, Krempl CD, Schmitt-Graff A, Ehl S.** 2008. Role of T cells in virus control and disease after infection with pneumonia virus of mice. J Virol **82:**11619-11627.

168. **Hamada H, Garcia-Hernandez Mde L, Reome JB, Misra SK, Strutt TM, McKinstry KK, Cooper AM, Swain SL, Dutton RW.** 2009. Tc17, a unique subset of CD8 T cells that can protect against lethal influenza challenge. J Immunol **182:**3469-3481.

169. **Zalinger ZB, Elliott R, Rose KM, Weiss SR.** 2015. MDA5 Is Critical to Host Defense during Infection with Murine Coronavirus. J Virol **89:**12330-12340.

170. **Kato H, Takeuchi O, Sato S, Yoneyama M, Yamamoto M, Matsui K, Uematsu S, Jung A, Kawai T, Ishii KJ, Yamaguchi O, Otsu K, Tsujimura T, Koh CS, Reis e Sousa C, Matsuura Y, Fujita T, Akira S.** 2006. Differential roles of MDA5 and RIG-I helicases in the recognition of RNA viruses. Nature **441:**101-105.

171. **Kim WK, Jain D, Sanchez MD, Koziol-White CJ, Matthews K, Ge MQ, Haczku A, Panettieri RA, Jr., Frieman MB, Lopez CB.** 2014. Deficiency of melanoma differentiation-associated protein 5 results in exacerbated chronic postviral lung inflammation. Am J Respir Crit Care Med **189:**437-448.

172. **Zhou H, Perlman S.** 2007. Mouse hepatitis virus does not induce Beta interferon synthesis and does not inhibit its induction by double-stranded RNA. J Virol **81:**568-574.

173. **Versteeg GA, Bredenbeek PJ, van den Worm SH, Spaan WJ.** 2007. Group 2 coronaviruses prevent immediate early interferon induction by protection of viral RNA from host cell recognition. Virology **361:**18-26.

174. **Han B, Ma X, Zhang J, Zhang Y, Bai X, Hwang DM, Keshavjee S, Levy GA, McGilvray I, Liu M.** 2012. Protective effects of long pentraxin PTX3 on lung injury in a severe acute respiratory syndrome model in mice. Lab Invest **92:**1285-1296.

175. **Rogers E, Wang BX, Cui Z, Rowley DR, Ressler SJ, Vyakarnam A, Fish EN.** 2012. WFDC1/ps20: a host factor that influences the neutrophil response to murine hepatitis virus (MHV) 1 infection. Antiviral Res **96:**158-168.

176. **Tate MD, Deng YM, Jones JE, Anderson GP, Brooks AG, Reading PC.** 2009. Neutrophils ameliorate lung injury and the development of severe disease during influenza infection. J Immunol **183:**7441-7450.

177. **Sun J, Madan R, Karp CL, Braciale TJ.** 2009. Effector T cells control lung inflammation during acute influenza virus infection by producing IL-10. Nat Med **15:**277-284.

178. **Sheehan KC, Lazear HM, Diamond MS, Schreiber RD.** 2015. Selective Blockade of Interferon-alpha and -beta Reveals Their Non-Redundant Functions in a Mouse Model of West Nile Virus Infection. PLoS One **10:**e0128636.

179. **Strehl B, Seifert U, Kruger E, Heink S, Kuckelkorn U, Kloetzel PM.** 2005. Interferon-gamma, the functional plasticity of the ubiquitin-proteasome system, and MHC class I antigen processing. Immunological Reviews **207:**19-30.

180. **Lykens JE, Terrell CE, Zoller EE, Divanovic S, Trompette A, Karp CL, Aliberti J, Flick MJ, Jordan MB.** 2010. Mice with a Selective Impairment of IFN-gamma Signaling in Macrophage Lineage Cells Demonstrate the Critical Role of IFN-gamma-Activated Macrophages for the Control of Protozoan Parasitic Infections In Vivo. Journal of Immunology **184:**877-885.

181. **Walunas TL, Bakker CY, Bluestone JA.** 1996. CTLA-4 ligation blocks CD28-dependent T cell activation. Journal of Experimental Medicine **183:**2541-2550.

182. **Walunas TL, Lenschow DJ, Bakker CY, Linsley PS, Freeman GJ, Green JM, Thompson CB, Bluestone JA.** 1994. Ctla-4 Can Function as a Negative Regulator of T-Cell Activation. Immunity **1:**405-413.

183. **Afonina IS, Cullen SP, Martin SJ.** 2010. Cytotoxic and non-cytotoxic roles of the CTL/NK protease granzyme B. Immunological Reviews **235:**105-116.

184. **Verhelst J, Parthoens E, Schepens B, Fiers W, Saelens X.** 2012. Interferon-Inducible Protein Mx1 Inhibits Influenza Virus by Interfering with Functional Viral Ribonucleoprotein Complex Assembly. Journal of Virology **86:**13445-13455.

185. **Pavlovic J, Haller O, Staeheli P.** 1992. Human and Mouse Mx-Proteins Inhibit Different Steps of the Influenza-Virus Multiplication Cycle. Journal of Virology **66:**2564-2569.

186. **Ehre C, Worthington EN, Liesman RM, Grubb BR, Barbier D, O'Neal WK, Sallenave JM, Pickles RJ, Boucher RC.** 2012. Overexpressing mouse model demonstrates the protective role of Muc5ac in the lungs. Proceedings of the National Academy of Sciences of the United States of America **109:**16528-16533.

187. **Hewson CA, Haas JJ, Bartlett NW, Message SD, Laza-Stanca V, Kebadze T, Caramori G, Zhu J, Edbrooke MR, Stanciu LA, Kon OM, Papi A, Jeffery PK, Edwards MR, Johnston SL.** 2010. Rhinovirus induces MUC5AC in a human infection model and in vitro via NF-kappa B and EGFR pathways. European Respiratory Journal **36:**1425-1435.

188. **Nakanishi A, Morita S, Iwashita H, Sagiya Y, Ashida Y, Shirafuji H, Fujisawa Y, Nishimura O, Fujino M.** 2001. Role of gob-5 in mucus overproduction and airway hyperresponsiveness in asthma. Proceedings of the National Academy of Sciences of the United States of America **98:**5175-5180.

189. **Zhou YH, Dong Q, Louahed J, Dragwa C, Savio D, Huang MX, Weiss C, Tomer Y, McLane MP, Nicolaides NC, Levitt RC.** 2001. Characterization of a calcium-activated chloride channel as a shared target of Th2 cytokine pathways and its potential involvement in asthma. American Journal of Respiratory Cell and Molecular Biology **25:**486-491.

190. **Brenner D, Blaser H, Mak TW.** 2015. Regulation of tumour necrosis factor signalling: live or let die. Nature Reviews Immunology **15:**362-374.

191. **Chu WM.** 2013. Tumor necrosis factor. Cancer Letters **328:**222-225.

192. **Honda K, Yanai H, Negishi H, Asagiri M, Sato M, Mizutani T, Shimada N, Ohba Y, Takaoka A, Yoshida N, Taniguchi T.** 2005. IRF-7 is the master regulator of type-I interferon-dependent immune responses. Nature **434:**772-777.

193. **Sawant KV, Xu RL, Cox R, Hawkins H, Sbrana E, Kolli D, Garofalo RP, Rajarathnam K.** 2015. Chemokine CXCL1-Mediated Neutrophil Trafficking in the Lung: Role of CXCR2 Activation. Journal of Innate Immunity **7:**647-658.

194. **Chintakuntlawar AV, Chodosh J.** 2009. Chemokine CXCL1/KC and its Receptor CXCR2 Are Responsible for Neutrophil Chemotaxis in Adenoviral Keratitis. Journal of Interferon and Cytokine Research **29:**657-666.

195. **Prince LR, Allen L, Jones EC, Hellewell PG, Dower SK, Whyte MKB, Sabroe I.** 2004. The role of interleukin-1 beta in direct and toll-like receptor 4-mediated neutrophil activation and survival. American Journal of Pathology **165:**1819-1826.

196. **Matzinger SR, Carroll TD, Fritts L, McChesney MB, Miller CJ.** 2011. Exogenous IFN-alpha administration reduces influenza A virus replication in the lower respiratory tract of rhesus macaques. PLoS One **6:**e29255.

197. **Kugel D, Kochs G, Obojes K, Roth J, Kobinger GP, Kobasa D, Haller O, Staeheli P, von Messling V.** 2009. Intranasal administration of alpha interferon reduces seasonal influenza A virus morbidity in ferrets. J Virol **83:**3843-3851.

198. **Iwai A, Shiozaki T, Kawai T, Akira S, Kawaoka Y, Takada A, Kida H, Miyazaki T.** 2010. Influenza A virus polymerase inhibits type I interferon induction by binding to interferon beta promoter stimulator 1. J Biol Chem **285:**32064-32074.

199. **Cheung CY, Poon LL, Lau AS, Luk W, Lau YL, Shortridge KF, Gordon S, Guan Y, Peiris JS.** 2002. Induction of proinflammatory cytokines in human macrophages by influenza A (H5N1) viruses: a mechanism for the unusual severity of human disease? Lancet **360:**1831-1837.

200. **Sugamata R, Dobashi H, Nagao T, Yamamoto K, Nakajima N, Sato Y, Aratani Y, Oshima M, Sata T, Kobayashi K, Kawachi S, Nakayama T, Suzuki K.** 2012. Contribution of neutrophil-derived myeloperoxidase in the early phase of fulminant acute respiratory distress syndrome induced by influenza virus infection. Microbiol Immunol **56:**171-182.

201. **Watanabe T, Tisoncik-Go J, Tchitchek N, Watanabe S, Benecke AG, Katze MG, Kawaoka Y.** 2013. 1918 Influenza virus hemagglutinin (HA) and the viral RNA polymerase complex enhance viral pathogenicity, but only HA induces aberrant host responses in mice. J Virol **87:**5239-5254.

202. **Long JP, Kotur MS, Stark GV, Warren RL, Kasoji M, Craft JL, Albrecht RA, Garcia-Sastre A, Katze MG, Waters KM, Vasconcelos D, Sabourin PJ, Bresler HS, Sabourin CL.** 2013. Accumulation of CD11b(+)Gr-1(+) cells in the lung, blood and bone marrow of mice infected with highly pathogenic H5N1 and H1N1 influenza viruses. Arch Virol **158:**1305-1322.

203. **Bonville CA, Percopo CM, Dyer KD, Gao J, Prussin C, Foster B, Rosenberg HF, Domachowske JB.** 2009. Interferon-gamma coordinates CCL3-mediated neutrophil recruitment in vivo. BMC Immunol **10:**14.

204. **Akaike T, Noguchi Y, Ijiri S, Setoguchi K, Suga M, Zheng YM, Dietzschold B, Maeda H.** 1996. Pathogenesis of influenza virus-induced pneumonia: involvement of both nitric oxide and oxygen radicals. Proc Natl Acad Sci U S A **93:**2448-2453.

205. **Yasui K, Baba A, Iwasaki Y, Kubo T, Aoyama K, Mori T, Yamazaki T, Kobayashi N, Ishiguro A.** 2005. Neutrophil-mediated inflammation in respiratory syncytial viral bronchiolitis. Pediatr Int **47:**190-195.

206. **Rigaux P, Killoran KE, Qiu Z, Rosenberg HF.** 2012. Depletion of alveolar macrophages prolongs survival in response to acute pneumovirus infection. Virology **422:**338-345.

207. **Dyer KD, Schellens IM, Bonville CA, Martin BV, Domachowske JB, Rosenberg HF.** 2007. Efficient replication of pneumonia virus of mice (PVM) in a mouse macrophage cell line. Virol J **4:**48.

208. **Zhao X, Dai J, Xiao X, Wu L, Zeng J, Sheng J, Su J, Chen X, Wang G, Li K.** 2014. PI3K/Akt signaling pathway modulates influenza virus induced mouse alveolar macrophage polarization to M1/M2b. PLoS One **9:**e104506.

209. **Bender BS, Croghan T, Zhang L, Small PA, Jr.** 1992. Transgenic mice lacking class I major histocompatibility complex-restricted T cells have delayed viral clearance and increased mortality after influenza virus challenge. J Exp Med **175:**1143-1145.

210. **Wu H, Haist V, Baumgartner W, Schughart K.** 2010. Sustained viral load and late death in Rag2-/- mice after influenza A virus infection. Virol J **7:**172.

211. **Frey S, Krempl CD, Schmitt-Graff A, Ehl S.** 2008. Role of T Cells in Virus Control and Disease after Infection with Pneumonia Virus of Mice. Journal of Virology **82:**11619-11627.

212. **Walsh KB, Teijaro JR, Brock LG, Fremgen DM, Collins PL, Rosen H, Oldstone MBA.** 2014. Animal Model of Respiratory Syncytial Virus: CD8(+) T Cells Cause a Cytokine Storm That Is Chemically Tractable by Sphingosine-1-Phosphate 1 Receptor Agonist Therapy. Journal of Virology **88:**6281-6293.

213. **Califano D, Furuya Y, Roberts S, Avram D, McKenzie ANJ, Metzger DW.** 2018. IFN-gamma increases susceptibility to influenza A infection through suppression of group II innate lymphoid cells. Mucosal Immunol **11:**209-219.

214. **Topham NJ, Hewitt EW.** 2009. Natural killer cell cytotoxicity: how do they pull the trigger? Immunology **128:**7-15.

215. **Gazit R, Gruda R, Elboim M, Arnon TI, Katz G, Achdout H, Hanna J, Qimron U, Landau G, Greenbaum E, Zakay-Rones Z, Porgador A, Mandelboim O.** 2006. Lethal influenza infection in the absence of the natural killer cell receptor gene Ncr1. Nature Immunology **7:**517-523.

216. **Mandelboim O, Lieberman N, Lev M, Paul L, Arnon TI, Bushkin Y, Davis DM, Strominger JL, Yewdell JW, Porgador A.** 2001. Recognition of haemagglutinins on virus-infected cells by NKp46 activates lysis by human NK cells. Nature **409:**1055-1060.

217. **Steinstreilein J, Guffee J.** 1986. Invivo Treatment of Mice and Hamsters with Antibodies to Asialo-Gm1 Increases Morbidity and Mortality to Pulmonary Influenza Infection. Journal of Immunology **136:**1435-1441.

218. **Kim TK, Bheda-Malge A, Lin Y, Sreekrishna K, Adams R, Robinson MK, Bascom CC, Tiesman JP, Isfort RJ, Gelinas R.** 2015. A systems approach to understanding human rhinovirus and influenza virus infection. Virology **486:**146-157.

219. **Honda K, Yanai H, Takaoka A, Taniguchi T.** 2005. Regulation of the type I IFN induction: a current view. Int Immunol **17:**1367-1378.

220. **Mordstein M, Kochs G, Dumoutier L, Renauld JC, Paludan SR, Klucher K, Staeheli P.** 2008. Interferon-lambda contributes to innate immunity of mice against influenza A virus but not against hepatotropic viruses. PLoS Pathog **4:**e1000151.

221. **Mahlakoiv T, Ritz D, Mordstein M, DeDiego ML, Enjuanes L, Muller MA, Drosten C, Staeheli P.** 2012. Combined action of type I and type III interferon restricts initial replication of severe acute respiratory syndrome coronavirus in the lung but fails to inhibit systemic virus spread. J Gen Virol **93:**2601-2605.

222. **Mordstein M, Neugebauer E, Ditt V, Jessen B, Rieger T, Falcone V, Sorgeloos F, Ehl S, Mayer D, Kochs G, Schwemmle M, Gunther S, Drosten C, Michiels T, Staeheli P.** 2010. Lambda interferon renders epithelial cells of the respiratory and gastrointestinal tracts resistant to viral infections. J Virol **84:**5670-5677.

223. **Talon J, Horvath CM, Polley R, Basler CF, Muster T, Palese P, Garcia-Sastre A.** 2000. Activation of interferon regulatory factor 3 is inhibited by the influenza A virus NS1 protein. J Virol **74:**7989-7996.

224. **Kochs G, Garcia-Sastre A, Martinez-Sobrido L.** 2007. Multiple anti-interferon actions of the influenza A virus NS1 protein. J Virol **81:**7011-7021.

225. **Percopo CM, Ma M, Brenner TA, Krumholz JO, Break TJ, Laky K, Rosenberg HF.** 2019. Critical Adverse Impact of IL-6 in Acute Pneumovirus Infection. J Immunol **202:**871-882.

226. **Schneider C, Nobs SP, Heer AK, Kurrer M, Klinke G, van Rooijen N, Vogel J, Kopf M.** 2014. Alveolar macrophages are essential for protection from respiratory failure and associated morbidity following influenza virus infection. PLoS Pathog **10:**e1004053.

227. **Wang J, Li F, Sun R, Gao X, Wei H, Li LJ, Tian Z.** 2013. Bacterial colonization dampens influenza-mediated acute lung injury via induction of M2 alveolar macrophages. Nat Commun **4:**2106.

228. **Moskophidis D, Kioussis D.** 1998. Contribution of virus-specific CD8+ cytotoxic T cells to virus clearance or pathologic manifestations of influenza virus infection in a T cell receptor transgenic mouse model. J Exp Med **188:**223-232.

229. **Zitzow LA, Rowe T, Morken T, Shieh WJ, Zaki S, Katz JM.** 2002. Pathogenesis of avian influenza A (H5N1) viruses in ferrets. J Virol **76:**4420-4429.

230. **Herlocher ML, Elias S, Truscon R, Harrison S, Mindell D, Simon C, Monto AS.** 2001. Ferrets as a transmission model for influenza: sequence changes in HA1 of type A (H3N2) virus. J Infect Dis **184:**542-546.

231. **Maines TR, Chen LM, Matsuoka Y, Chen H, Rowe T, Ortin J, Falcon A, Nguyen TH, Mai le Q, Sedyaningsih ER, Harun S, Tumpey TM, Donis RO, Cox NJ, Subbarao K, Katz JM.** 2006. Lack of transmission of H5N1 avian-human reassortant influenza viruses in a ferret model. Proc Natl Acad Sci U S A **103:**12121-12126.

232. **Yen HL, Lipatov AS, Ilyushina NA, Govorkova EA, Franks J, Yilmaz N, Douglas A, Hay A, Krauss S, Rehg JE, Hoffmann E, Webster RG.** 2007. Inefficient transmission of H5N1 influenza viruses in a ferret contact model. J Virol **81:**6890-6898.

233. **de Waal L, Smits SL, Veldhuis Kroeze EJB, van Amerongen G, Pohl MO, Osterhaus A, Stittelaar KJ.** 2018. Transmission of Human Respiratory Syncytial Virus in the Immunocompromised Ferret Model. Viruses **10**.

234. **van den Brand JM, Haagmans BL, Leijten L, van Riel D, Martina BE, Osterhaus AD, Kuiken T.** 2008. Pathology of experimental SARS coronavirus infection in cats and ferrets. Vet Pathol **45:**551-562.

235. **Darnell ME, Plant EP, Watanabe H, Byrum R, St Claire M, Ward JM, Taylor DR.** 2007. Severe acute respiratory syndrome coronavirus infection in vaccinated ferrets. J Infect Dis **196:**1329-1338.